



Scientific Report

Intensive Rehabilitation
Technologies

RESEARCH

Open Access



Video mirror feedback induces more extensive brain activation compared to the mirror box: an fNIRS study in healthy adults

Julien Bonnal^{1,2,3,4*}, Canan Ozsancak^{1,5}, Fabrice Prieur^{2,3,4} and Pascal Auzou^{1,5}

Abstract

Background Mirror therapy (MT) has been shown to be effective for motor recovery of the upper limb after a stroke. The cerebral mechanisms of mirror therapy involve the precuneus, premotor cortex and primary motor cortex. Activation of the precuneus could be a marker of this effectiveness. MT has some limitations and video therapy (VT) tools are being developed to optimise MT. While the clinical superiority of these new tools remains to be demonstrated, comparing the cerebral mechanisms of these different modalities will provide a better understanding of the related neuroplasticity mechanisms.

Methods Thirty-three right-handed healthy individuals were included in this study. Participants were equipped with a near-infrared spectroscopy headset covering the precuneus, the premotor cortex and the primary motor cortex of each hemisphere. Each participant performed 3 tasks: a MT task (right hand movement and left visual feedback), a VT task (left visual feedback only) and a control task (right hand movement only). Perception of illusion was rated for MT and VT by asking participants to rate the intensity using a visual analogue scale. The aim of this study was to compare brain activation during MT and VT. We also evaluated the correlation between the precuneus activation and the illusion quality of the visual mirrored feedback.

Results We found a greater activation of the precuneus contralateral to the visual feedback during VT than during MT. We also showed that activation of primary motor cortex and premotor cortex contralateral to visual feedback was more extensive in VT than in MT. Illusion perception was not correlated with precuneus activation.

Conclusion VT led to greater activation of a parieto-frontal network than MT. This could result from a greater focus on visual feedback and a reduction in interhemispheric inhibition in VT because of the absence of an associated motor task. These results suggest that VT could promote neuroplasticity mechanisms in people with brain lesions more efficiently than MT.

Clinical trial registration NCT04738851.

Keywords Mirror therapy, Virtual reality, Precuneus, Motor cortex, Cerebral activation, fNIRS

*Correspondence:

Julien Bonnal
julien.bonnal@chu-orleans.fr

¹Service de Neurologie, Centre Hospitalier Universitaire d'Orléans, 14
Avenue de l'Hôpital, Orleans 45100, France

²CIAMS, Université Paris-Saclay, Orsay Cedex 91405, France

³CIAMS, Université d'Orléans, Orléans 45067, France

⁴SAPRÉM, Université d'Orléans, Orléans, France

⁵L2RSO, Université d'Orléans, Orléans, France



© The Author(s) 2024. **Open Access** This article is licensed under a Creative Commons Attribution 4.0 International License, which permits use, sharing, adaptation, distribution and reproduction in any medium or format, as long as you give appropriate credit to the original author(s) and the source, provide a link to the Creative Commons licence, and indicate if changes were made. The images or other third party material in this article are included in the article's Creative Commons licence, unless indicated otherwise in a credit line to the material. If material is not included in the article's Creative Commons licence and your intended use is not permitted by statutory regulation or exceeds the permitted use, you will need to obtain permission directly from the copyright holder. To view a copy of this licence, visit <http://creativecommons.org/licenses/by/4.0/>. The Creative Commons Public Domain Dedication waiver (<http://creativecommons.org/publicdomain/zero/1.0/>) applies to the data made available in this article, unless otherwise stated in a credit line to the data.

Introduction

Mirror therapy (MT) is commonly used for stroke rehabilitation. This technique consists of using the reflection in a mirror of the movements of a healthy limb to give the illusion of movement of the pathological limb. First proposed for phantom limb pain [1], MT was then used for motor rehabilitation of the post-stroke hemiparetic upper limb [2]. Recent meta-analyses have reported a beneficial effect of MT on upper limb motor recovery after stroke [3, 4].

Despite its effectiveness, the use of MT may be limited by difficulty with positioning for individuals with postural deficits, the need for bilateral training, or associated disorders such as aphasia or hemispatial neglect [5, 6]. New MT tools using virtual reality have been developed to improve the technique [7]. In this study, we focused on video therapy (VT) in which the mirror is replaced by a digital screen [8–10]. The use of these recent tools has been found to be feasible [11]. To our knowledge, there is no evidence of clinical superiority of VT over MT. The relatively high cost of these technologies makes it necessary to determine if they are indeed more effective than simpler, lower cost tools [7]. As such, it seems relevant to compare brain activation patterns between both modalities (MT and VT).

Many studies have explored the brain mechanisms of MT in both people after stroke and healthy individuals. MT activates the motor cortex, in particular the primary motor cortex (M1), premotor cortex (PMC) [12–15] and the precuneus (PC) [16–19] contralaterally to the side of visual feedback. In this study we focused more specifically on the activation of the PC as a determining factor of the effectiveness of the technique. Indeed, it has been shown that motor recovery following MT is correlated with PC activation [19]. One of the roles of the PC is to integrate the visual information from the environment and its transmission to the motor cortex to create a body self-perception [20]. Therefore, in MT the PC could be activated when the visual feedback gives the illusion of ownership of the visualized limb. It then seems relevant to assess the correlation between this activation and the quality of perception of the illusion.

Among the studies evaluating brain activity during MT, some used a real mirror [12, 13, 15, 17] and others a VT tool [14, 16, 18, 19], often for reasons of compatibility with the imaging method. To our knowledge, no study has directly compared the brain activation profiles of these 2 techniques. It seems appropriate to study these mechanisms in healthy subjects as a first step, in order to provide a rationale for future studies in patients. The literature on MT has shown similar activation patterns between healthy subjects [13, 16] and stroke subjects [14, 19]. A MT study conducted in healthy and stroke subjects found precuneus activation in both populations [21].

We chose to use fNIRS to determine the amount of activation of the cerebral regions of interest. This technique enables the evaluation of neurovascular coupling by measuring changes in both oxyhemoglobin (HbO₂) and deoxyhemoglobin (HbR) in the cortex. The portability of the fNIRS device means it can be used in the real-life environment, including to determine the cerebral mechanisms involved in rehabilitation [12, 13, 16, 19].

The first aim of the study was to compare cerebral activation (PC, PMC and M1) induced by MT and VT tasks using functional near infrared spectroscopy (fNIRS). We hypothesized that VT would lead to greater activation of each region. The second aim of this study was to evaluate the correlation between individuals' perceptions of the illusion of movement for the two mirrored feedback modalities (MT and VT) and brain activation. We hypothesized that the stronger the illusion of movement, the greater the activation of the PC.

Materials and methods

Participants and ethical statement

Thirty-three right-handed individuals (9 males, 24 females; mean (SD) age 24.5 (3.4) years, range 19–40) with no history of neurological, physical, or psychiatric illness were included in this study. Two other individuals were initially recruited, but their data could not be analysed owing to the poor quality of the fNIRS signal. The Edinburgh Handedness Inventory [22] was used to evaluate handedness. All participants had an Edinburgh laterality ratio ≥ 80 . Full written consent was obtained from all participants in accordance with the Declaration of Helsinki. This study was approved by the Institutional Review Board CPP NORD-OUEST I on 21st January 2021 (no. 2020-A02936-33) and was registered on clinical trials.gov (NCT04738851). The study is reported according to the Strengthening the Reporting of Observational Studies in Epidemiology (STROBE) guidelines.

Experimental design and procedure

Participants were required to sit in a comfortable, upright position during the experiment. Experiments were organized in a block paradigm (Fig. 1A). The block design included 10 20-s trials for each task. Rest time between trials varied from 20 to 30 s to minimize the physiological effects of respiration, heart rate, and Mayer waves (low-frequency oscillations in blood pressure) on hemodynamic responses to the task [23].

Each participant completed 3 separate recordings (with a 10-minute rest period in between) for 3 different tasks. The control task involved performing a movement with the right hand while looking at the left hand (Fig. 1B). During this task, the left hand is motionless. So, this task has been carried out to check that the results related to the mirror techniques are not only attributable to the

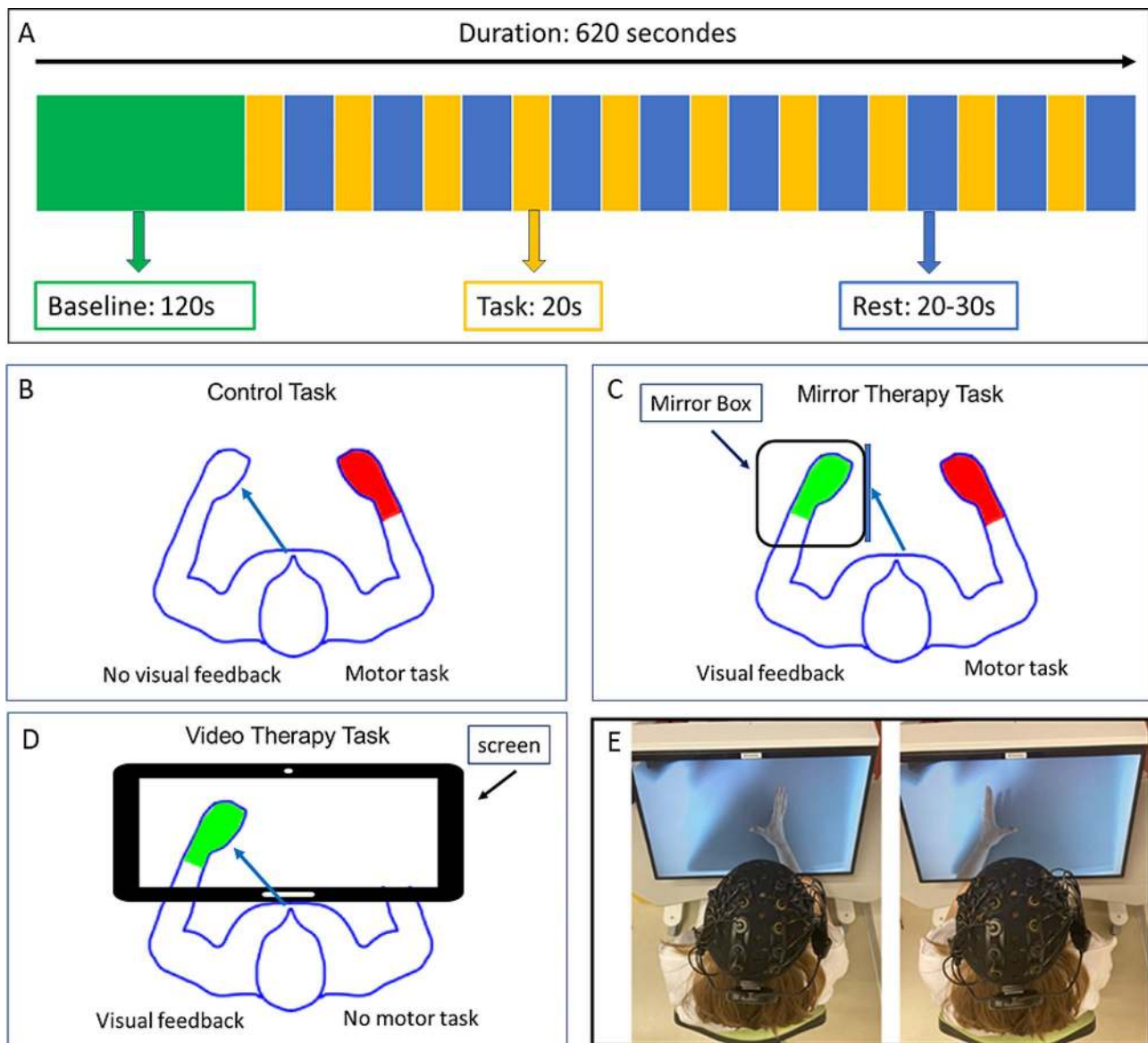


Fig. 1 experimental design. (A) Block design for each recording. (B) Control Task. (C) Mirror Therapy Task. (D) Video Therapy Task. The blue arrow represents the direction of the participant's gaze. The green hand indicates the provision of mirrored feedback and the red hand indicates that the participant is performing a motor task. (E) Picture of the setup of the Video Therapy Task: on the left, the movement recording with the right hand and on the right the visualization of the movement on the left after flipping the image

observation of the hand (in this case, the left hand) but require the visualization of a movement. The mirror therapy task involved performing a movement with the right hand while observing the reflection of that movement in a mirror (Fig. 1C). For this task, a mirror box was used in which the left hand was positioned. The video therapy task involved observing a left-hand movement on a screen (with the left hand placed under the screen) (Fig. 1D). During VT task, no movement was performed by the participant's right hand. For VT task, we used an innovative device based on the principle of mirror therapy and action observation using a screen instead of a

normal mirror. We used the IVS3 (Dessintey[®], Saint-Etienne, France). This tool requires the pre-recording of a movement with one hand (the healthy hand in the case of a stroke), which is then flipped into the contralateral hand (the impaired hand in the case of a stroke). For this study, movement of the participant's right hand was recorded before the performance of the task and then the illusion of movement of the left hand was provided on the screen (Fig. 1E). For each task, the movement studied was a hand opening/closing movement performed at a frequency of 0.5 Hz (using a metronome) [24]. The order of the 3 conditions was counterbalanced to avoid

any effect of the order. The perception of the illusion was rated for each of the mirror feedback tasks (MT and VT) by asking participants to rate the intensity of any sensations they experienced (tingling, warmth, desire to move the hand, sensation of contraction, etc.) using a visual analogue scale.

fNIRS data acquisition

Changes in the concentrations of oxyhemoglobin (HbO₂) and deoxyhemoglobin (HbR) within the cerebral cortex were measured using a continuous wave optical system Brite 24 system (Artinis Medical Systems, Netherlands). The sources of this system generate 2 wavelengths of near-infrared light at 670 and 850 nm, and the sampling rate is fixed at 10 Hz. A total of 10 light sources and 8 detectors with an inter-optode distance of 3 cm constituted 18 channels (Fig. 2).

To localize the coordinates of each channel in the Montreal Neurological Institute standard brain [25], a 3D digitizer (FASTRACK, Polhemus) was used, and the coordinates were further imported to the NIRS SPM toolbox for spatial registration [26]. The coordinates were then used to define the channels constituting the different regions of interest (ROI) that were used for the statistical analysis (Fig. 2). We defined 3 ROI for each hemisphere as follows: Right PC (Channels 1,2), Right M1 (channels 6,8,9), Right PMC (Channels 3,4,5,7), Left PC (Channels 10,11), Left M1 (channels 13,17,18) and Left PMC (channels 12,14,15,16).

Preprocessing of fNIRS data

We used both HbO₂ and HbR signals to measure the hemodynamic response because they provide different and complementary information [27, 28]. The Homer2 toolbox in Matlab (The MathWorks Inc.) was used for offline data preprocessing [29].

The processing was performed as follows:

1. Identification and exclusion of bad channels: channels were considered as bad and excluded from the analysis if the coefficient of variation ($[\text{standard deviation}/\text{mean}] * 100$) of the raw data was $> 33\%$. The function `hmrPruneChannels` was used ($\text{SNRthres} = 3$). For each subject, the number of channels excluded ranged from 0 to 6. Overall, 5% of channels were excluded from the analysis.
2. Optical density conversion: raw data were converted into optical density with the `hmrIntensity2OD` function.
3. Filtering periodic noise: respiration, cardiac activity and high frequency noise were attenuated with `hmrBandpassFilt` ($\text{hpf} = 0, \text{lpf} = 0.1$).
4. For the remaining artifacts (physiological and motion artifacts), Principal Component Analysis was used with the `enPCAfilter_nSV` function.
5. Concentration conversion: corrected optical density data were converted into relative concentration changes with the modified Beer-Lambert law [30]. The age-dependent differential path length factor

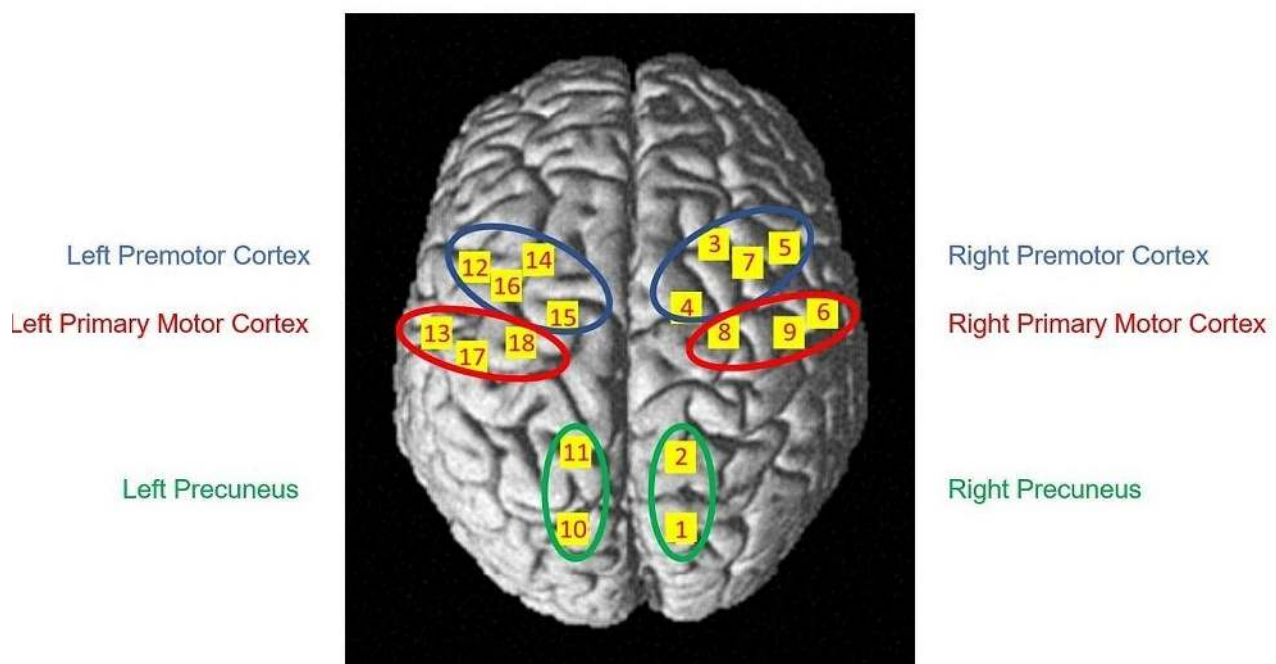


Fig. 2 Anatomical locations of the channels and representation of the Regions of Interest superimposed onto the normalized brain surface in the MNI standard brain template

(DPF) value was calculated for each participant [31]. DPF values were calculated for each wavelength according to the mean age. They were respectively 6.2 and 5.1 for the 760 and 840 nm wavelengths.

6. The hemodynamic response function was estimated by solving a general linear deconvolution model using the `hmrDeconvTB_SS3rd` function (t range = [-5, 25], $gstd = 1$, $gms = 1$, $\rho_{SD_ssThresh} = 1$).

Data analysis

Data analysis was performed with Matlab (The MathWorks Inc.). Mean values were calculated for the rest (from 5 s before, to the beginning of the task) and trial periods (from +5 s to +25 s) for each channel. To detect cerebral activation, the mean changes in HbO₂ and HbR between the rest period and task for each channel and for each ROI were compared using the unilateral paired Student t test. For the ROI analysis, an average of the corresponding channels was made. We applied a Benjamini–Hochberg procedure [32] to control the growth of the false discovery rate (FDR) caused by multiple comparisons. The task comparisons were analysed using one-way repeated measures ANOVA (factor task) for each ROI and HbO₂, which seems to be a better marker of cerebral activation than HbR [28, 33]. A post-hoc analysis was performed using unilateral paired t -tests. Significance was set at $p < 0.05$ (Bonferroni correction $p < 0.017$).

Finally, we evaluated the link between movement illusion during mirrored feedback (for MT and VT tasks) and PC activation using a Pearson correlation between the Visual Analog Scale and the mean HbO₂ changes for the Right PC ROI.

Results

Comparison of baseline and task hemodynamic responses: cerebral activation

The hemodynamic responses for the 3 conditions (Table 1) are illustrated by the plotograms (Fig. 3) and a NIRS-SPM (statistical parametric mapping for near-infrared spectroscopy) representation (Fig. 4). Overall, responses were canonical with an increase in HbO₂ concentration and a tendency towards a decrease in HbR concentration.

Control Task

HbO₂ concentration increased ($t = 5$, $p < 0.01$) and HbR concentration decreased ($t = -3.65$, $p < 0.01$) only in the left M1. No significant changes were found for the other ROI or channels.

Mirror therapy task

HbO₂ concentration increased ($t = 6.37$, $p < 0.01$) and HbR concentration decreased ($t = -5.29$, $p < 0.01$) in the left

M1. No significant changes were found for the other ROI, but Channel 15 (part of left PMC) showed a significant decrease in HbR concentration ($t = -3.95$, $p < 0.01$) and channel 6 (part of right M1) showed a significant increase in HbO₂ concentration ($t = 2.55$, $p < 0.05$).

Video therapy task

HbO₂ concentration increased ($t = 2.58$, $p < 0.05$) and HbR concentration decreased ($t = -2.85$, $p < 0.05$) in the right PC. HbO₂ concentration also increased in the left PC ($t = 2.43$, $p < 0.05$) and the right M1 ($t = 4.19$, $p < 0.01$). No significant changes were found for the other ROI, but Channel 5 (part of the right PMC) showed an increase in HbO₂ concentration ($t = 3.72$, $p < 0.01$) and a decrease in HbR concentration ($t = -2.88$, $p < 0.05$).

Task comparisons

The results of the ANOVA and the post-hoc analysis are shown in Fig. 5.

Precuneus

For the right PC, one-way ANOVA showed a significant effect of task ($F = 5.36$, $p = 0.007$). Post-hoc analysis showed that activation was greater during VT task than MT task ($t = 2.57$, $p = 0.008$) and control task ($t = 4.38$, $p < 0.001$).

For the left PC, the one-way ANOVA showed a significant effect of task ($F = 4.17$, $p = 0.02$). Post-hoc analysis showed that activation was greater during VT task than control task ($t = 2.56$, $p = 0.008$).

Primary motor cortex

The one-way ANOVA showed a significant effect of task only for the left M1 ($F = 22.32$, $p < 0.001$). Post-hoc analysis showed that activation was greater during MT task than VT task ($t = 5.7$, $p < 0.001$) and during control task than VT task ($t = 3.74$, $p < 0.001$).

There was no significant effect on the right M1 ($F = 1.17$, $p = 0.32$).

Premotor Cortex

The one-way ANOVA showed a significant effect of task only for the left PMC ($F = 7.32$, $p = 0.001$). Post-hoc analysis showed that activation was greater during MT task than VT task ($t = 2.65$, $p = 0.007$) and during control task than VT task ($t = 2.67$, $p = 0.007$).

There was no significant effect on the right PMC ($F = 2.44$, $p = 0.1$).

Illusion of movement

Illusion of movement was evaluated after MT task (mean (SD) 4.5 (2.4)) and VT task (mean (SD) 5.2 (2.2)). There was no correlation between perception of illusion and

Table 1 Changes in HbO₂ and HbR concentrations for ROI and individual channels, and the corresponding *p*-values between rest and task for each condition

	Control Task			Mirror Therapy Task			Video Therapy Task		
	HbO ₂	HbR	<i>p</i> value	HbO ₂	HbR	<i>p</i> value	HbO ₂	HbR	<i>p</i> value
Right PC	-0.066(0.163)	0.001(0.068)	0.598	-0.039(0.183)	0.883	0.392	0.043(0.096)	-0.031(0.063)	0.004*
Channel 1	-0.111(0.184)	0.004(0.081)	0.610	-0.083(0.218)	0.982	0.387	0.0414(0.114)	-0.039(0.082)	0.005*
Channel 2	-0.027(0.159)	0.001(0.067)	0.509	0.005(0.181)	0.436	0.417	0.046(0.115)	-0.024(0.059)	0.014
Right PMC	-0.032(0.112)	0.005(0.060)	0.674	-0.011(0.134)	0.796	0.545	0.019(0.067)	-0.014(0.049)	0.136
Channel 3	-0.046(0.120)	0.015(0.058)	0.920	-0.041(0.162)	0.913	0.902	0.004(0.101)	-0.015(0.066)	0.097
Channel 4	-0.072(0.247)	-0.008(0.117)	0.350	-0.070(0.245)	0.931	0.231	-0.030(0.132)	-0.010(0.102)	0.291
Channel 5	0.012(0.121)	0.015(0.073)	0.866	0.049(0.157)	0.037	0.607	0.055(0.084)	-0.024(0.046)	0.004*
Channel 7	-0.024(0.117)	0.001(0.067)	0.508	-0.016(0.159)	0.711	0.895	0.027(0.088)	-0.002(0.047)	0.407
Right M1	0.008(0.118)	-0.006(0.073)	0.352	0.029(0.138)	0.078	0.298	0.047(0.082)	-0.016(0.058)	0.026
Channel 6	0.041(0.138)	-0.014(0.084)	0.170	0.075(0.172)	0.008*	0.138	0.078(0.096)	-0.023(0.057)	0.014
Channel 8	-0.023(0.174)	0.004(0.071)	0.633	0.002(0.178)	0.469	0.639	0.011(0.105)	-0.009(0.057)	0.175
Channel 9	0.003(0.124)	-0.008(0.087)	0.293	0.014(0.154)	0.289	0.212	0.060(0.095)	-0.018(0.072)	0.081
Left PC	-0.048(0.172)	-0.002(0.072)	0.422	-0.019(0.185)	0.595	0.253	0.060(0.134)	-0.013(0.073)	0.117
Channel 10	-0.077(0.184)	0.007(0.073)	0.694	-0.037(0.194)	0.850	0.425	0.059(0.144)	-0.027(0.079)	0.034
Channel 11	-0.013(0.193)	-0.012(0.087)	0.219	0.009(0.214)	0.404	0.111	0.065(0.158)	-0.004(0.093)	0.417
Left PMC	0.052(0.140)	-0.011(0.123)	0.258	0.054(0.146)	0.049	0.066	-0.026(0.107)	0.001(0.040)	0.265
Channel 12	0.033(0.153)	0.029(0.129)	0.894	0.035(0.167)	0.129	0.267	0.009(0.154)	-0.003(0.037)	0.366
Channel 14	0.012(0.106)	-0.012(0.111)	0.268	0.020(0.192)	0.279	0.185	-0.047(0.118)	0.002(0.033)	0.634
Channel 15	0.077(0.244)	-0.057(0.147)	0.027	0.077(0.204)	0.027	<0.001**	-0.043(0.101)	-0.030(0.078)	0.032
Channel 16	0.033(0.142)	-0.007(0.168)	0.394	0.064(0.196)	0.037	0.196	-0.055(0.178)	0.027(0.081)	0.961
Left M1	0.151(0.157)	-0.061(0.090)	<0.001**	0.204(0.168)	<0.001*	<0.001**	0.015(0.101)	0.004(0.061)	0.684
Channel 13	0.174(0.183)	-0.045(0.099)	0.006*	0.244(0.238)	<0.001*	<0.001**	0.045(0.130)	0.002(0.062)	0.591
Channel 17	0.201(0.212)	-0.092(0.108)	<0.001**	0.243(0.249)	<0.001*	<0.001**	-0.003(0.156)	0.002(0.075)	0.567
Channel 18	0.071(0.130)	-0.042(0.092)	0.006*	0.125(0.148)	<0.001*	<0.001**	0.003(0.085)	0.008(0.064)	0.762

Data are mean(SEM), unit: μMol/L.

Abbreviations: HbO₂ = oxyhemoglobin; HbR = deoxyhemoglobin; PC = Precuneus; PMC = Premotor Cortex; M1 = Primary Motor Cortex

Significance levels were corrected for multiple comparisons using the Benjamini–Hochberg procedure: * *p* < 0.05; ** *p* < 0.01

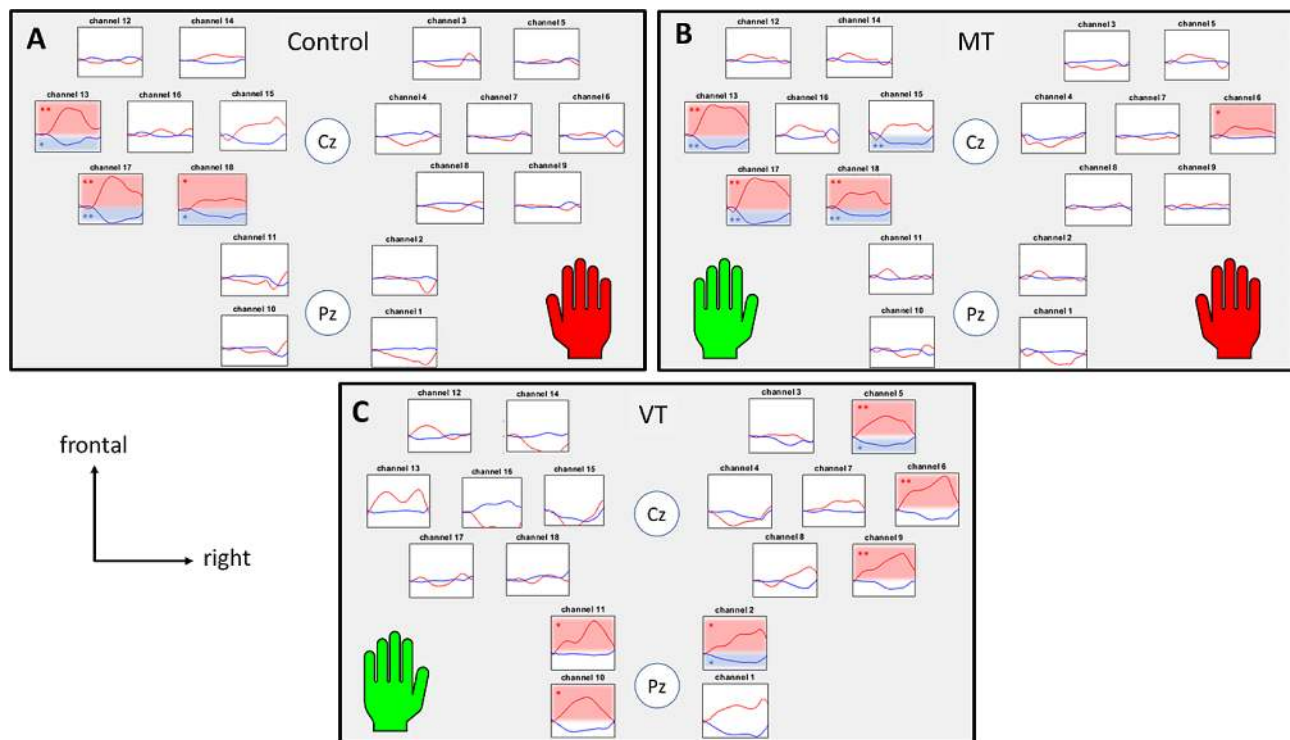


Fig. 3 Results of the hemodynamic response by task for each channel. (A) Control Task. (B) Mirror Therapy Task. (C) Video Therapy Task. Results are expressed as means (average of the participants' HbR and HbO₂ concentrations). The green left hand indicates that the task involved mirrored feedback and the red right hand indicates that the task involved motor execution. Graph locations were organised according to the anatomical correspondence using the EEG 10/20 system. The time window analysed was 30 s: from 5 s before the beginning of the task to 25 s after. The red traces indicate HbO₂ concentrations and the blue traces indicate HbR concentrations. The red boxes indicate a significant difference between rest and task periods for HbO₂ concentration. The blue boxes indicate a significant difference between rest and task periods for HbR concentrations. *: $p < 0.05$; **: $p < 0.01$; FDR corrected

changes in HbO₂ for the right PC area of interest for MT task ($r^2 = 0.03$, $p = 0.76$) or VT task ($r^2 = 0.07$, $p = 0.14$).

Discussion

To our knowledge, this study is the first to compare the cerebral activation induced by conventional mirror therapy (MT) with that induced by video therapy (VT). In VT, the visualised movements are pre-recorded and projected onto a large screen positioned in front of the individual. Compared with conventional MT, VT could provide a higher quality illusion and encourage attention to visual feedback. This new modality could therefore improve the effectiveness of MT by optimising the mechanisms that induce neuroplasticity. In this study we focused on the regions of interest that are involved in MT, the precuneus (PC), primary motor cortex (M1) and premotor cortex (PMC). We explored mirror tasks with no movement intention, which allowed us to specifically assess the effect of visual feedback. Our main aim was to evaluate the difference in activation of the PC between the two techniques since PC activation could be correlated with the effectiveness of the technique [19]. As we had hypothesized, we found greater activation of the PC contralateral to visual feedback during VT than

during conventional MT. We also showed that activation of M1 and PMC contralateral to visual feedback was more extensive in VT than in MT.

Activation of the PC: movement illusion or attentional mechanisms?

The involvement of the PC in MT has been previously widely demonstrated [16, 17, 19, 34]. The PC plays a major role in visual processing and self-perception [20], and more particularly in the perception of the hand [35]. We initially hypothesized that during the MT and the VT tasks, the PC would be activated if the participants perceived the illusion of seeing their own hand during the visual feedback situation, and we hypothesized that the quality of the illusion would be greater with VT. To verify our hypothesis, we assessed the participants' perceptions of the quality of the illusion (impression that the hand was moving, tingling, sensations of contraction, etc.), as suggested by Rossiter [36]. We found that the perception of the illusion did not differ between the VT and MT tasks and that it was not correlated with the level of PC activation. Illusion perception is subjective and difficult to assess, in particular because no validated scales exist for that purpose. However, some studies have found

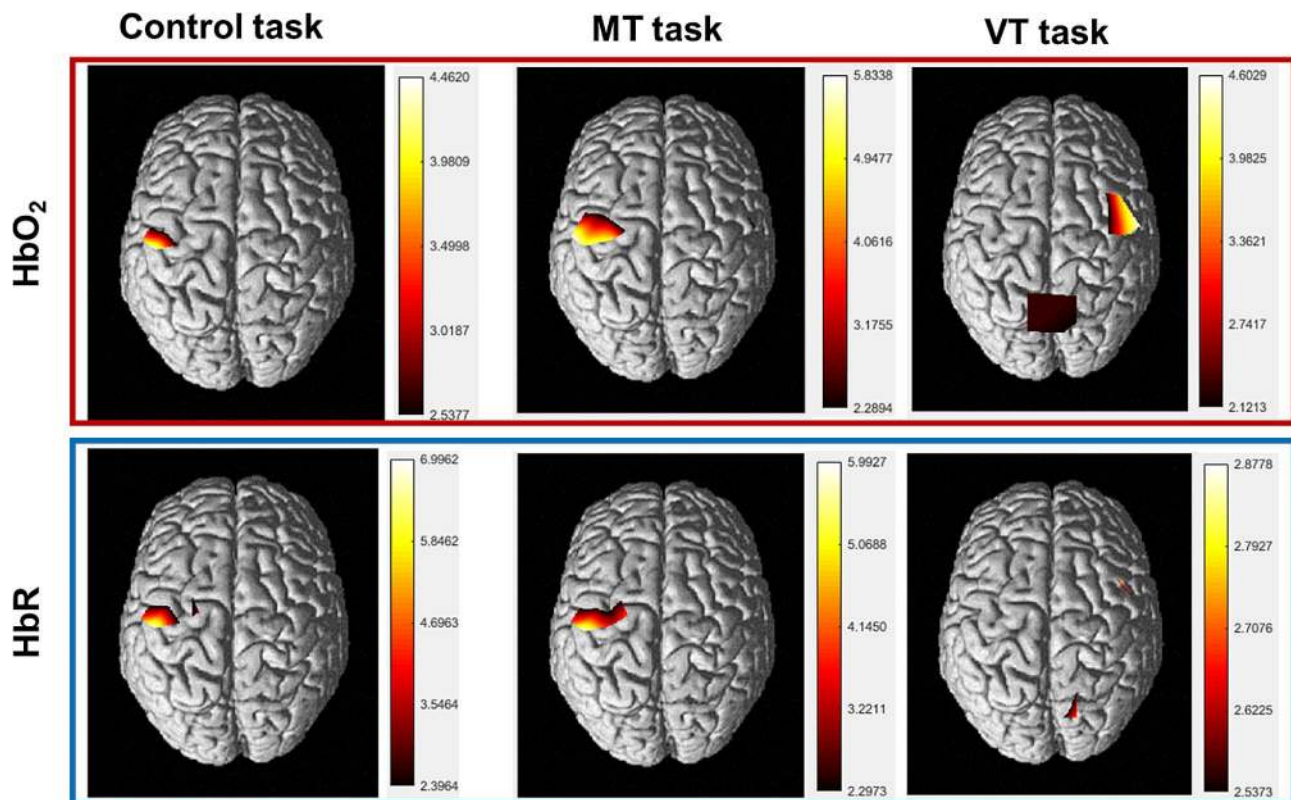


Fig. 4 Mean cerebral cortex activation maps for oxyhemoglobin and deoxyhemoglobin during the 3 tasks. Data are t values, t : statistical value of sample t -test with a significance level of $p < 0.05$ (FDR corrected). The change from red to yellow indicates that the degree of activation is from low to high. Only statistically significant responses are illustrated. The data and maps were calculated and generated by NIRS-SPM.

PC activation during VT without a real illusion [16, 19]. In those studies, the screen was located at a distance from the participant that did not allow visual continuity between the upper limb and the visual feedback. Thus, we cannot conclude that the greater PC activation found in this study with VT than MT was the result of a higher quality movement illusion with VT.

Another explanation for these results could relate to the role of the PC in attentional tasks. When a person is focused on a given task, the PC may be recruited to support the cognitive engagement. A functional MRI (fMRI) study on 10 healthy individuals showed that the PC was activated during a visuospatial attention task [37]. In addition, a meta-analysis showed that PC lesions could cause spatial hemineglect [38]. The PC therefore seems to be particularly involved in visual attention processes. In our study, the lack of an associated motor task during the VT task may have focused attention on the visual feedback to a greater extent than the MT task. Thus, the more extensive PC activation during VT than MT may have been due to a higher level of attention.

Moreover, in our study PC activation was not only contralateral to the side of feedback but bilateral. This could be explained by the fact that the function of the PC is not as lateralized as that of other brain structures. Indeed,

although several MT studies have found that PC activation was strictly contralateral in response to visual feedback [16, 18, 19], two motor imaging studies reported that lateralization of the PC was random across individuals. This result is interesting insofar as in the event of a hemispheric lesion including the PC, its activity could be compensated for by the contralesional PC.

The activity of the PC seems important for rehabilitation, as it could have a predominant role in the stimulation of neuroplasticity. Indeed, it has been shown that the PC is closely connected to the motor cortex [39]. The motor cortex is often damaged after a stroke in individuals with residual upper limb impairment. Activating the PC during rehabilitation could therefore stimulate the ipsilesional M1. Based on these results, it is possible that VT, by improving recruitment of precuneus, is an effective technique for improving neuroplasticity and therefore motor recovery in stroke patients. These hypotheses will need to be verified in future clinical studies.

Other cortical regions of interest: M1 and PMC

First, we only found activation of the left M1 during the MT and control tasks, i.e., the tasks that required motor activity of the right hand. These results are in line with

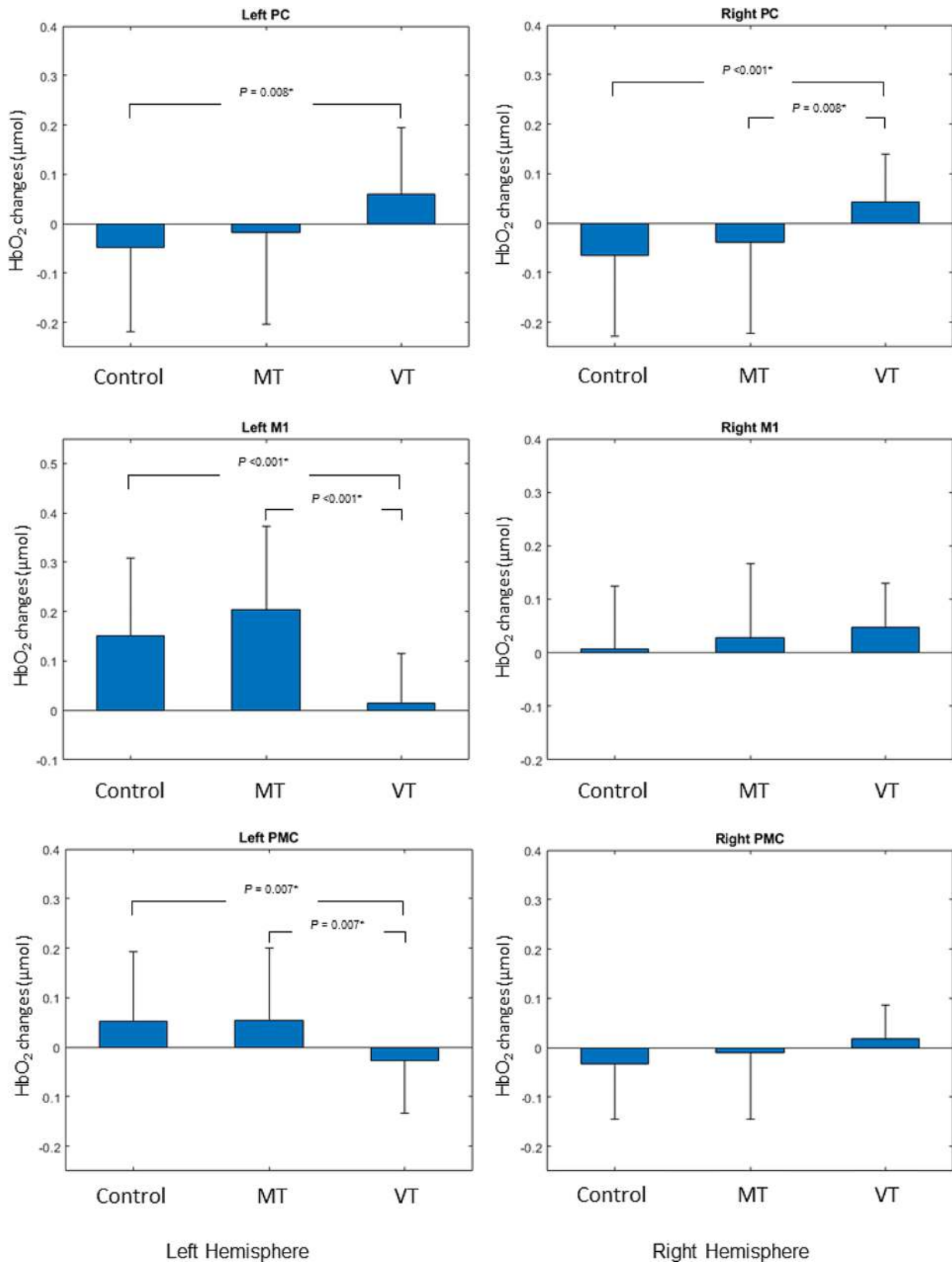


Fig. 5 Post-hoc analysis with the paired t-test results that remained significant after Bonferroni correction

the classical literature regarding the contralateral cortical control of motor activity [40].

Second, we found activation of the right M1 for the tasks involving mirror feedback (MT and VT). These results are also in agreement with the existing literature [12, 13]. However, although we didn't find any statistical difference in the task comparison for this region, our results show a more extensive activation during VT task than during MT task (for this ROI, one channel was activated during MT task and two channels during VT task). We previously argued that the lack of a motor task during the VT is interesting because it encourages attention on the visual feedback. This absence of a motor task could also explain the difference in M1 activation between VT and MT for two reasons. First, the VT used here, due to the absence of a motor task, could be considered as action observation (AO) therapy associated with visual illusion. A study has shown that AO regulates interhemispheric interaction, with a facilitatory effect on the M1 contralateral to the observed movement and an inhibitory effect on the M1 ipsilateral [41]. However, the VT used here also provided the visual illusion of movement of the own limb. One study showed that AO was able to induce neuroplasticity on M1 only if associated with an illusion of movement (kinaesthetic in the study) [42]. Therefore, the VT used here could have a facilitatory effect on the ipsilesional side (in the case of a stroke) and stimulate neuroplasticity in the M1. Second, the less extensive activation during MT may result from interhemispheric inhibition induced by the right-hand motor task. Indeed, it has been shown that unilateral movement leads to inhibition of the ipsilateral hemisphere via the transcallosal pathway [43]. Interhemispheric balance is altered by stroke [44], even in a resting situation [45], and MT in particular helps to restore this balance [46]. Therefore, it is likely that the difference found in this study would be more marked in a group of people after stroke. However, these results need to be interpreted with caution. Indeed, even though activation involves more channels in VT and is consequently more extensive, our results show no statistically significant difference between the two techniques for the whole ROI. It has also been shown that these interhemispheric interactions can be both inhibitory and facilitatory, depending on stimulus intensity [47, 48]. Here, our results seem to show that the stimulus (the motor task) had an inhibitory effect, since activation was more extensive in the absence of motor task. However, it might be interesting to investigate a possible facilitating effect of the motor task during MT on activation of the M1 contralateral to visual feedback by varying the intensity of the task.

To resume our results concerning M1, they can be explained by a facilitatory effect of VT or an inhibitory

effect of MT. In both cases, the absence of a motor task in VT could lead to better stimulation of M1.

Finally, our results showed activation of the PMC contralateral to the visual feedback only during the VT task. This activation was limited to a single channel. This could correspond to activation of mirror neurons located in the ventral part of the PMC [49]. This system is particularly involved in action observation therapy [50]. As mentioned above, the VT used here could be considered as 1st-person AO, which leads to greater activation of mirror neurons than 3rd-person AO [51]. The activation found here could therefore be linked solely to movement observation (with no associated motor task) and would not be dependent on illusion perception, which is the basis of mirror therapy.

In summary, contralateral to the visual feedback, our results show a greater activation of PC during VT compared to MT and an activation of the motor cortex during MT and VT, but this activation was more extensive during VT. These results are mainly explained by the absence of a motor task during VT, which favours increased attention to the visual feedback (greater activation of PC) and possibly reduces interhemispheric inhibition mechanisms (larger activation of M1). Therefore, VT appears to optimise recruitment of the parietofrontal motor network compared with MT [52]. This network induces neuroplasticity after a brain lesion. Indeed, this network is more activated during a motor task in people after stroke than in healthy subjects [53]. Our results therefore suggest that VT may be clinically more effective than MT because of a greater stimulation of neuroplasticity, but this needs to be demonstrated in clinical studies of people after stroke. While the literature shows similar activation patterns between healthy subjects and stroke patients in the exploration of MT mechanisms [13, 14, 16, 17, 34], these mechanisms may be impacted by the location of the lesion. A study of 36 stroke patients showed that the clinical efficacy of MT was linked to the integrity of dorsal and ventral streams [54]. In view of the results of Brunetti et al. [19], we can also assume that a lesion of the PC would also impact the clinical efficacy of MT. Thus, future studies in stroke patients, whether imaging or clinical, should consider results according to lesion location.

Limitations and perspectives

This study has several limitations. First, the MT modalities differed from those used in clinical practice. Usually, individuals are asked to accompany the visualized movement by trying to move the impaired hand. This condition was not applicable to healthy individuals, as the intention would have resulted in a movement that would have masked the brain activation related to the visual feedback. Although this modality without movement

intention can be applied to the patient, it does not appear to be optimal. A magnetoencephalography study in healthy individuals showed that contralateral M1 activation was greater when feedback was associated with the intention to perform the movement [15]. Another limitation concerns the task. We analysed a simple task (hand opening/closing). However, a study conducted in healthy individuals and people after stroke showed that MT-related brain activation was greater when the task was complex [55]. It would have been interesting to explore differences between simple and complex motor tasks.

Moreover, our study has some recruitment-related limitations. This study was carried out only on healthy subjects, whereas it investigates rehabilitation methods (i.e. MT and VT) used in the rehabilitation of stroke patients. While this was an important step, it will be necessary to evaluate these activation patterns and any clinical differences between the two techniques in stroke patients in future studies. In addition, we only recruited right-handed individuals, and the motor tasks were performed on the right side with left visual feedback. Therefore, our results cannot be extrapolated to the use of MT for the non-dominant side or to left-handed individuals. An electroencephalogram study of 13 healthy individuals found increased intracortical contralateral inhibition to movement and activation of mirror neurons [46]. However, the authors showed that the former effect was greater when participants moved their right (dominant) hand, and the latter was greater when the feedback was to the right (thus left-handed motor skills). To our knowledge, the specificity of left-handedness has not been evaluated in MT, but it is likely that different brain mechanisms are involved. Indeed, it has been shown that left-handed individuals have more bilateral activation patterns during the execution of motor tasks [56]. These different parameters should be considered in future studies.

Another limitation regarding the sample is that we only recruited young subjects, whereas some studies have shown that cortical activation patterns during motor task performance are different in older subjects. For example, one study showed that activation was more bilateral in older participants during a hand rehabilitation exercise using a multisensory glove [57]. Therefore, our results cannot be directly generalized to older adults or people after stroke, who are usually older than our study participants. Further studies in older subjects are thus warranted.

Finally, the fNIRS device did not allow us to cover the whole cortex. Therefore, we selected regions of interest (PC, PMC, and M1). However, other zones are activated during MT, such as the supplementary motor area, parietal and occipital cortices [34]. Unfortunately, this is a limitation of the fNIRS technique [12, 16]. In addition,

some regions are not accessible by fNIRS, such as the cerebellum, which appears to be involved in MT [58].

Conclusion

The results of this study reinforce the data in the literature concerning the mechanisms behind the effectiveness of mirror therapy and demonstrate the reliability of fNIRS for this type of exploration. Our results showed the involvement of a parieto-frontal network in which the precuneus appears to play a major role. This network seems to be more activated by VT than MT, which could be due in particular to the absence of a motor task. These results provide physiological data that could serve as a rationale for conducting clinical trials of activation patterns and efficacy in acute stage stroke patients.

Abbreviations

MT	mirror therapy
VT	video therapy
M1	primary motor cortex
PMC	premotor cortex
PC	precuneus
HbO ₂	oxyhemoglobin
HbR	deoxyhemoglobin
fNIRS	functional near infrared spectroscopy
ROI	region of interest
DPF	differential path length factor
FDR	false discovery rate
AO	action observation

Acknowledgements

We thank Johanna Robertson, PT, PhD, medical writer and translator for language assistance. We also thank Céline Gay, Mathieu Bruneau and Amandine Mathou for technical assistance.

Author contributions

J.B. and P.A. conceived the study design. J.B. carried out the experiment and conducted analysis of fNIRS data. J.B. drafted the manuscript with inputs from all other authors. P.A., F.P. and C.O. contributed to the critical revision of the manuscript. All authors read and approved the final manuscript.

Funding

Not applicable.

Data availability

The data that support the findings of this study are available from the corresponding author on reasonable request.

Declarations

Ethics approval and consent to participate

This study was approved by the Institutional Review Board CPP NORD-OUEST I on 21st January 2021 (no. 2020-A02936-33). Full written consent was obtained from all participants in accordance with the Declaration of Helsinki.

Consent for publication

Not applicable.

Competing interests

The authors declare no competing interests.

Received: 28 November 2023 / Accepted: 10 May 2024

Published online: 14 May 2024

References

- Ramachandran VS, Rogers-Ramachandran D, Cobb S. Touching the phantom limb. *Nature*. 1995;377:489–90.
- Altschuler EL, Wisdom SB, Stone L, Foster C, Galasko D, Llewellyn DME, et al. Rehabilitation of hemiparesis after stroke with a mirror. *Lancet*. 1999;353:2035.
- Zeng W, Guo Y, Wu G, Liu X, Fang Q. Mirror therapy for motor function of the upper extremity in patients with stroke: a meta-analysis. *J Rehabil Med*. 2018;50:8–15.
- Thieme H, Morkisch N, Mehrholz J, Pohl M, Behrens J, Borgetto B et al. Mirror therapy for improving motor function after stroke. *Cochrane Database Syst Rev* [Internet]. 2018 [cited 2021 Apr 30];2018. <https://www.ncbi.nlm.nih.gov/pmc/articles/PMC6513639/>.
- Colomer C, Noé E, Llorens R. Mirror therapy in chronic stroke survivors with severely impaired upper limb function: a randomized controlled trial. *Eur J Phys Rehabil Med*. 2016;52:8.
- Arya KN, Pandian S, Vikas null, Puri V. Mirror Illusion for Sensori-Motor Training in Stroke: a Randomized Controlled Trial. *J Stroke Cerebrovasc Dis*. 2018;27:3236–46.
- Darbois N, Guillaud A, Pinsault N. Do Robotics and Virtual Reality Add Real Progress to Mirror Therapy Rehabilitation? A Scoping Review. *Rehabil Res Pract* [Internet]. 2018 [cited 2021 Apr 30];2018. <https://www.ncbi.nlm.nih.gov/pmc/articles/PMC6120256/>.
- Giroux P, Sirigu A. Illusory movements of the paralyzed limb restore motor cortex activity. *NeuroImage*. 2003;20(Suppl 1):S107–111.
- Li Y, Wu C, Hsieh Y, Lin K, Yao G, Chen C, et al. The Priming effects of Mirror Visual feedback on bilateral Task Practice: a randomized controlled study. *Occup Therapy Int*. 2019;2019:e3180306.
- Chang C-S, Lo Y-Y, Chen C-L, Lee H-M, Chiang W-C, Li P-C. Alternative Motor Task-Based Pattern Training With a Digital Mirror Therapy System Enhances Sensorimotor Signal Rhythms Post-stroke. *Front Neurol* [Internet]. 2019 [cited 2021 Jun 12];10. <https://www.frontiersin.org/articles/https://doi.org/10.3389/fneur.2019.01227/full>.
- Hoermann S, dos Santos LF, Morkisch N, Jettkowski K, Sillis M, Devan H, et al. Computerised mirror therapy with augmented Reflection Technology for early stroke rehabilitation: clinical feasibility and integration as an adjunct therapy. *Disabil Rehabil*. 2017;39:1503–14.
- Inagaki Y, Seki K, Makino H, Matsuo Y, Miyamoto T, Ikoma K. Exploring Hemodynamic Responses Using Mirror Visual Feedback With Electromyogram-Triggered Stimulation and Functional Near-Infrared Spectroscopy. *Front Hum Neurosci* [Internet]. 2019 [cited 2021 May 28];13. <https://www.ncbi.nlm.nih.gov/pmc/articles/PMC6399579/>.
- Bai Z, Fong KNK, Zhang J, Hu Z. Cortical mapping of mirror visual feedback training for unilateral upper extremity: a functional near-infrared spectroscopy study. *Brain Behav*. 2020;10:e01489.
- Saleh S, Adamovich SV, Tunik E. Mirrored feedback in chronic stroke: recruitment and effective connectivity of ipsilesional sensorimotor networks. *Neurorehabil Neural Repair*. 2014;28:344–54.
- Cheng C-H, Lin S-H, Wu C-Y, Liao Y-H, Chang K-C, Hsieh Y-W. Mirror Illusion modulates M1 activities and functional connectivity patterns of perceptual-attention circuits during Bimanual movements: a Magnetoencephalography Study. *Front Neurosci*. 2019;13:1363.
- Mehnert J, Brunetti M, Steinbrink J, Niedeggen M, Dohle C. Effect of a mirror-like illusion on activation in the precuneus assessed with functional near-infrared spectroscopy. *J Biomed Opt*. 2013;18:066001.
- Michielsen ME, Smits M, Ribbers GM, Stam HJ, van der Geest JN, Bussmann JBJ, et al. The neuronal correlates of mirror therapy: an fMRI study on mirror induced visual illusions in patients with stroke. *J Neurol Neurosurg Psychiatry*. 2011;82:393–8.
- Dohle C, Stephan KM, Valvoda JT, Hosseiny O, Tellmann L, Kühlen T, et al. Representation of virtual arm movements in precuneus. *Exp Brain Res*. 2011;208:543–55.
- Brunetti M, Morkisch N, Fritzsche C, Mehnert J, Steinbrink J, Niedeggen M, et al. Potential determinants of efficacy of mirror therapy in stroke patients—A pilot study. *Restor Neurol Neurosci*. 2015;33:421–34.
- Cavanna AE, Trimble MR. The precuneus: a review of its functional anatomy and behavioural correlates. *Brain*. 2006;129:564–83.
- Wang J, Fritzsche C, Bernarding J, Holtze S, Mauritz K-H, Brunetti M, et al. A comparison of neural mechanisms in mirror therapy and movement observation therapy. *J Rehabil Med*. 2013;45:410–3.
- Oldfield RC. The assessment and analysis of handedness: the Edinburgh inventory. *Neuropsychologia*. 1971;9:97–113.
- Leff DR, Orihuela-Espina F, Elwell CE, Athanasiou T, Delpy DT, Darzi AW, et al. Assessment of the cerebral cortex during motor task behaviours in adults: a systematic review of functional near infrared spectroscopy (fNIRS) studies. *NeuroImage*. 2011;54:2922–36.
- Bae SJ, Jang SH, Seo JP, Chang PH. The Optimal Speed for Cortical Activation of Passive Wrist Movements Performed by a Rehabilitation Robot: A Functional NIRS Study. *Front Hum Neurosci* [Internet]. 2017 [cited 2021 May 3];11. <https://www.ncbi.nlm.nih.gov/pmc/articles/PMC5398011/>.
- Lancaster JL, Woldorff MG, Parsons LM, Liotti M, Freitas CS, Rainey L, et al. Automated Talairach atlas labels for functional brain mapping. *Hum Brain Mapp*. 2000;10:120–31.
- Ye JC, Tak S, Jang KE, Jung J, Jang J. NIRS-SPM: statistical parametric mapping for near-infrared spectroscopy. *NeuroImage*. 2009;44:428–47.
- Hoshi Y. Hemodynamic signals in fNIRS. *Prog Brain Res*. 2016;225:153–79.
- Strangman G, Culver JP, Thompson JH, Boas DA. A quantitative comparison of simultaneous BOLD fMRI and NIRS recordings during functional brain activation. *NeuroImage*. 2002;17:719–31.
- Huppert TJ, Diamond SG, Franceschini MA, Boas DA. HomER: a review of time-series analysis methods for near-infrared spectroscopy of the brain. *Appl Opt*. 2009;48:D280–298.
- Kocsis L, Herman P, Eke A. The modified Beer-Lambert law revisited. *Phys Med Biol*. 2006;51:N91–98.
- Scholkmann F, Spichtig S, Muehlemann T, Wolf M. How to detect and reduce movement artifacts in near-infrared imaging using moving standard deviation and spline interpolation. *Physiol Meas*. 2010;31:649–62.
- Benjamini Y, Hochberg Y. Controlling the false Discovery rate: a practical and powerful Approach to multiple testing. *J Roy Stat Soc: Ser B (Methodol)*. 1995;57:289–300.
- Zama T, Shimada S. Simultaneous measurement of electroencephalography and near-infrared spectroscopy during voluntary motor preparation. *Sci Rep*. 2015;5:16438.
- Wang J, Fritzsche C, Bernarding J, Krause T, Mauritz K-H, Brunetti M, et al. Cerebral activation evoked by the mirror illusion of the hand in stroke patients compared to normal subjects. *NeuroRehabilitation*. 2013;33:593–603.
- Fattori P, Breveglieri R, Marzocchi N, Filippini D, Bosco A, Galletti C. Hand Orientation during Reach-to-grasp movements modulates neuronal activity in the medial posterior parietal area V6A. *J Neurosci*. 2009;29:1928–36.
- Rossiter HE, Borrelli MR, Borchert RJ, Bradbury D, Ward NS. Cortical mechanisms of Mirror Therapy after Stroke. *Neurorehabil Neural Repair*. 2015;29:444–52.
- Simon O, Mangin JF, Cohen L, Le Bihan D, Dehaene S. Topographical layout of hand, eye, calculation, and language-related areas in the human parietal lobe. *Neuron*. 2002;33:475–87.
- Molenberghs P, Cunnington R, Mattingley JB. Brain regions with mirror properties: a meta-analysis of 125 human fMRI studies. *Neurosci Biobehavioral Reviews*. 2012;36:341–9.
- Jitsuishi T, Yamaguchi A. Characteristic cortico-cortical connection profile of human precuneus revealed by probabilistic tractography. *Sci Rep*. 2023;13:1936.
- Bonnal J, Ozsancak C, Monnet F, Valery A, Prieur F, Auzou P. Neural Substrates for Hand and Shoulder Movement in Healthy Adults: A Functional near Infrared Spectroscopy Study. *Brain Topogr* [Internet]. 2023 [cited 2023 May 22]; <https://doi.org/10.1007/s10548-023-00972-x>.
- Gueugneau N, Bove M, Ballay Y, Papaxanthis C. Interhemispheric inhibition is dynamically regulated during action observation. *Cortex*. 2016;78:138–49.
- Bisio A, Biggio M, Avanzino L, Ruggeri P, Bove M. Kinaesthetic illusion shapes the cortical plasticity evoked by action observation. *J Physiol*. 2019;597:3233–45.
- Grefkes C, Eickhoff SB, Nowak DA, Dafotakis M, Fink GR. Dynamic intra- and interhemispheric interactions during unilateral and bilateral hand movements assessed with fMRI and DCM. *NeuroImage*. 2008;41:1382–94.
- Murase N, Duque J, Mazzocchio R, Cohen LG. Influence of interhemispheric interactions on motor function in chronic stroke. *Ann Neurol*. 2004;55:400–9.
- Carter AR, Astafiev SV, Lang CE, Connor LT, Rengachary J, Strube MJ, et al. Resting interhemispheric functional magnetic resonance imaging connectivity predicts performance after stroke. *Ann Neurol*. 2010;67:365–75.
- Bartur G, Pratt H, Dickstein R, Frenkel-Toledo S, Geva A, Soroker N. Electrophysiological manifestations of mirror visual feedback during manual movement. *Brain Res*. 2015;1606:113–24.
- Liepert J, Dettmers C, Terborg C, Weiller C. Inhibition of ipsilateral motor cortex during phasic generation of low force. *Clin Neurophysiol*. 2001;112:114–21.

48. Belyk M, Banks R, Tendera A, Chen R, Beal DS. Paradoxical facilitation alongside interhemispheric inhibition. *Exp Brain Res*. 2021;239:3303–13.
49. Rizzolatti G, Craighero L. The Mirror-Neuron System. *Annu Rev Neurosci*. 2004;27:169–92.
50. Hardwick RM, Caspers S, Eickhoff SB, Swinnen SP. Neural correlates of action: comparing meta-analyses of imagery, observation, and execution. *Neurosci Biobehav Rev*. 2018;94:31–44.
51. Ge S, Liu H, Lin P, Gao J, Xiao C, Li Z. Neural Basis of Action Observation and understanding from First- and third-person perspectives: an fMRI study. *Front Behav Neurosci*. 2018;12:283.
52. Hamzei F, Dettmers C, Rijntjes M, Glauche V, Kiebel S, Weber B, et al. Visuo-motor control within a distributed parieto-frontal network. *Exp Brain Res*. 2002;146:273–81.
53. Bönstrup M, Schulz R, Schön G, Cheng B, Feldheim J, Thomalla G, et al. Parietofrontal network upregulation after motor stroke. *Neuroimage Clin*. 2018;18:720–9.
54. Hamzei F, Erath G, Kücking U, Weiller C, Rijntjes M. Anatomy of brain lesions after stroke predicts effectiveness of mirror therapy. *Eur J Neurosci*. 2020;52:3628–41.
55. Bello UM, Chan CCH, Winser SJ. Task Complexity and Image Clarity Facilitate Motor and Visuo-Motor activities in Mirror Therapy in Post-stroke patients. *Front Neurol*. 2021;12:722846.
56. Solodkin A, Hlustik P, Noll DC, Small SL. Lateralization of motor circuits and handedness during finger movements. *Eur J Neurol*. 2001;8:425–34.
57. Yuan X, Li Q, Gao Y, Liu H, Fan Z, Bu L. Age-related changes in brain functional networks under multisensory-guided hand movements assessed by the functional near – infrared spectroscopy. *Neurosci Lett*. 2022;781:136679.
58. Bello UM, Kranz GS, Winser SJ, Chan CCH. Neural Processes Underlying Mirror-Induced Visual Illusion: An Activation Likelihood Estimation Meta-Analysis. *Front Hum Neurosci [Internet]*. 2020 [cited 2021 May 12];14. <https://www.ncbi.nlm.nih.gov/pmc/articles/PMC7412952/>.

Publisher's Note

Springer Nature remains neutral with regard to jurisdictional claims in published maps and institutional affiliations.



RESEARCH

Open Access



Distinct and additive effects of visual and vibratory feedback for motor rehabilitation: an EEG study in healthy subjects

Adham Ahmed^{1,2,4*}, Bessagnet Hugo^{1,3}, Struber Lucas⁴, Rimaud Diana¹, Ojardias Etienne^{1,2} and Giroux Pascal^{1,2}

Abstract

Introduction The use of visual and proprioceptive feedback is a key property of motor rehabilitation techniques. This feedback can be used alone, for example, for vision in mirror or video therapy, for proprioception in focal tendon vibration therapy, or in combination, for example, in robot-assisted training. This Electroencephalographic (EEG) study in healthy subjects explored the distinct neurophysiological impact of adding visual (video therapy), proprioceptive (focal tendinous vibration), or combined feedback (video therapy and focal tendinous vibration) to a motor imagery task.

Methods Sixteen healthy volunteers performed 20 mental imagery (MI) tasks involving right wrist extension and flexion under four conditions: MI alone (IA), MI + video feedback observation (IO), MI + vibratory feedback (IV), and MI + observation + vibratory feedback (IOV). Brain activity was monitored with EEG, and time-frequency neurophysiological markers of movement were computed. The emotions of the patients were also measured during the task.

Results In the alpha band, we observed bilateral ERD in the visual feedback conditions (IO, IOV). In the beta band, the ERD was bilateral in the IA, IV and IOV but more lateralized in the IV and IOV. After movement, we observed strong ERS in the IO and IOV but not in the IA or IV. Embodiment was stronger in conditions with vibratory feedback (IOV > IV > IA and IO)

Conclusion Conditions with visual feedback (IO, IOV) recruit the mirror neurons system (alpha ERD) and provide more accurate feedback of the task than IA and IV, which triggers motor validation pathways (beta rebound analysis). Vibratory feedback enhances the recruitment of the left sensorimotor areas, with a synergistic effect in the IOV (beta ERD analysis), thus maximizing embodiment. Visual and vibratory feedback recruits the sensorimotor cortex during motor imagery in different ways and can be combined to maximize the benefits of both techniques

Trial registration <https://clinicaltrials.gov/study/NCT04449328>.

Keywords Motor imagery, Video therapy, Focal vibration therapy, EEG, Rehabilitation

*Correspondence:
Adham Ahmed
ahmed.adham@chu-st-etienne.fr

Full list of author information is available at the end of the article



© The Author(s) 2024. **Open Access** This article is licensed under a Creative Commons Attribution-NonCommercial-NoDerivatives 4.0 International License, which permits any non-commercial use, sharing, distribution and reproduction in any medium or format, as long as you give appropriate credit to the original author(s) and the source, provide a link to the Creative Commons licence, and indicate if you modified the licensed material. You do not have permission under this licence to share adapted material derived from this article or parts of it. The images or other third party material in this article are included in the article's Creative Commons licence, unless indicated otherwise in a credit line to the material. If material is not included in the article's Creative Commons licence and your intended use is not permitted by statutory regulation or exceeds the permitted use, you will need to obtain permission directly from the copyright holder. To view a copy of this licence, visit <http://creativecommons.org/licenses/by-nc-nd/4.0/>.

Introduction

Mental imagery (MI) is defined as the voluntary activation of a mental representation of a movement without the movement actually being performed [1]. It can be kinesthetic (the subject feels that he or she is performing a movement) or visual (the subject visualizes himself/herself in the first or third person performing a movement) [2]. For healthy subjects, MI allows the subjects to stimulate and maintain the cortical networks involved in motor function, particularly the motor, premotor, prefrontal and parietal regions [3]. MI has also been shown effective in addition to conventional rehabilitation in poststroke rehabilitation, with improvements in motor function of the upper limb, walking speed and functional independence [4, 5]. From a neurophysiological perspective, MI increases functional connectivity between motor and premotor regions [6], corticospinal excitability [7] and induces structural connectivity reorganization [8].

Current rehabilitation techniques propose enriching MI with various feedback, notably visual (visual feedback therapies: mirror therapy, virtual reality therapy) and kinesthetic feedback (i.e., tendinous vibration therapies), to facilitate motor imagery and to provide proprioceptive and/or visual feedback on a correctly performed action.

Visual feedback therapies (VfT) are diverse. Historically, mirror therapy (MT) was the first rehabilitation technique to offer patients subjective visual feedback of correct movement performed by a paretic limb [9, 10]. However, during the last decade, video observational therapy (VOT) has emerged as an alternative to mirror therapy. In this therapy, the subject observes on a screen a projection of the paretic limb performing the action. This projection is made using a prerecorded video of the healthy limb performing the action flipped on the horizontal axis (mirror image) and displayed on a screen (Fig. 1). The VOT provides the subject with the subjective visual illusion of a correctly performed movement



Fig. 1 Video observational feedback therapy (IVS-3TM - Dessintey)

without requiring the use of a healthy limb. The benefits of VfT have been widely demonstrated not only in motor rehabilitation for central nervous system impairments, such as stroke [11, 12], but also in peripheral nervous system rehabilitation, such as brachial plexus palsy [13].

Vibratory feedback therapy consists of exciting muscle spindles by means of vibratory stimulation. These vibrations can be applied to the whole body or in a focal manner (focal vibration, FV). Vibratory stimulation devices are generally applied to tendons or related muscles (e.g., *biceps brachialis* and *extensor radialis longus carpi*). In stroke rehabilitation but also in other neurological disease rehabilitation (i.e., multiple sclerosis, cerebral palsy), FV has shown benefits for balance, motor function and spasticity [14, 15].

Visual and proprioceptive feedback, whether provided by video therapy devices, focal vibration, or other devices, is at the heart of modern rehabilitation techniques (i.e., robotic therapy seeks to provide somato-sensory feedback to the subject, along with a visual feedback of the moving arm). We know that visual feedback induces a rebalance of interhemispheric inhibition in healthy subjects [16] and stroke patients [17]. Similarly, we know that FV facilitates the recruitment of the sensory-motor regions of the subject [18, 19], with an improvement in the efficiency of the sensorimotor network [20]. However, the way each of these feedbacks might act precisely on the sensorimotor cortex remains imperfectly understood. Additionally, the synergy between visual and proprioceptive feedback remains to be explored. The addition of a vibration device to mirror therapy or virtual reality promotes the illusion of subjectivity of movements [21] as well as the perceived motor illusion of the subjects [22]. In electroencephalography (EEG), Le Franc et al. reported increased recruitment in sensory-motor regions under combined FV and VOT conditions compared to imaging conditions alone [23]. Interestingly, proprioceptive afferences alone [24] but also coupled to visual feedback [25] also enhance classification performances in motor imagery tasks in Brain Computer Interfaces training.

However, despite those results, a major challenge remains in to create a standardized and easily reproducible neurophysiological experiment in healthy subjects, that can be later extended to stroke patients, to specifically explore the integration of each type of feedback with the aim to personalize the rehabilitation therapy [26]. The aim of the study is to get a better understanding of the integration of visual, somato-sensory, and coupled feedback, along with a point of comparison for subsequent data for stroke patients.

To build this model, we recorded the EEG activity of healthy subjects performing motor imagery tasks of the right wrist under experimental conditions with visual, proprioceptive, or double feedback. For visual feedback,

we chose the VOT since it enabled us to study the specific effect of visual feedback without being disturbed by the cortical activities inherent to the production of the movement of the other limb in the MT. For proprioceptive feedback, the FV allowed us to study the specific effects of proprioceptive feedback. Four experimental conditions were tested: [1] imagery alone—IA; [2] imagery with visual feedback observation—IO; [3] imagery with vibratory feedback—IV; and [4] imagery with visual and vibratory feedback—IOV; with the study of EEG alpha and beta desynchronization during the task and beta rebound after the task.

Materials and methods

Participants

We recruited right-handed healthy volunteers. We excluded subjects who presented with neurological, epileptic, or psychiatric illness and subjects who were receiving neuromodulatory treatments or neuromodulatory drugs. Participants signed a consent form prior to participating in the study. Participants underwent the Edinburgh Handedness Inventory test of laterality, and we also tested their visual imagery performance with the Movement Imagery Questionnaire-Revised (MIQ-RS) questionnaire [27].

The inclusions were conducted between January and April 2023. The STROBE guidelines were used to report our study. The study was registered at NCT (NCT04449328). The study was conducted in accordance with the Declaration of Helsinki and was approved by the ethics committee. Comité de protection des personnes Sud Ouest et Outre Mer IV" (04/12/2019. N°: CPP2019-11-084a / 2019-A01673-54 / 19.09.12.44858 with amendment N°: 19.01592.201984-MS03 allowing EEG data collection for healthy subjects).

Material

Visual feedback was provided using a VOT device (IVS-3™-Dessintey™). It consists of a large screen precisely placed between the subject's eye and his trained hand. The device is equipped with a camera behind its screen that records a hand movement as if it were in first-person view. When a recorded video is displayed on the screen, it results in the illusion of subjective movement. Medical foam was placed under the wrist to sur-elevate the hand and make movements more comfortable. This device can easily provide congruent feedback with the visual axis, thus maximizing the subjective illusion (Fig. 2A).

Vibratory feedback was provided using the Vibrasens device (VB 115, Techno Concept™). The Vibrasens is composed of a generator with adjustable vibration frequency, as well as a vibrator with an interchangeable tip, which can be placed on the wrist of the subjects (Fig. 2A). The device was placed on the tendon of the *extensor radialis longus carpi*, with the adapted tip.

EEG data were recorded with a 32-channel ENO-BIO™ device placed on the head of the subjects with Ag/AgCl electrodes. The data were sampled at 500 Hz, and the impedance was maintained below 5 kΩ. The protocol displayed on the IVS panel was designed with OpenSesame software [28]. An OpenSesame Time To Live (TTL) trigger was sent on the EEG recording at the beginning of each experimental condition for accurate synchronization of the visual cues in further analysis.

Experimental device

During the experiment, the subjects were comfortably installed in a standardized position on a chair in front of a height-adjustable table on which they trained on VOT.

Before the beginning of the session and during the entire duration of the experiment, the subject's right hand was positioned behind the screen of the VOT device. Then, the vibration device was applied to the subject's right *extensor radialis longus carpi* tendon. For each

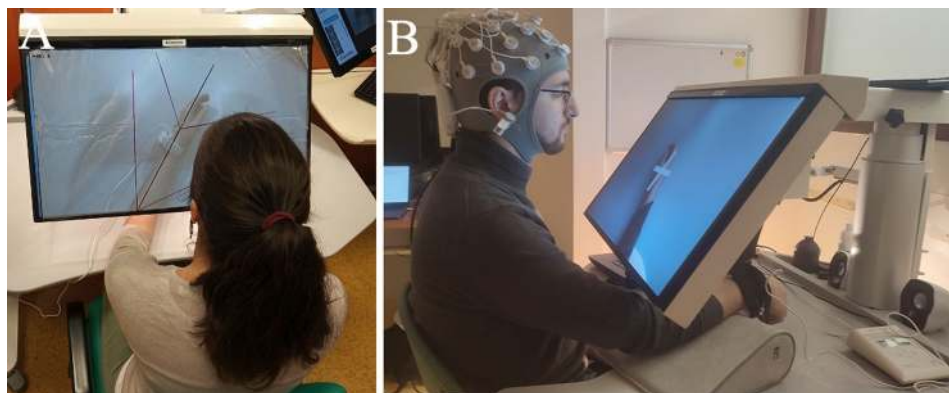


Fig. 2 (A) Standardization of movement amplitude with a transparent layer. (B) Experimental setup, with a video-feedback therapy device, an EEG device and a vibratory feedback device

subject, we searched the vibration frequency that maximized the subject’s self-declared kinesthetic illusion in a 70 to 100 Hz vibratory range [29]. The vibration amplitude was set to 1 mm [18]. We then recorded the following with VOT device:

1. A video of the subject’s hand performing a wrist extension and returning to a neutral position. The video was then manually extracted from the VOT device, shortened, and resampled for the whole movement to last exactly three seconds, with two seconds of pause before and after. The movement displayed and performed by the subjects consisted of a slow extension of the wrist and fingers (two seconds) immediately followed by quick flexion (one second). At rest, the wrist was in a neutral position on the axis of the arm and was completely relaxed. The amplitude of the movement and position of the hand on the screen were standardized due to the use of a transparent layer with angle markers placed on the screen during the recording of the video and removed afterward (Fig. 2B). The timing of the movement was as follows: two seconds of presentation of the arm with a white cross, 3 s of task (2 s of hand opening and one second of return to rest), and then 2 s of rest with the return of the cross, added to a randomized time of 500 to 1000 milliseconds. This video was used for the imagery + observation (IO) and imagery + observation + vibration conditions (IOV).

2. In the six-second video of the panel of the VOT device, we added the same cross as in the first video. This video was used for the imagery alone (IA) and imagery + vibration conditions (IV). We deliberately did not show a video of the subject’s immobile hand to prevent incongruent feedback interference (feeling of a hand movement while watching an immobile hand).

Each session was divided into four subsessions, separated by a one-minute pause, and proposed in a randomized order to each subject. In each subsession, the subject performed a motor imagery task of right wrist dorsiflexion twenty times and returned to rest (Fig. 3). The subsessions differed in the type of feedback offered in addition to the motor imagery task. In the IA subsession, the subject had to imagine only the MI task without visual or vibratory feedback. In the IO subsession, the subject performed the MI task while observing the movement performed on the VOT device. In the IV task, the subject had to perform MI with congruent vibratory feedback during wrist extension but without visual feedback. The vibratory feedback was manually synchronized with the action by the same operator in all the studies. In the IOV subsession, the subject had to perform MI, with vibratory feedback and visual feedback.

After each group of 20 movements for each condition, a one-minute break was observed. During this time, the subjects were asked to rate the intensity of their subjective imagery perception on a Likert scale ranging from 1 to 10. They were also asked to mimic the angle of









Duration:	2 seconds	2 seconds	1 second	2 seconds
Task:	Rest	Motor imagery of wrist extension	Motor imagery of wrist coming back to position	Rest
Visual feedback in: IA, IV				
Visual feedback in: IV, IOV				
Vibratory feedback in: IV, IOV	No	Yes	Yes	No
Vibratory feedback in: IA, IO	No (The vibratory device remains on the subject's hand but is not working)			

Fig. 3 Experimental paradigm for the imagery alone (IA), imagery + observation (IO), imagery + vibration (IV), and imagery + observation + vibration (IOV) conditions

movement felt with their right hand. The angle was measured with an electronic goniometer.

Data analysis

EEG

After filtering (0.5–70 Hz bandpass filter, 50 Hz notch filter), the data were segmented into 7-second epochs (2 s before the onset of movement and 2 s after the end of movement). The epochs containing a peak-to-peak voltage above 100 mV were considered too noisy and rejected. Then, a visual inspection of the data was conducted with rejection of the remaining noisy epochs, and bad channels were interpolated. Approximately 80% of the data in our study were considered valid. Ocular artifacts were removed with independent component analysis (ICA). This whole process was conducted using the MATLAB EEGLab Toolbox (UC San Diego, USA) [30]. The data were referenced to infinite sources using the REST algorithm [31]. After this preprocessing, for each epoch and each EEG channel, time-frequency maps were generated. We implemented time-frequency analysis by convolving the signal with a set of complex Morlet wavelets, defined as complex sine waves tapered by a Gaussian distribution. The frequencies of the wavelets ranged from 2 Hz to 40 Hz in 80 linearly spaced steps. The full width at half maximum (FWHM) ranged from 1000 to 200 ms [32, 33]. To avoid border effect artifacts during wavelet analysis, we removed 500 ms on each side of the epochs after wavelet convolution.

For each electrode, event-related desynchronization (ERD) and event-related synchronization (ERS) magnitudes were then expressed as percentages of the power in the defined time and frequency window relative to the power measured during the corresponding baseline [34] and were expressed as percent changes. The baseline was chosen between 1500 ms and 500 ms before the onset of the movement. We analyzed [1] alpha band power (8–12 Hz) during the task (2500–4500 ms) to obtain the alpha component of the mu motor rhythm, [2] beta band power (12–25 Hz) during the task (2500–4500 ms) to obtain the beta component of the mu motor rhythm, and [3] beta band power after the task (5000–6000 ms) to obtain the postmovement beta rebound power. The average of all the time-frequency maps for each condition and electrode was computed.

Statistical comparison

EEG data

For statistical analysis, we evaluated the modulations of alpha, beta ERD and beta ERS intensity values for each motor imagery task in two regions of interest, the C3 and C4 electrodes, which represent the activity over the left and right sensory-motor cortex, respectively. This allowed us to explore the effects of the different types of

feedback. Statistical analysis over time-frequency regions of interest was conducted using a Friedman test to assess whether the means of illusion intensities differed significantly across the feedback conditions due to nonnormality of the data. Subsequently, to determine which pairs of conditions exhibited significant differences, post hoc tests were performed with a Wilcoxon signed-rank test with a significance threshold of $p < 0.05$.

To improve statistical relevancy, we also performed time-frequency mapping on C3, C4, CP5, CP6, and occipital region electrodes (mean of Oz, O1 and O2 maps) using permutation testing with 10,000 permutations under the null hypothesis, with a significance threshold of $p < 0.05$ for each test, followed by cluster-based correction to identify contiguous regions exhibiting significant differences [35]. The results of this permutation test, along with the time-frequency maps, are shown in the Supplementary Materials.

Kinesthetic illusion data

For kinesthetic illusion comparison between conditions, the statistical analysis was conducted at first with a Friedman test, to assess whether the means of illusion intensities declared by the subjects significantly differed across the four feedback conditions. If the Friedman test was positive ($p < 0.05$), a Wilcoxon signed-rank post hoc tests was performed to determine which pairs of conditions exhibited significant differences, with a significance threshold of $p < 0.05$ for each pairwise comparison.

Results

Participants

Sixteen healthy volunteers (age: 47.1 years \pm 14.9, with 9 females and 7 males) were recruited for the study from the University of Saint-Etienne. Fifteen subjects were right-handed, and 1 subject was left-handed.

Time-frequency analysis during motor imagery

Alpha band desynchronization

In the alpha band, the time course analysis of the signal over the C3 electrode (Fig. 4A) revealed quick desynchronization in the IA condition (approximately one second) rather than maintained desynchronization during the other three conditions (IO, IV, IOV).

We found no clear desynchronization in the global map analysis under the IA condition. However, we highlighted bilateral desynchronization during IO conditions, centered over the C3 and C4 electrodes, which was completed with bilateral centro-parietal (CP5, CP6) desynchronization. During the IOV condition, we also observed bilateral desynchronization, which was much stronger than that in the other conditions and was mainly centered over the centro-parietal regions and frontal regions. Interestingly, we observed parieto-occipital

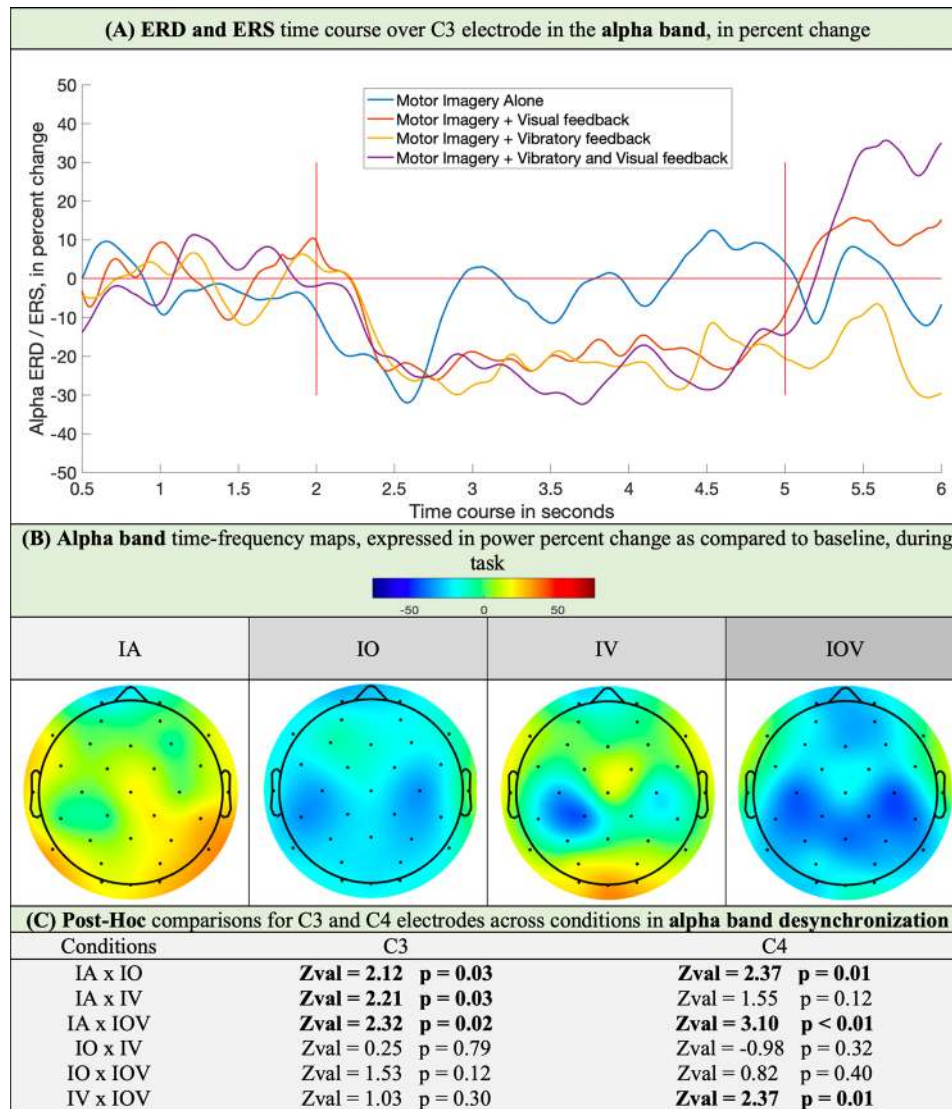


Fig. 4 (A) ERS and ERD time course over the C3 electrode in the alpha band expressed as percent change; the motor imagery task lasted between 2 and 5 s. (B) Time-frequency cortical maps in the alpha band during the motor imagery task with different feedbacks. (C) Statistical analysis of C3 and C4 electrodes between conditions (IA: Motor Imagery Alone, IO: Motor Imagery and Action Observation, IV: Motor Imagery and Focal Vibration, IOV: Motor Imagery and Action Observation and Focal Vibration). For statistical comparison, * indicates significant results

hypersynchrony in the conditions without visual feedback (IA, IV), which was absent in the conditions with visual feedback (IO, IOV) (Fig. 4B).

A statistical comparison of conditions with a Friedman test revealed a significant difference in desynchronization strength across conditions over C3 ($\chi^2(3)=5.4, p=0.021$) and C4 ($\chi^2(3)=8.76, p=0.032$). Post hoc analysis over C3 showed stronger desynchronization over the C3 electrode in the IO, IV and IOV conditions than in the IA condition. Other comparisons over C3 did not show differences between conditions. At the C4 electrode, there was greater desynchronization in the IO and IOV than in the IA and greater desynchronization in the IOV than in the IV (Fig. 4C).

The time-frequency maps of the central (C3, C4), occipital (mean of O1, Oz and O2) and central-parietal (CP5, CP6) regions and the results of the statistical analysis with permutation testing can be found in Tables 1, 2, 3, 4 and 5 of the Supplementary Material.

Beta band desynchronization

In the beta band, the time course analysis of the signal over the C3 electrode showed that in all conditions, desynchronization was maintained throughout the task (Fig. 5A).

In the IA condition, we found weak desynchronization over C3. In the IO condition, there was bilateral desynchronization centered over the C3 and C4 electrodes as

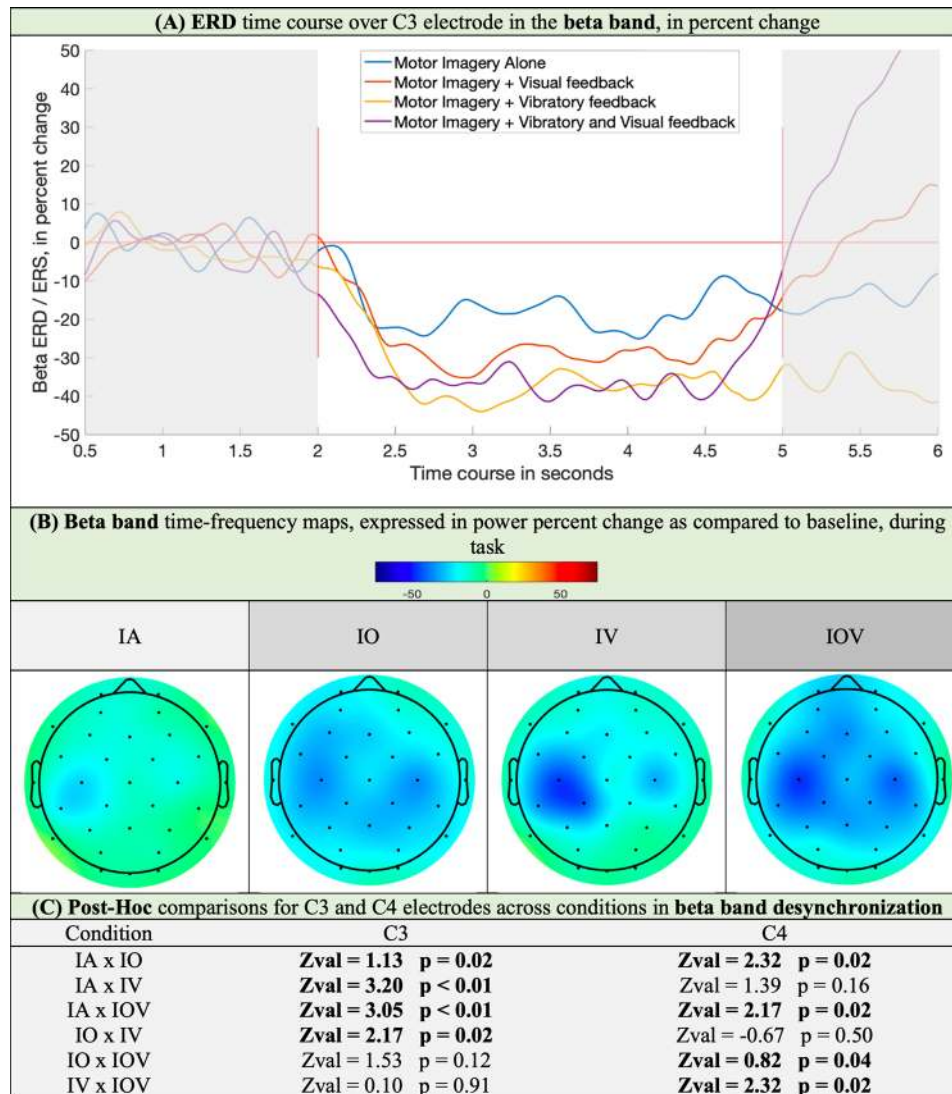


Fig. 5 (A) ERD time course (2 to 5 s) over the C3 electrode in the beta band expressed as percent change; the motor imagery task lasted between 2 and 5 s. (B) Time-frequency cortical maps in the beta band during the motor imagery (MI) task with different feedbacks. (C) Statistical analysis of C3 and C4 electrodes between conditions (IA: motor imagery alone, IO: motor imagery and action observation, IV: motor imagery and focal vibration, IOV: motor imagery and action observation and focal vibration)

well as the left prefrontal and bilateral parietal electrodes. In the IV condition, there was strong left centro-parietal desynchronization, which also involved left precentral electrodes, and weak desynchronization over the right central region (C4). In the IOV condition, the desynchronization was bilateral, much stronger than that in the other conditions, and was mainly centered in bilateral centro-parietal electrodes (CP5, CP6) and left prefrontal electrodes. There were no changes in the occipital electrodes (Fig. 5B).

Statistical comparison of conditions with a Friedman test revealed a significant difference in desynchronization strength across conditions over C3 ($\chi^2(3) = 13.96, p = 0.03$) and C4 ($\chi^2(3) = 10.36, p = 0.015$). Post hoc statistical analysis revealed a significant change in C3 in the

IO, IV, and IOV conditions compared to the IA condition. Desynchronization was also greater in the IV group than in the IO group. At the C4 electrode, desynchronization was greater in the IO and IOV than in the IA. Desynchronization was also greater in the IOV group than in the IV and IO groups (Fig. 5C).

The time-frequency maps of the central (C3, C4) and centro-parietal (CP5, CP6) regions and the results of the statistical analysis with permutation testing can be found in Tables 1, 2, 3, 4 of the Supplementary Material.

Time-frequency analysis after motor imagery

The beta band ERS time course over the C3 electrode can be seen in Fig. 5A between 5 and 6 s.

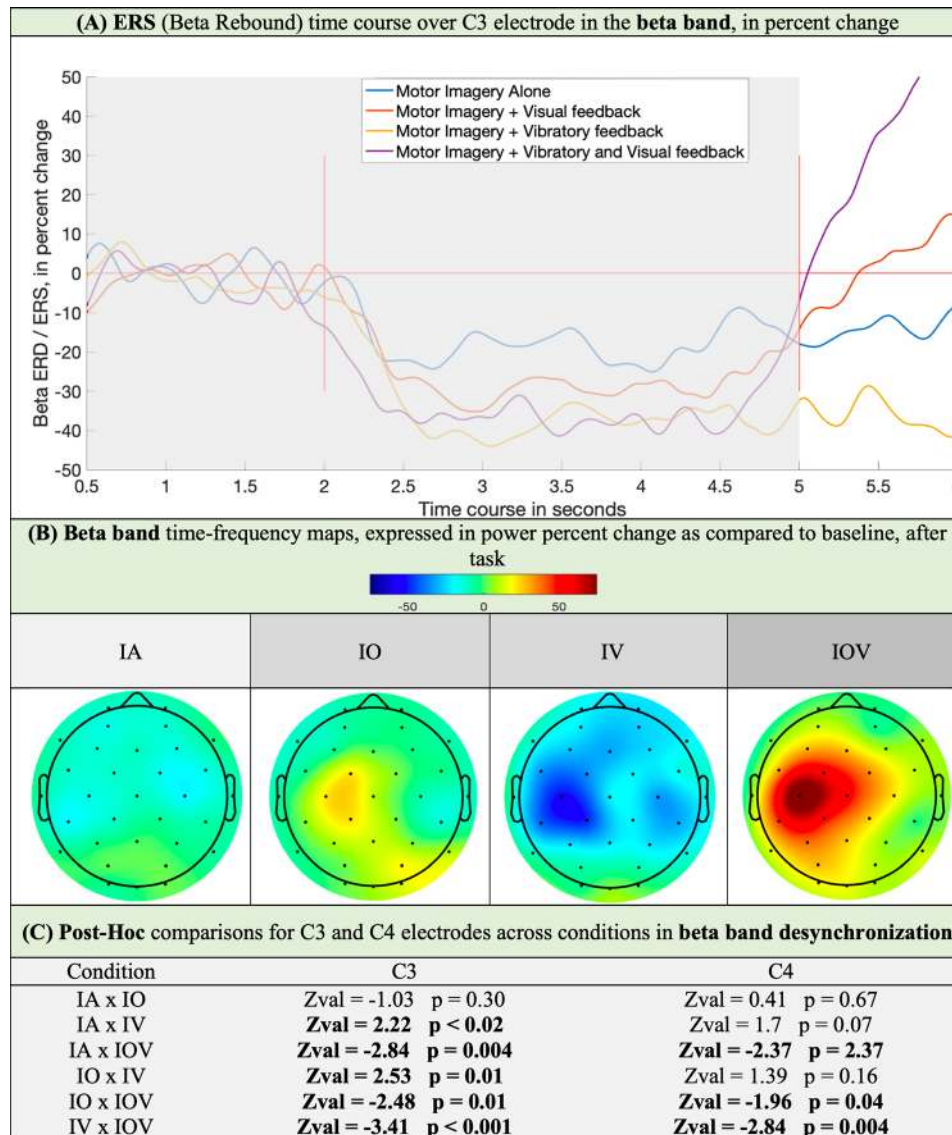


Fig. 6 (A) ERS time course (5 to 6 s) over the C3 electrode in the beta band expressed as percent change; duration of the motor imagery task ranged between 2 and 5 s. (B) Time-frequency cortical maps in the beta band after the motor imagery (MI) task with different feedbacks. (C) Statistical analysis of C3 and C4 electrodes between conditions (IA: motor imagery alone, IO: motor imagery and action observation, IV: motor imagery and focal vibration, IOV: motor imagery and action observation and focal vibration)

After the movement (Fig. 6A, B), there was no ERS (or beta rebound) in the IA condition. With visual feedback (IO, IOV), there was a rebound centered above the C3 electrode, which was stronger in the IOV than in the IO. Under IV conditions, we did not observe any rebound but rather prolonged desynchronization. Analysis of the power time course over C3 showed that in IV, this desynchronization lasts approximately 1 s after the end of the task and then returns to baseline with no rebound. Statistical comparison of conditions with a Friedman test revealed a significant difference in desynchronization strength across conditions over C3 ($\chi^2(3)=21.246, p<0.0001$) and C4 ($\chi^2(3)=11.72, p=0.008$). Post hoc statistical analysis of C3 (Fig. 6C) revealed significant

differences between all conditions except for the IA × IO comparison. At the C4 electrode, differences were found in the IOV compared to all other conditions.

Motor illusion assessment

Double feedback (IOV) maximized the embodiment in the task (Fig. 7A) and the perceived angle of movement (Fig. 7B). Vibratory feedback also provided a strong kinesthetic illusion (31°, 6/10 illusion intensity), whereas visual feedback alone and motor imagery alone provided weaker embodiment in the task. A statistical comparison of conditions with a Friedman test revealed a significant difference in the perceived intensity of the illusion across the four sensory feedback conditions ($\chi^2(3)=21.41,$

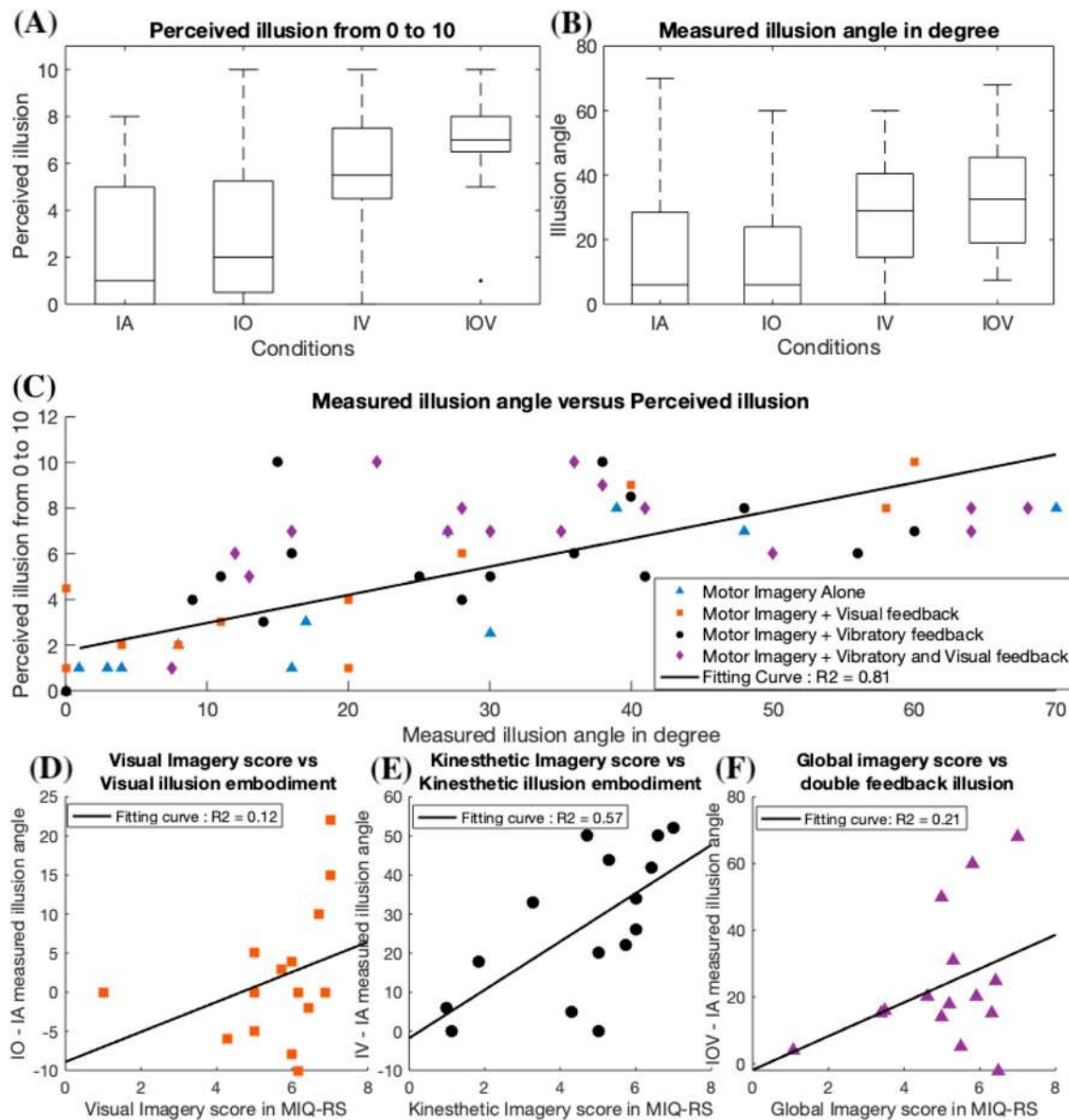


Fig. 7 (A) Mean perceived kinetic illusion amplitude on a Likert scale from 0 (no movement) to 10 (maximum illusion) with standard deviation (red line) in the different conditions. (B) Measured mimicked illusion angle after the task with standard deviation (red line) in the different conditions. (C) Measured illusion angle versus perceived illusion intensity for each condition. (D) Improvement in the illusion angle in the IO condition versus the IA condition (IO angle - IA angle) according to visual imagery performance. (E) Improvement in illusion angle in the IV condition versus the IA condition (IV angle - IA angle) according to kinesthetic imagery performance. (F) Improvement in the illusion angle in the IOV condition versus the IA condition (IOV angle - IA angle) according to global imagery performance (IA: imagery alone, IO: imagery and observation, IV: imagery and vibration, IOV: imagery and observation and vibration)

$p < 0.001$). Subsequent pairwise comparisons using the Wilcoxon signed-rank test indicated that participants perceived a significantly greater illusion intensity in IV compared with IA ($Z = -2.34, p = 0.006$), IOV compared with IA ($Z = -3.2, p = 0.001$), IV compared with IO ($Z = -2.27, p = 0.02$), IOV compared with IO ($Z = -3.04, p = 0.002$) and IOV compared with IV ($Z = -2.47, p = 0.01$). However, we found no significant difference in IO compared with IA ($Z = -1.98, p = 0.04$) (Fig. 7A, B).

We found a good correlation between the subjects' self-declared kinesthetic illusion intensity and the measured angle of their hand mimicking the movement ($R^2 = 0.81$) (Fig. 7C).

We found no significant correlation between the improvement in the illusion angle during IO and the MIQ-RS visual imagery score ($R^2 = 0.12$, Fig. 7D). We found a correlation between embodiment in vibratory therapy and kinesthetic imagery scores on the MIQ-RS

($R^2=0.57$, Fig. 7E). However, we found no significant difference between the improvement in the illusion angle in IOV and the MIQ-RS global imagery score ($R^2=0.21$, Fig. 7F). Compared with neurophysiological data, we did not find any correlation between desynchronization intensity and global motor imagery abilities on the MIQ-RS ($R^2=0.07$) or between desynchronization intensity and perceived motion angle ($R^2=0.009$).

Discussion

The main aim of this study was to highlight brain activation topographic differences among four different conditions of neurofeedback during motor imagery: no feedback, visual feedback, proprioceptive feedback, and combined feedback (visual and proprioceptive).

Visual feedback favors the recruitment of neurons to the visual cortex and mirror system

In the alpha band, we observed strong desynchronization in conditions with visual feedback (IO, IOV) above the bilateral central and parietal regions. In conditions without visual feedback (IA, IV), this desynchronization was much more lateralized in central regions contralateral to the imagined hand movement. In addition, we observed strong parieto-occipital hypersynchrony (increase in alpha activity) in conditions without visual feedback. In contrast, this hypersynchrony was not observed in conditions with visual feedback.

Concerning the modulations of alpha activity in the parieto-occipital regions, we know that these regions support the occipital alpha rhythm, which is well known to electrophysiologists. Indeed, alpha occipital is a brain rhythm. Its power increases when people's eyes are closed, and occipital alpha activity can be used as an index of the degree to which visual brain activity is subjected to inhibition [36]. Occipital alpha activity also reacts to retinotopic amplitude modulation during shifts in visual attention [37], and it is strongly associated with reductions in visual attention [38, 39]. It also acts as a clock on visuo-temporal processing [40]. In sEEG, the occipital alpha rhythm is localized over a large portion of the visual cortex, in the cuneus and calcarine cortex, to a lesser extent in the superior parietal lobule, and in the temporal regions [41]. It originates from the basal ganglia, more specifically in the pulvinar nucleus of the thalamus [42]. Thus, we can reasonably consider that the presence of strong occipital alpha activity in conditions without visual feedback (IA, IV) reflects a relative resting of the occipital cortex and, more specifically, visual areas compared to conditions with visual feedback (IO and IOV) that require visual attention.

The dynamics of alpha desynchronization above central regions correspond to different brain rhythms. Conditions with visual feedback (IO, IOV) are associated

with bilateral centro-parietal alpha desynchronization. Above the sensory-motor regions, alpha band desynchronization is generally associated with Mu desynchronization [43]. The Mu rhythm is a well-known EEG rhythm containing two independent components, one in the alpha band and one in the beta band, encoding different parameters related to motricity [44]. In the alpha band, although it supports a wide range of activities, Mu desynchronization is generally a good marker of the activity of the mirror neuron system (MNS) [45]. This activity is present not only during action observation, motor imagery, and motor execution but also in other more complex tasks recruiting mirror neurons, notably in social cognition [46]. Mu rhythms are generated around bilateral centro-parietal regions [47]. We thus assume that the bilateral alpha desynchronization (absent in IA) we observed corresponds to Mu desynchronization and is proof of the recruitment of the mirror neuron system specific to visual feedback conditions, whereas the lateralized alpha desynchronization in the IV condition is due to another mechanism that we will describe later. This bilateral recruitment has also been observed in other works in healthy subjects [48, 49] and stroke subjects [50]. This hypothesis of MNS recruitment is also supported by the recruitment of the visual cortex in both the IO and IOV conditions (no occipital alpha hypersynchrony), which is a prerequisite for MNS recruitment. This MNS recruitment during visual feedback therapies has already been documented for MT after stroke [1].

Visual feedback enhances motor validation mechanisms

After movement, we observed a stronger beta rebound over the C3 electrode in conditions with visual feedback than in the IA condition. Beta rebound corresponds to hypersynchrony in the beta band following movement [34, 51]. It originates in the motor cortex and can be measured throughout the precentral gyrus [52, 53]. Beta rebound was described as participating in the maintenance of an idling state in sensorimotor regions. However, its interpretation has been broadened: beta rebound is modulated by motor validation phenomena and temporal integration of somatosensory and motor parameters [54] and is related to post-movement motor validation mechanisms. For example, the observation of an erroneous movement modulates beta rebound [55], as can the introduction of errors in a motor task [56]. It is possible that this modulation of beta rebound emerges following the detection of a mismatch between the forward model and the sensory afferents, allowing an update of the motor pattern [57]. The very weak or absent rebound in the IA task may be related to the absence of sensory afference (visual or kinesthetic) to compare with the motor imagery forward model. In contrast, in the IO and IOV conditions, the visual feedback provided to the

subjects, with the precise parameters of the movement, allows this forward model versus sensory afferential comparison, leading to the emergence of a beta rebound. Interestingly, the double feedback condition, which also leads to the strongest embodiment, leads to stronger beta rebound.

Concerning beta rebounds, another point of interest is the absence of beta rebound in the IV condition and the pursuit of desynchronization for approximately 1 s before returning to baseline. Proprioceptive feedback has also been shown to modulate beta rebound, as abolition of proprioceptive feedback leads to a suppression of beta rebound [58]. The presence of beta rebound has been documented after tendinous focal vibration [59], but it is not clear whether, in this experimental paradigm, the subject was allowed to watch his arm during the illusion. In our study, this delay in desynchronization may have been caused by inertia when the vibration device was stopped. However, this hypothesis does not seem valid because the vibration is stopped at the end of the wrist extension phase (at 4 s). Moreover, in the IOV condition, the rebound appears at the end of the movement. Furthermore, even after the return to baseline, between 6 and 7 s, we observed no beta rebound in the IV condition. It is possible that long desynchronization is related to a remanent effect of vibration on sensorimotor regions due to the intensity of vibratory feedback and incongruent signals of neuromuscular bundles that cannot be evened by visual observation. Another hypothesis would be that vibratory feedback alone is insufficient to trigger beta rebound in the absence of visual feedback during motor imagery; indeed, vibration offers a single, continuous sensory afference modality on a single tendon, which is hardly congruent with the actual feeling of a subject who breaks down all the phases of a movement with his hand involving numerous muscles and different movements. One method of testing this hypothesis would be to evaluate beta rebound modulations in two tendon vibration situations: one where the subjects can see their vibrated hand and one where the hand is invisible. We believe that the rebound would be present but weak in the situation where the hand is visible, but this hypothesis remains to be demonstrated.

Vibratory feedback enhances sensorimotor cortex recruitment

When assessing the correlation between the EEG signal intensity of the IV and differences between the IA and IO conditions during the task, we found that there was strong and very lateralized left central (C3) and left centro-parietal (CP1, CP5) desynchronization in both the alpha and beta bands in the IV condition. Having no visual feedback in the IV condition and a different and very lateralized ERD topography, we cannot interpret this

desynchronization as the recruitment of the MNS system, as we observed in IO and IOV. Previous work also demonstrated that when combining MT to FV, stronger alpha desynchronization over C3 occurred under vibration conditions [21]. In fact, in the alpha band, this very lateralized desynchronization in IV during upper limb FV has also been observed in acute stroke patients with an enhancement of alpha ERD (but not beta) over the C3 electrode during right limb FV, suggesting a specific effect of vibration on contralateral S1–M1 excitability [60]. For healthy subjects, vibrotactile vibration is also significantly associated with vibration intensity in the alpha band [61]. For the IV condition, we thus hypothesize that the strong and lateralized desynchronization in the alpha band we observed could be due to specific recruitment of the contralateral sensorimotor cortex due to the right wrist FV.

In the beta band, IV desynchronization is also very lateralized. Beta ERD corresponds to disinhibition of somatomotor neuronal populations [44], with a correlation between motor response intensity and desynchronization strength in stroke patient populations [62]. Beta ERD is also correlated with M1 excitability [63]. For upper limb movements, beta ERD is classically mainly localized on the sensorimotor cortex opposite to the moving limb [64]. These data suggest that the beta band ERD observed in our study during IV conditions reflects strong, specific, and lateralized recruitment of the sensorimotor cortex and primary motor cortex induced by FV therapy. This strong C3 beta ERD is also present in the IOV condition (but more lateralized probably due to the addition of visual feedback effects), which is still consistent with this interpretation.

Kinesthetic feedback is a prerequisite for strong motor illusions in healthy subjects

When assessing motor illusion, it appears that subjects feel more embodiment (declared illusion and measured illusion angle) in conditions with vibratory feedback (IV, IOV) compared with conditions without vibratory feedback (IA, IO), with a good correlation between self-declared illusion and measured illusion angle, increasing the reliability of the data. We found a relatively good correlation ($R^2=0.58$) between the kinesthetic motor imagery score on the MIQ-RS and the measured illusion angle in the IV condition. However, we found no such correlation between the visual imagery score on the MIQ-RS and the measured illusion angle in the IO condition ($R^2=0.12$) or between the global imagery score on the MIQ-RS and the measured illusion angle in the double feedback condition ($R^2=0.21$).

The sense of limb position depends on a convergence of visual and proprioceptive cues [65], and both occipital and somatosensory cortexes are involved in the

constitution of feelings of body ownership and the sense of agency in relation to multisensory regions (fronto-parietal cortex), the precuneus and the insular cortex [66]. Our result may seem unexpected because we would have thought that subjects with stronger visual imagery scores would feel more embodiment in the visual feedback condition and that subjects with kinesthetic imagery scores would feel more embodiment in the vibratory feedback condition.

We explain this difference by the presence of a visual-proprioceptive mismatch in the visual feedback (IO) condition, which could diminish the embodiment of the subjects in the task. Indeed, in the IV condition, the subject's hand is masked; thus, he relies exclusively on proprioceptive feedback to build a sense of agency. This finding explains the good correlation between kinesthetic motor imagery performance and the measured illusion angle. In contrast, in the IO condition, the subject can see the hand's movement on the screen but also receives proprioceptive feedback from his or her nonmoving hand, thus creating a visuo-proprioceptive mismatch that reduces embodiment. Adding vibratory feedback to the IO condition (IOV) corrects this visuo-proprioceptive mismatch and thus provides maximal embodiment during therapy.

We did not find any significant correlation between global motor imagery performance on the MIQ-RS and illusion performance in the IOV condition. Furthermore, the addition of the two feedbacks in the IOV condition did not lead to the maximum illusion effect for all the subjects. This may be due to qualitative aspects of the feedback, which may not perfectly reproduce the imagined movement but possibly to the imaging task needed. Subjects may also have different strategies to interpret both proprioceptive and visual feedback. Some subjects reported that they were helped by the feedback, whereas others reported that they were disturbed by it during their motor imagery. Notably, these points remain to be explored through the study of incongruent proprioceptive feedback.

Building a global understanding model

Based on the literature and the results of this research, we propose a general theoretical model for the integration of visual and vibratory feedback in healthy subjects (Fig. 8).

In video feedback therapy, visual feedback is integrated into the occipital cortex and visual areas (no alpha hypersynchrony). This visual feedback of subjective movement recruits mirror neurons (bilateral alpha desynchronization), the involvement of which has been described in visual feedback therapies (MT, virtual reality therapy, etc.) [67–69]. This recruitment of mirror neurons by action observation is also accompanied by the recruitment of sensory-motor regions [67], with an increase in the excitability of the M1 cortex [70–72], connectivity changes [73], and a shift in the interhemispheric balance in healthy subjects and patients in MT [16, 17]. Interestingly, this modulation of M1 by the MNS has been demonstrated in other situations, such as disturbed versus undisturbed movements [74], also suggesting this relationship between the MNS involved in the direct matching model mechanism during action observation [68] and M1 recruitment [75]. This visual feedback also enables the subject to concentrate and work on the fine parameters of movement, which results in a greater beta rebound than during motor imagery alone because the subject is provided with feedback on the movement. Beta rebound relations with the mirror neuron system and Mu rhythms have been explored in autism [76], but we have few points of comparison for healthy subjects or neurological patients. A pitfall of visual feedback therapy alone is that the visual illusion seems to conflict, at least for some subjects, with the proprioceptive feedback of the immobile limb, which diminishes the movement illusion at the group level.

In FV therapy, feedback integration is mediated by a different pathway involving somatosensory cortex recruitment (alpha desynchronization) [60], leading to global recruitment of sensory-motor regions (beta desynchronization) in healthy subjects [77] and stroke

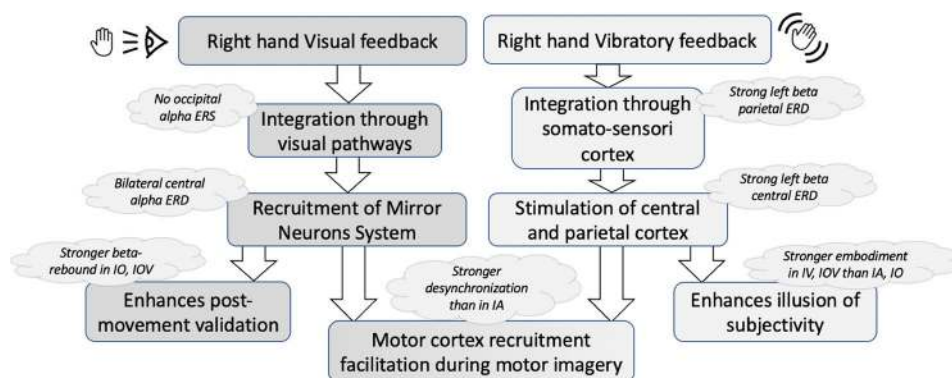


Fig. 8 Global model for visual and vibratory feedback with cortical recruitment consequences and neurophysiological correlates

patients [78]. This recruitment may also be accompanied by modulation of corticospinal excitability, although this point is still discussed in the literature [18, 79, 80]; corticospinal plasticity [81]; connectivity changes and improvement of efficiency parameters in stroke patients [19, 20]; and remnant and additive effects of M1 excitability immediately following the end of vibrations [60]. This recruitment also favors the emergence of a strong kinesthetic illusion, at least in situations where visual feedback is hidden, with a good correlation between the subjects' kinesthetic imagery abilities and their sensation of embodiment. However, vibration of a single tendon does not provide the subject with a precise model of the movement on which to base his motor imagery (on/off vibration of a single tendon) and may therefore not favor the emergence of beta rebound and postmovement validation mechanisms. However, further studies are needed to study beta rebound after vibration therapy.

In the double feedback condition, these two pathways are solicited concomitantly (strong bilateral desynchronization, but that also seems reinforced over the left central regions) with probable potentiation because we observe a statistically significantly reinforced rebound (visual pathway) along with a strong sensation of embodiment (vibratory pathway). A stronger sense of embodiment has also been documented when combining MT and vibrotactile stimulation [82, 83], leading to strong M1 excitability [84], which is a function of the vividness of the kinesthetic illusion perceived by the subjects [85]. Congruent visuo-proprioceptive feedback induces strong M1 excitability, whereas simple tactical stimulation coupled with action observation alone does not. This study focused on healthy subjects. However, in our view, these data suggest that during neurological rehabilitation (stroke, brachial plexus palsy, etc.), the types of feedback should be adapted for each subject while remaining as varied as possible for stimulating both integration pathways.

From healthy subjects to neurological patients

Since this study was conducted on healthy subjects, we must exercise caution when applying these results to a pathological population, as they may have significantly different brain rhythms and functional cortical dynamics [86]. However, some general conclusions can be drawn.

Firstly, this study confirms that both visual and proprioceptive feedback enhance the recruitment of the sensorimotor cortex compared to motor imagery tasks alone. This effect is even more pronounced in the double feedback condition. Based on these results, which demonstrate stronger cortical recruitment in the double feedback condition, as well as findings from the literature showing better functional outcomes with double

feedback [87], we recommend providing patients with combined feedback whenever possible.

Another point of interest is the presence of different feedback integration networks, which are based on distinct anatomical structures. Although the exact mechanisms by which visual and proprioceptive feedback recruit the motor cortex are still debated, we can speculate that specific lesions in these pathways may impair feedback integration in pathological subjects. For instance, the modulation of cortical recruitment varies according to lesion topography in focal vibration [88], with a stronger recruitment observed in patients with basal ganglia ischemia and other subcortical ischemia, compared to those with cortical strokes. There are few comparable studies in the literature for visual feedback therapies. In a context where patients often engage with various rehabilitation devices indiscriminately, determining which type of feedback most effectively promotes motor cortex recruitment for each patient may be crucial for personalizing therapies [26].

Limitations

The main limitation of this study lies in the small number of subjects included. Although statistically significant results were obtained in the areas of interest, these findings need to be validated in a larger sample. Furthermore, this study included only right-handed subjects. It would be interesting to investigate the effect of feedback lateralization on handedness in a larger cohort (e.g., left-hand motor imagery and feedback for right-handed subjects). Finally, it will be necessary to test these results with other rehabilitation methods (such as virtual reality, robotic therapy, etc.), both in healthy subjects and patients, to confirm the validity of this model.

Additionally, we did not include a sham condition for the vibration to distinguish between the specific recruitment of the sensorimotor cortex caused by tendinous vibration and the recruitment induced by the sensation of the vibratory device's movements. Indeed, both proprioceptive and sensory feedback have correlates in the alpha and beta bands [89], which can be confounded in the analysis. Given the strong motor illusion reported by the subjects, we believe the cortical effects were primarily due to the proprioceptive aspect of the feedback. However, further research should investigate this point and include a vibratory sham condition.

Finally, a longer time at the beginning of the epochs should also be considered. Indeed, our baseline may also have been contaminated by some motor-preparation rhythms. Statistical comparison was performed between time-frequency maps with different baselines (500-1500ms baseline versus 500-1200ms baseline) and found no difference. Even if this did not change the overall significance of our results, further studies should include

at least three seconds of pause at the beginning of each epoch.

Conclusion

This study compared differences in cortical activation around sensory-motor regions during a motor imagery task with different neurofeedback modalities: no feedback, visual feedback, tendon vibration feedback, and visual and vibratory feedback.

We found differences in cortical recruitment, indicating different modalities of integration of visual and proprioceptive feedback. Visual feedback leads to the recruitment of the MNS, favors motor validation mechanisms, and recruits sensorimotor areas but does not provide a strong movement illusion. Vibratory feedbacks recruit sensorimotor areas and enhances the illusion of movement but does not specifically favor motor validation. Double feedback combines the effects of both techniques, strongly recruits the sensorimotor cortex with a potentiation effect and maximizes post-movement validation and the feeling of embodiment.

In this work, we propose a specific model for studying the visual and proprioceptive afferents involved in all motor rehabilitation techniques. Our next step is to study this model on a larger set of healthy subjects and in a pathological situation (i.e., stroke) to evaluate how these afferences are integrated on the assumption that, in a pathological situation, certain patients would be more receptive to one type of feedback than another.

Abbreviations

EEG	Electroencephalography
ERD	Event Related Desynchronization
ERS	Event Related Synchronization
fMRI	Functional Magnetic Resonance Imagery
FV	Focal Vibration
FWHM	Full Width at Half Maximum
MI	Mental Imagery
MNS	Mirror Neuron System
IA	Mental Imagery Alone condition
IO	Mental Imagery + Action Observation condition
IOV	Mental Imagery + Action Observation + Focal Vibration condition
IV	Mental Imagery + Focal Vibration condition
MNS	Mirror Neurons System
MT	Mirror Therapy
VFT	Visual Feedback Therapies
VOT	Video Observational Therapy
VR	Virtual Reality

Supplementary Information

The online version contains supplementary material available at <https://doi.org/10.1186/s12984-024-01453-3>.

Supplementary Material 1
Supplementary Material 2
Supplementary Material 3
Supplementary Material 4
Supplementary Material 5

Acknowledgements

The EEG device and disposable were funded by the Association AIRE (St-Etienne, France) and by the Foundation Neurodis (St-Etienne, France). The funders had no role in the study design, data collection and analysis, decision to publish or preparation of the manuscript. This article was edited for proper English language at AJE: EB03-07F6-62DD-8C91-4298.

Author contributions

AA and RD performed the experiments. AA analyzed the data, with help of SL. AA wrote the paper with BH and OE. AA, RD and GP conceived the study. GP supervised the study. All the authors contributed to the editing of this paper.

Funding

The EEG device and disposable were funded by the *Association AIRE* (St-Etienne, France) and by the *Foundation Neurodis* (St-Etienne, France). The funders had no role in the study design, data collection and analysis, decision to publish or preparation of the manuscript.

Data availability

The datasets supporting the conclusions of this article are available upon reasonable request.

Declarations

Ethical approval

The study OPTIVIBE was registered and approved by the ethics committee CPP: "Comité de protection des personnes Sud Ouest et Outre Mer IV" (04/12/2019. N°: CPP2019-11-084a / 2019-A01673-54 / 19.09.12.44858 with amendment N°: 19.01592.201984-MS03 allowing EEG data collection for healthy subjects). The study was conducted in accordance with the Declaration of Helsinki.

Human ethics and consent to participate

Written consent was obtained from all the subjects for participation and publication.

Competing interests

The authors declare no competing interests.

Author details

¹Department of Physical Rehabilitation, CHU of St Etienne, St-Etienne, France

²Laboratory Trajectoires, INSERM 1028, CNRS 5229, University of Lyon-St-Etienne, St-Etienne, France

³Inter-University Laboratory of Human Movement Biology, "Physical Ability and Fatigue in Health and Disease" Team, Saint-Etienne "Jean Monnet" & Lyon 1 & "Savoie Mont-Blanc" Universities, Saint-Etienne F-42023, France

⁴Univ. Grenoble Alpes, CEA, LETI, Clinatex, Grenoble, France

Received: 7 April 2024 / Accepted: 20 August 2024

Published online: 12 September 2024

References

1. Villa-Berges E, Laborda Soriano AA, Lucha-López O, Tricas-Moreno JM, Hernández-Secorún M, Gómez-Martínez M, et al. Motor Imagery and Mental Practice in the Subacute and Chronic Phases in Upper Limb Rehabilitation after Stroke: a systematic review. *Costi S, éditeur. Occup Therapy Int* 24 janv. 2023;2023:1–12.
2. Filgueiras A, Quintas Conde EF, Hall CR. The neural basis of kinesthetic and visual imagery in sports: an ALE meta-analysis. *Brain Imaging Behav Oct.* 2018;12(5):1513–23.
3. Héту S, Grégoire M, Saimpont A, Coll MP, Eugène F, Michon PE, et al. The neural network of motor imagery: an ALE meta-analysis. *Neurosci Biobehavioral Reviews* juin. 2013;37(5):930–49.
4. Monteiro KB, Cardoso M, dos S, Cabral VR da, Santos C, dos AOB, Silva PS da, de Castro JBP et al. Effects of Motor Imagery as a Complementary Resource on the Rehabilitation of Stroke Patients: A Meta-Analysis of Randomized Trials. *Journal of Stroke and Cerebrovascular Diseases.* août. 2021;30(8):105876.

5. Machado TC, Carregosa AA, Santos MS, Ribeiro NM, da Melo S. Efficacy of motor imagery additional to motor-based therapy in the recovery of motor function of the upper limb in post-stroke individuals: a systematic review. *Top Stroke Rehabil.* oct 2019;3(7):548–53.
6. Bajaj S, Butler AJ, Drake D, Dhamala M. Brain effective connectivity during motor-imagery and execution following stroke and rehabilitation. *NeuroImage.* 2015;8:572–82.
7. Cicinelli P, Marconi B, Zaccagnini M, Pasqualetti P, Filippi MM, Rossini PM. Imagery-induced cortical excitability changes in stroke: a transcranial magnetic stimulation study. *Cereb Cortex* 1 févr. 2006;16(2):247–53.
8. Tavazzi E, Bergsland N, Pirastu A, Cazzoli M, Blasi V, Baglio F. MRI markers of functional connectivity and tissue microstructure in stroke-related motor rehabilitation: a systematic review. *NeuroImage: Clin.* 2022;33:102931.
9. Kim H, Lee E, Jung J, Lee S. Utilization of Mirror Visual Feedback for Upper Limb function in Poststroke patients: a systematic review and Meta-analysis. *Vis* 15 nov. 2023;7(4):75.
10. Altschuler EL, Wisdom SB, Stone L, Foster C, Galasko D, Llewellyn DME, et al. Rehabilitation of hemiparesis after stroke with a mirror. *Lancet* juin. 1999;353(9169):2035–6.
11. Ding L, Wang X, Chen S, Wang H, Tian J, Rong J, et al. Camera-based Mirror Visual Input for Priming Promotes Motor Recovery, daily function, and Brain Network Segregation in Subacute Stroke patients. *Neurorehabilitation Neural Repair* avr. 2019;33(4):307–18.
12. Borges LR, Fernandes AB, Melo LP, Guerra RO, Campos TF. Action observation for upper limb rehabilitation after stroke. *Cochrane Database Syst Rev.* 2018;10(10).
13. Giroux P, Sirigu A. Illusory movements of the paralyzed limb restore motor cortex activity. *NeuroImage* Nov. 2003;20:S107–11.
14. Moggio L, de Sire A, Marotta N, Demeco A, Ammendolia A. Vibration therapy role in neurological diseases rehabilitation: an umbrella review of systematic reviews. *Disabil Rehabil.* sept 2022;25(20):5741–9.
15. Alashram AR, Padua E, Romagnoli C, Annino G. Effectiveness of focal muscle vibration on hemiplegic upper extremity spasticity in individuals with stroke: a systematic review. *NeuroRehabilitation* 18 déc. 2019;45(4):471–81.
16. Bartur G, Pratt H, Dickstein R, Frenkel-Toledo S, Geva A, Soroker N. Electrophysiological manifestations of mirror visual feedback during manual movement. *Brain Res* mai. 2015;1606:113–24.
17. Bartur G, Pratt H, Frenkel-Toledo S, Soroker N. Neurophysiological effects of mirror visual feedback in stroke patients with unilateral hemispheric damage. *Brain Res* déc. 2018;1700:170–80.
18. Souron R, Baudry S, Millet GY, Lapole T. Vibration-induced depression in spinal loop excitability revisited. *J Physiol* nov. 2019;597(21):5179–93.
19. Li W, Li C, Xu Q, Ji L. Effects of Focal Vibration over Upper Limb Muscles on the activation of Sensorimotor Cortex Network: an EEG study. *J Healthc Eng.* 2019;2019:9167028.
20. Li W, Li C, Xiang Y, Ji L, Hu H, Liu Y. Study of the activation in sensorimotor cortex and topological properties of functional brain network following focal vibration on healthy subjects and subacute stroke patients: an EEG study. *Brain Res* nov. 2019;1722:146338.
21. Ding L, He J, Yao L, Zhuang J, Chen S, Wang H, et al. Mirror Visual Feedback combining Vibrotactile Stimulation promotes Embodiment Perception: an Electroencephalogram (EEG) pilot study. *Front Bioeng Biotechnol.* oct 2020;26:8:553270.
22. Le Franc S, Bonan I, Fleury M, Butet S, Barillot C, Lécuyer A, et al. Visual feedback improves movement illusions induced by tendon vibration after chronic stroke. *J Neuro-Engineering Rehabilitation* déc. 2021;18(1):156.
23. Le Franc S, Fleury M, Jeunet C, Butet S, Barillot C, Bonan I, et al. Influence of the visuo-proprioceptive illusion of movement and motor imagery of the wrist on EEG cortical excitability among healthy participants. *Aspell JE*, éditeur. *PLoS ONE* 2 sept. 2021;16(9):e0256723.
24. Vidaurre C, Ramos Murguialday A, Haufe S, Gómez M, Müller KR, Nikulin VV. Enhancing sensorimotor BCI performance with assistive afferent activity: an online evaluation. *Neuroimage* 1 oct. 2019;199:375–86.
25. Zhang L, Chen L, Wang Z, Zhang X, Liu X, Ming D. Enhancing visual-guided motor imagery performance via sensory threshold Somatosensory Electrical Stimulation Training. *IEEE Trans Biomedical Eng* févr. 2023;70(2):756–65.
26. Le Franc S, Herrera Altamira G, Guillen M, Butet S, Fleck S, Lécuyer A, et al. Toward an adapted Neurofeedback for Post-stroke Motor Rehabilitation: state of the art and perspectives. *Front Hum Neurosci* 14 Juill. 2022;16:917909.
27. Lorient J, Nicolas A. Validation de la traduction française Du Movement Imagery Questionnaire-revised (MIQ-R). *Sci Motricité.* 2004;53:57–68.
28. Mathôt S, Schreiij D, Theeuwes J, OpenSesame. An open-source, graphical experiment builder for the social sciences. *Behav Res Methods* juin. 2012;44(2):314–24.
29. Avvantaggiato C, Casale R, Cinone N, Facciorusso S, Turitto A, Stuppiello L, Picelli A, Ranieri M, Intiso D, Fiore P, Ciritella C, Santamato A. Localized muscle vibration in the treatment of motor impairment and spasticity in post-stroke patients: a systematic review. *Eur J Phys Rehabil Med.* 2021;57(1):44–60.
30. Delorme A, Makeig S. EEGLAB: an open source toolbox for analysis of single-trial EEG dynamics including independent component analysis. *J Neurosci Methods* mars. 2004;134(1):9–21.
31. Dong L, Li F, Liu Q, Wen X, Lai Y, Xu P, et al. MATLAB Toolboxes for Reference Electrode standardization technique (REST) of scalp EEG. *Front NeuroSci.* oct 2017;30:1:1601.
32. Cohen MX. A better way to define and describe Morlet wavelets for time-frequency analysis. *NeuroImage* Oct. 2019;199:81–6.
33. Allen DP, MacKinnon CD. Time–frequency analysis of movement-related spectral power in EEG during repetitive movements: a comparison of methods. *J Neurosci Methods* janv. 2010;186(1):107–15.
34. Pfurtscheller G, Lopes da Silva FH. Event-related EEG/MEG synchronization and desynchronization: basic principles. *Clin Neurophysiol Nov.* 1999;110(11):1842–57.
35. Maris E, Oostenveld R. Nonparametric statistical testing of EEG- and MEG-data. *J Neurosci Methods* août. 2007;164(1):177–90.
36. Hohaia W, Saurels BW, Johnston A, Yarrow K, Arnold DH. Occipital alpha-band brain waves when the eyes are closed are shaped by ongoing visual processes. *Sci Rep* déc. 2022;12(1):1194.
37. Searwards TV, Searwards MA. Alpha-band oscillations in visual cortex: part of the neural correlate of visual awareness? *Int J Psychophysiol* 1 avr. 1999;32(1):35–45.
38. Peylo C, Hilla Y, Sauseng P. Cause or consequence? Alpha oscillations in visuospatial attention. *Trends Neurosciences* Sept. 2021;44(9):705–13.
39. Sauseng P, Klimesch W, Stadler W, Schabus M, Doppelmayr M, Hanslmayr S, et al. A shift of visual spatial attention is selectively associated with human EEG alpha activity. *Eur J Neurosci* déc. 2005;22(11):2917–26.
40. Freschl J, Azizi LA, Balboa L, Kaldy Z, Blaser E. The development of peak alpha frequency from infancy to adolescence and its role in visual temporal processing: a meta-analysis. *Dev Cogn Neurosci* oct. 2022;57:101146.
41. Frauscher B, Von Ellenrieder N, Zemann R, Doležalová I, Minotti L, Olivier A, et al. Atlas of the normal intracranial electroencephalogram: neurophysiological awake activity in different cortical areas. *Brain* 1 avr. 2018;141(4):1130–44.
42. Attal Y, Schwartz D. Assessment of Subcortical Source Localization Using Deep Brain Activity Imaging Model with Minimum Norm Operators: A MEG Study. *Barnes GR*, éditeur. *PLoS ONE.* 20 mars. 2013;8(3):e59856.
43. Debnath R, Salo VC, Buzzell GA, Yoo KH, Fox NA. Mu rhythm desynchronization is specific to action execution and observation: evidence from time-frequency and connectivity analysis. *NeuroImage* janv. 2019;184:496–507.
44. Stolk A, Brinkman L, Vansteensel MJ, Aarnoutse E, Leijten FS, Dijkerman CH et al. Electroencephalographic dissociation of alpha and beta rhythmic activity in the human sensorimotor system. *eLife* 9 oct 2019;8:e48065.
45. Fox NA, Bakermans-Kranenburg MJ, Yoo KH, Bowman LC, Cannon EN, Vanderwert RE, et al. Assessing human mirror activity with EEG mu rhythm: a meta-analysis. *Psychol Bull.* 2016;142(3):291–313.
46. Hobson HM, Bishop DVM. The interpretation of mu suppression as an index of mirror neuron activity: past, present and future. *Royal Soc Open Sci* mars. 2017;4(3):160662.
47. Thorpe SG, Cannon EN, Fox NA. Spectral and source structural development of mu and alpha rhythms from infancy through adulthood. *Clin Neurophysiol* Janv. 2016;127(1):254–69.
48. Cole EJ, Barraclough NE. Timing of mirror system activation when inferring the intentions of others. *Brain Res* 1 déc. 2018;1700:109–17.
49. Caspers S, Zilles K, Laird AR, Eickhoff SB. ALE meta-analysis of action observation and imitation in the human brain. *Neuroimage* 15 avr. 2010;50(3):1148–67.
50. Franceschini M, Ottaviani M, Romano P, Goffredo M, Pournajaf S, Lofrumento M et al. sept. The reaching phase of feeding and self-care actions optimizes Action Observation effects in chronic stroke subjects. *Neurorehabilitation and neural repair.* 1 2022;36(9):574–86.
51. Pfurtscheller G, Neuper C, Brunner C, Da Silva FL. Beta rebound after different types of motor imagery in man. *Neurosci Lett* Avr. 2005;378(3):156–9.
52. Jurkiewicz MT, Gaetz WC, Bostan AC, Cheyne D. Post-movement beta rebound is generated in motor cortex: evidence from neuromagnetic recordings. *NeuroImage* Sept. 2006;32(3):1281–9.

53. Mary A, Bourguignon M, Wens V, Op De Beeck M, Leproult R, De Tiège X, et al. Aging reduces experience-induced sensorimotor plasticity. A magnetoencephalographic study. *NeuroImage* janv. 2015;104:59–68.
54. Cardellicchio P, Hilt PM, Dolfini E, Fadiga L, D'Ausilio A. Beta rebound as an index of temporal integration of Somatosensory and Motor signals. *Front Syst Neurosci* 2 sept. 2020;14:63.
55. Koelewijn T, Van Schie HT, Bekkering H, Oostenveld R, Jensen O. Motor-cortical beta oscillations are modulated by correctness of observed action. *NeuroImage* Avr. 2008;40(2):767–75.
56. Torrecillos F, Alayrangues J, Kilavik BE, Malfait N. Distinct modulations in Sensorimotor Postmovement and Foreperiod β -Band activities related to Error Salience Processing and Sensorimotor Adaptation. *J Neurosci* 16 sept. 2015;35(37):12753–65.
57. Cao L, Hu YM. Beta rebound in Visuomotor Adaptation: still the Status Quo? *J Neurosci* 15 juin. 2016;36(24):6365–7.
58. Cassim F, Monaca C, Szurhaj W, Bourriez JL, Defebvre L, Derambure P, Guieu JD. Does post-movement beta synchronization reflect an idling motor cortex? *NeuroReport*. 2001;12(17):3859–63.
59. Keinrath C, Wriessnegger S, Müller-Putz GR, Pfurtscheller G. Post-movement beta synchronization after kinesthetic illusion, active and passive movements. *Int J Psychophysiol* nov. 2006;62(2):321–7.
60. Lopez S, Bini F, Del Percio C, Marinuzzi F, Celletti C, Suppa A, et al. Electroencephalographic sensorimotor rhythms are modulated in the acute phase following focal vibration in healthy subjects. *Neurosci* 3 juin. 2017;352:236–48.
61. Park W, Kim SP, Eid M. Neural coding of vibration intensity. *Front Neurosci* 11 Nov. 2021;15:682113.
62. Shiner CT, Tang H, Johnson BW, McNulty PA. Cortical beta oscillations and motor thresholds differ across the spectrum of post-stroke motor impairment, a preliminary MEG and TMS study. *Brain Res* déc. 2015;1629:26–37.
63. Takemi M, Masakado Y, Liu M, Ushiba J. Event-related desynchronization reflects downregulation of intracortical inhibition in human primary motor cortex. *J Neurophysiol* sept. 2013;110(5):1158–66.
64. Zhao M, Marino M, Samogin J, Swinnen SP, Mantini D. Hand, foot and lip representations in primary sensorimotor cortex: a high-density electroencephalography study. *Sci Rep* 19 déc. 2019;9(1):19464.
65. Graziano MSA. Where is my arm? The relative role of vision and proprioception in the neuronal representation of limb position. *Proceedings of the National Academy of Sciences*. 31 août. 1999;96(18):10418–21.
66. Schneider C, Marquis R, Jöhr J, Lopes da Silva M, Ryvlin P, Serino A, De Lucia M, Diserens K. Disentangling the percepts of illusory movement and sensory stimulation during tendon vibration in the EEG. *NeuroImage*. 2021;241:118431.
67. Zhang JQ, Fong KNK, Welage N, Liu KPY. The activation of the Mirror Neuron System during Action Observation and Action execution with Mirror Visual Feedback in Stroke: a systematic review. *Neural Plast*. 2018;2018:1–14.
68. Kemmerer D. What modulates the Mirror Neuron System during action observation? Multiple factors involving the action, the actor, the observer, the relationship between actor and observer, and the context. *Progress Neurobiol* oct. 2021;205:102128.
69. Brihmat N, Tarri M, Quidé Y, Anglio K, Pavard B, Castel-Lacanal E, et al. Action, observation or imitation of virtual hand movement affect differently regions of the mirror neuron system and the default mode network. *Brain Imaging Behav* Oct. 2018;12(5):1363–78.
70. Lepage JF, Tremblay S, Théoret H. Early non-specific modulation of corticospinal excitability during action observation. *Eur J Neurosci* mars. 2010;31(5):931–7.
71. Strafella AP, Paus T. Modulation of cortical excitability during action observation: a transcranial magnetic stimulation study. *Neuroreport* 14 Juill. 2000;11(10):2289–92.
72. Novaes MM, Palhano-Fontes F, Peres A, Mazzetto-Betti K, Pelicioni M, Andrade KC, et al. Neurofunctional changes after a single mirror therapy intervention in chronic ischemic stroke. *Int J Neurosci* oct. 2018;128(10):966–74.
73. Lin SH, Cheng CH, Wu CY, Liu CT, Chen CL, Hsieh YW. Mirror Visual Feedback Induces M1 Excitability by Disengaging Functional Connections of Perceptuo-Motor-Attentional Processes during Asynchronous Bimanual Movement: A Magnetoencephalographic Study. *Brain Science*. 20 août. 2021;11(8):1092.
74. Cheng CH, Sun HH, Weng JQ, Tseng YJ. Differential motor cortex excitability during observation of normal and abnormal goal-directed movement patterns. *Neurosci Res* oct. 2017;123:36–42.
75. Liepelt R, Cramon DYV, Brass M. What is matched in direct matching? Intention attribution modulates motor priming. *J Experimental Psychology: Hum Percept Perform* juin. 2008;34(3):578–91.
76. Honaga E, Ishii R, Kurimoto R, Canuet L, Ikezawa K, Takahashi H, et al. Post-movement beta rebound abnormality as indicator of mirror neuron system dysfunction in autistic spectrum disorder: an MEG study. *Neurosci Lett* 12 Juill. 2010;478(3):141–5.
77. Ramu V, Lakshminarayanan K. Enhanced motor imagery of digits within the same hand via vibrotactile stimulation. *Front NeuroSci*. 2023;17:1152563.
78. Snyder DB, Beardsley SA, Hyngstrom AS, Schmit BD. Cortical effects of wrist tendon vibration during an arm tracking task in chronic stroke survivors: an EEG study. *PLoS ONE*. 2023;18(12):e0266586.
79. Kolbaşı EN, Huseynsinoglu BE, Bayraktaroğlu Z. Effect of upper limb focal muscle vibration on cortical activity: a systematic review with a focus on primary motor cortex. *Eur J Neurosci* août. 2022;56(3):4141–53.
80. Lauzier L, Perron MP, Munger L, Bouchard É, Abboud J, Nougareou F, et al. Variation of corticospinal excitability during kinesthetic illusion induced by musculotendinous vibration. *J Neurophysiol* 1 nov. 2023;130(5):1118–25.
81. Rocchi L, Suppa A, Leodori G, Celletti C, Camerota F, Rothwell J, et al. Plasticity Induced in the human spinal cord by focal muscle vibration. *Front Neurol*. 2018;9:935.
82. Ding L, He J, Yao L, Zhuang J, Chen S, Wang H, et al. Mirror Visual Feedback combining Vibrotactile Stimulation promotes Embodiment Perception: an Electroencephalogram (EEG) pilot study. *Front Bioeng Biotechnol*. 2020;8:553270.
83. Schlienger R, De Giovanni C, Guerraz M, Kavounoudias A. When proprioceptive feedback enhances visual perception of self-body movement: rehabilitation perspectives. *Front Hum Neurosci* 12 mai. 2023;17:1144033.
84. Bisio A, Biggio M, Canepa P, Faelli E, Ruggeri P, Avanzino L, et al. Primary motor cortex excitability as a marker of plasticity in a stimulation protocol combining action observation and kinesthetic illusion of movement. *Eur J Neurosci* avr. 2021;53(8):2763–73.
85. Bisio A, Biggio M, Avanzino L, Ruggeri P, Bove M. Kinaesthetic illusion shapes the cortical plasticity evoked by action observation. *J Physiol* juin. 2019;597(12):3233–45.
86. Kancheva I, Van Der Salm SMA, Ramsey NF, Vansteensel MJ. Association between lesion location and sensorimotor rhythms in stroke – a systematic review with narrative synthesis. *Neurol Sci* déc. 2023;44(12):4263–89.
87. He J, Li C, Lin J, Shu B, Ye B, Wang J, et al. Proprioceptive training with visual feedback improves Upper Limb function in Stroke patients: a pilot study. *Neural Plast*. 2022;2022:1588090.
88. Li W, Li C, Liu A, Lin PJ, Mo L, Zhao H, et al. Lesion-specific cortical activation following sensory stimulation in patients with subacute stroke. *J Neuroeng Rehabil*. nov 2023;13(1):155.
89. Schneider C, Marquis R, Jöhr J, Lopes da Silva M, Ryvlin P, Serino A, et al. Disentangling the percepts of illusory movement and sensory stimulation during tendon vibration in the EEG. *Neuroimage* 1 nov. 2021;241:118431.

Publisher's note

Springer Nature remains neutral with regard to jurisdictional claims in published maps and institutional affiliations.

@ | D

EFFICACY OF A NEW VIDEO OBSERVATIONAL TRAINING METHOD (INTENSIVE VISUAL SIMULATION) FOR MOTOR RECOVERY IN THE UPPER LIMB IN SUBACUTE STROKE: A FEASIBILITY AND PROOF-OF-CONCEPT STUDY

Etienne OJARDIAS, MD, PhD^{1,2}, Ahmed ADHAM, MD^{1,2}, Hugo BESSAGUET, MD^{1,3}, Virginie PHANER, MD¹, Diana RIMAUD, PhD^{1,3} and Pascal GIRAUX, MD, PhD^{1,2}

From the ¹Physical Medicine & Rehabilitation Department, University Hospital of Saint-Étienne, Saint-Étienne, France; ²Lyon Neuroscience Research Center, Trajectoires team (Inserm UMR-S 1028, CNRS UMR 5292, Lyon1 & Saint-Etienne Universities), France; ³Inter-University Laboratory of Human Movement Biology, EA 7424, Jean Monnet University, Saint-Etienne, France

Objective: To demonstrate the feasibility and efficacy of a new video-observation training method (intensive visual simulation) to improve upper limb function.

Design: Small sample, randomized, evaluator-blind, monocentric study.

Patients: Seventeen early subacute ischaemic stroke patients with complete hemiplegia were randomly assigned to the therapeutic group ($n=8$) or control group (CG, $n=9$).

Methods: Thirty sessions of intensive visual simulation combined with corrected visual feedback (therapeutic group) or uncorrected visual feedback (control group) were performed over 6 weeks on top of a standard rehabilitation programme. Main outcome measure: 400p-HA. Secondary outcome measures: Box and Blocks (B&B), Purdue Pegboard test, Minnesota.

Results: The 400p-HA test improved significantly from T0 to 6 months for both groups, with a significant difference between groups at 3 months (MW-UT $p=0.046$) and 4 months (MW-UT $p=0.046$) in favour of the therapeutic group. One-phase exponential modelling of 400p-HA showed a greater plateau for the therapeutic group (F test $p=0.0021$). There was also faster recovery of the ability to perform the B&B tests for the therapeutic group (log-rank test $p=0.03$).

Conclusion: This study demonstrated the feasibility and potential efficacy of an intensive visual simulation training programme to improve upper limb function in subacute stroke patients. A larger study is needed to confirm these results.

Key words: equipment and supplies; evaluation study; feedback; sensory; hemiplegia; stroke rehabilitation; upper extremity; intensive visual simulation; IVS.

Submitted Jan 5, 2024. Accepted after revision Jun 10, 2024

Published XX. DOI: 10.2340/jrm.v56.36119

J Rehabil Med 2024; 56: jrm36119.

Correspondence address: Pascal Giraux, Physical Medicine & Rehabilitation Department, Bellevue Hospital, University Hospital of Saint-Étienne, 25 Bd Pasteur, Saint-Etienne, F-42055, France. E-mail: pascal.giraux@univ-st-etienne.fr

Stroke is the leading cause of acquired disability in adults in the most developed countries, with up to 80% of stroke patients suffering an upper limb

LAY ABSTRACT

The recovery of poststroke upper-limb motor deficits remains challenging, and improvements in this deficit rely on a combination of intensive and specific rehabilitation techniques. The aim of this study was to demonstrate the feasibility and test the efficacy of a new video-observation training method named intensive visual simulation to improve upper-limb function. Seventeen subacute hemiplegic stroke patients were included in this study; they received a total of 30 sessions of either intensive visual simulation training (movement attempts with corrected visual feedback) for the therapeutic group or sham-intensive visual simulation (movement attempts with uncorrected visual feedback) for the control group. The global hand functioning assessment (400p-HA) was significantly better at 3 and 4 months in the therapeutic group than in the control group, and the recovery curve was better. We conclude that this intensive visual simulation training regimen demonstrates promising benefits for upper-limb motor recovery in hemiplegic patients at a subacute stage.

motor deficit (1, 2). After complete hemiplegia, the recovery of a functional hand is achieved by less than 20% of patients despite sustained rehabilitation care (3). New neurorehabilitation technologies based on the understanding of the neural mechanisms of motor control propose diverse and intensive motor training, which is intended to improve this poor outcome (4, 5).

Among these techniques, observational therapies can be defined as a set of motor rehabilitation techniques that rely on the visualization of body movements and activate the mirror neuron system as the main stimulation of the sensorimotor network (6). Mirror therapy (MT) is the princeps technique (7, 8) and is effective for motor recovery in stroke patients (9). However, its use is problematic in patients who have hemineglect, attentional deficit, apraxia, or aphasia. When they are specified, hemineglect or severe aphasia are common exclusion criteria in most of the clinical studies selected in the recent Cochrane review (9), which means that the effectiveness of MT is not clearly established in

patients with these associated impairments. The use of videos and a computerized device could overcome some of these difficulties. Action Observation Training therapies includes different set of techniques using video of movements that provide a model of correctly executed movements, either as an external model at a third-person point of view, or at first-person point of view if the screen is positioned in the optical axis between the subject's eyes and the impaired limb. The first-person point of view provides visual feedback with an embodiment effect comparable to MT, generating kinaesthetic illusions in most patients. If motor imagery alone can improve upper limb motor function (5, 10, 11), synchronous action observation and motor imagery can enhance excitability of the sensorimotor cortex and contribute to motor improvement following stroke (12). We previously developed the first experimental device to successfully enhance cortical motor activity (13) and relieve pain in patients with brachial plexus lesions (14). A library of movements performed with the intact upper limb was video recorded at the first-person point of view and horizontally flipped to serve as visual feedback during training of the impaired limb. This optical and computerized system provides the subject with an immersive 2D image of a correctly executed movement despite the motor deficit. A full device was consequently developed for motor training of the upper limb (IVS™, Dessintey Co., St-Jean-Bonnefonds, France).

In this proof-of-concept study, we tested the feasibility and effectiveness of intensive visuomotor training with the intensive visual simulation (IVS) device to improve upper limb function in a small sample of first-ever subacute stroke patients with an initially complete motor deficit in the upper limb. The objective was to test the effectiveness of the training with corrected visual feedback, where the device normally executes movements (therapeutic group), versus training with uncorrected feedback (control group), where the device actually delivers the movements of the impaired limb. For both groups, this intervention was given in addition to a standard rehabilitation programme.

METHODS

Design

A pilot, prospective, randomized parallel-group, examiner-blind trial was also conducted. During a 2-year period, all patients diagnosed with stroke and admitted to the Physical Medicine and Rehabilitation (PMR) inpatient clinic of the University Hospital of Saint-Étienne were screened for possible inclusion in the study. Baseline evaluation was performed prior to randomization. A computer-generated randomization table was generated by a person not involved in the study. Patients were randomly allocated to either the therapeutic (T) or control (C) group based on an assignment schedule and their details were stored in consecutively numbered, sealed envelopes to ensure

concealment. Outcome data were collected at baseline (i.e., a few days before intervention), every 2 weeks during the 6 weeks of intervention, and then monthly until 6 months poststroke. Outcome measurements were performed by an independent examiner blinded to group allocation. To maintain blinding, patients were instructed not to discuss any aspects of their intervention with the examiner. The protocol was approved by the ethics committee of the Saint-Étienne University Hospital (No. 200102-JV200125). Patients were provided with written information regarding the study, and written consent was obtained from all patients before participation in the study.

Patients

The inclusion criteria were male or female, aged 18 to 75 years, able to give consent, right-handed (Edinburgh Inventory >+40), with a complete motor deficit in the left or right upper limb at D0 poststroke (0 MRC score from shoulder to digits), related to a first ischaemic stroke, less than 30 days old at the time of inclusion, and proven by brain imaging. The main exclusion criteria were disabling general illness, a history of neurological or psychiatric disease, a very poor recovery prognosis due to a complete infarct of the middle cerebral artery territory, a visual deficit that could not be compensated for, and cognitive impairment that compromised comprehension or completion of the rehabilitation programme.

Intervention

Throughout the study, both groups received individualized standard rehabilitation therapy for the upper limb from a physiotherapist (1 hour) or an occupational therapist (1 hour), which was different from the approach used by the therapist who performed the IVS training and who was blinded to the patient's group assignment. This standard rehabilitation included hands-on therapy, passive and active mobilization, electrophysiotherapy, and task-oriented therapy. This standard therapy was delivered 5 days a week during a part of the day (morning or afternoon) different from the IVS sessions, thus preserving the patient's fatigue level. This standard treatment continued after the end of the intervention, either in hospital or on an outpatient basis, according to a programme and duration tailored to each patient.

Both groups received the intervention with an IVS™ setup (Dessintey Co., France) (Fig. 1). We used a research version of the IVS device, which also allowed direct video capture and display of the impaired limb. The therapeutic group (TG) received upper limb rehabilitation sessions with visual feedback correction (normally executed movements, with horizontally flipped, prerecorded video of the intact limb), whereas the control group (CG) had sessions without visual feedback correction (direct video capture and display of the impaired limb). The training consisted of functional reaching and grasping movements. A set of 10 objects was selected to include 2 examples of 5 types of prehensile postures according to Schlesinger's classification (cylindrical, tip, palmar, spherical, lateral). Before each movement, a static grey picture with the written name of the next movement to be performed was displayed on the screen for 5 sec, then a cross (preparation cue) for 1 sec, and a video was displayed for approximately 10 sec, either the normally executed movement (horizontally flipped, prerecorded video of the intact limb) for the TG or the direct video capture of the impaired limb for the CG. Patients were asked to perform a volitional movement attempt of the instructed movement during the video display, and for the TG patients were instructed to synchronize this movement attempt with the displayed movement. During



Fig. 1. Stroke patient during practice on the IVS device.

each training session, the 10 movements were repeated 20 times, for a total of 200 movements per session. The 2 groups received the same measure of rehabilitation. The therapist remained close to the patient during the training to provide instruction to the patient, ensure optical coherence of the display, eventually assist the patient, and specifically ensure the correct starting position of the patient's hand. Patients received this training 5 days a week for 6 weeks, for a total of 30 sessions.

Outcome measures

The main outcome measure was the 400-point Hand Assessment test (400pt-HA) (15–17). This validated test evaluates 57 usual manual activities that test simple distal analytical movements, unimanual grasping and displacement of objects, and the function of both hands (coordinated bimanual movements). By combining analytical and functional dimensions, this test covers a large range of sensitivities regarding motor recovery in the hand.

Additional validated grasping and dexterity tests were also conducted as secondary outcomes: the Box and Block Test (B&B) (18), the Purdue Pegboard Test (Purdue) (19, 20) and the Minnesota Rate of Manipulation Test (Minnesota) (21). To be performed with the impaired limb, these tests require minimal recovery of reaching and grasping capabilities with the impaired limb. These scores are consequently expected to be 0 (or close to 0) at the beginning of the intervention and may remain null in the case of nonfunctional recovery.

An inclusion visit was performed for each patient with a clinical examination, and data regarding associated deficits, such as sensitivity impairment, hemineglect, and praxis disorders, were collected to eventually assess the influence of these factors on therapeutic efficacy. At inclusion, a baseline motor evaluation of the upper limb was performed (400pt-HA, B&B, Minnesota, Purdue). This motor evaluation was repeated every

2 weeks during the 6 weeks of the rehabilitation programme and then monthly until 6 months poststroke. These numerous assessments (8 per patient in the case of complete data), with a relatively long follow-up period (6 months poststroke), were designed to allow temporal modelling (estimate of the recovery curves) in addition to the usual comparative analysis.

Data analysis

All the data were analysed using Prism 5 software (GraphPad Software, Inc; <https://www.graphpad.com/>). The Mann–Whitney U test was applied to determine the difference in age between the 2 groups, and Fisher's exact test was applied for the other characteristics of the patients. Comparisons of test results between the 2 groups were performed with Mann–Whitney U tests. Two-tailed results were considered significant if $p < 0.05$. In addition, one-phase exponential modelling was applied to the recovery curves of 400pt-HA for each group, and the fits of the 2 groups were compared with an extra sum-of-squares F test. Considering that dexterity tests (B&B Minnesota, Purdue) have an optional and delayed recovery (non-0 score), additional time-to-event statistics were performed (time-to-non-0 score), similar to survival curves, with a comparison of the two groups of curves using log-rank (Mantel–Cox) tests.

RESULTS

Patients included

Seventeen patients, with a mean age of 63.4 years (SD 7.8), who were suffering a first ischaemic stroke and met the inclusion criteria, were enrolled and randomly assigned to the control group (CG, $n=9$; mean age 64.2 years, SD 9.6) or the therapeutic group (TG, $n=8$; mean age 62.6 years, SD 5.7). The main characteristics of the population are described in Table I, and none of these characteristics significantly differed between the groups. There was an overall predominance of right hemiplegia (13 out of 17 patients), which was balanced between the groups.

400pt-HA results

The 400pt-HA test showed a significant improvement from T0 to the end of the intervention (Fig. 2a and Table II) and then a slower improvement until 6 months. The difference in the means between the TG 43.1 and CG 27.0 groups did not reach statistical significance (Mann–Whitney U test $p=0.07$) at the end of the intervention but became significant during the follow-up period at 3 months (TG 45.5; CG 27.8; $p=0.046$) or 4 months (TG 51.5; CG 29.9; $p=0.046$). This difference at 3 and 4 months is superior to the minimal clinically important difference (MCID) of 6. Modelling of the recovery of upper limb function based on all temporal data of patients in each group was performed with a one-phase exponential model, which was selected as the best suitable model for the recovery curve (Fig. 2b). This model differed significantly between the therapeutic

Table I. Main characteristics of the patients

Initials	Sex	Age	Affected limb	Brain lesion
Control				
DR01	M	62	R	Left centrum semiovale and thalamus
GA03	M	72	R	Left superficial MCA territory
SC07	M	49	L	Right lenticulo-striate territory
DY12	F	72	R	Left superficial MCA territory
GJ13	F	47	R	Left superficial MCA territory and partial lenticulo-striate territory
RL14	M	70	R	Left lenticulo-striate territory
DM15	F	66	R	Left superficial MCA territory
FG16	F	70	R	Left lenticulo-striate territory
GD17	F	69	L	Right superficial MCA territory
Therapeutic				
FJ02	M	58	R	Left superficial MCA territory
RM04	F	57	L	Right internal capsule and centrum semiovale
RE05	M	68	R	Left internal capsule and thalamus
VJ06	M	71	R	Left lenticulo-striate territory
GM08	F	66	L	Right lenticulo-striate territory
PL09	M	59	R	Left internal capsule and centrum semiovale
FF10	M	57	R	Left centrum semiovale
BL11	M	65	R	Left internal capsule

MCA: middle cerebral artery.

and control groups ($p=0.0021$; extra sum-of-squares F test), with the therapeutic group reaching a higher plateau (Ymax: TG 54.2 with 95% CI [40.3–68]; CG 29.2 with 95% CI [22.6–38.4]).

Dexterity tests

The mean evolution of the B&B, Purdue and Minnesota tests can be seen in the left column of Fig. 3. The mean values of the 3 tests were consistent in favour of the therapeutic group, although the Mann–Whitney *U* test did not differ significantly. The cumulative curves of the time-to-non-0 scores can be seen in the right-hand column of Fig. 3. This temporal time-to-event approach allows us to consider the duration of a 0-point interval as a marker of recovery. These curves show a consistently faster recovery of non-0 scores for the 3 tests, with a log-rank (Mantel–Cox) test indicating significant results for the B&B test ($p=0.03$); concretely, this finding indicates that the recovery of the ability to transfer at least 1 cube (from one side to the other) with the paretic hand is faster in the therapeutic group than in the control group.

Table II. Details of results for the total 400p-HA test and the 3 dexterity tests over time (T0, END of intervention, M3, M4, and M6) for the therapeutic group and the control group

Test	Therapeutic group					Control group					
	T0 Mean±SD	END Mean±SD	M3 Mean±SD	M4 Mean±SD	M6 Mean±SD	T0 Mean±SD	END Mean±SD	M3 Mean±SD	M4 Mean±SD	M6 Mean±SD	MCID Mean±SD
400p-HA	15.1±13.2	43.1 ± 25.0	45.51±20.9	51.6±23.3	40.±36.6	9.6±3.2	27.0±21.4	27.8± 22.4	29.9±26.5	57.6±25.1	3.3
Box& Block	0.7±1.9	2.4±3.7	7.7±10.0	10.1±4.0	2.8±4.1	0.6±1.2	1.9±3.8	4.7±9.5	6.0±10.5	5.0±4.4	5.5/7.8*
Purdue	8.3±2.1	13.8±12.9	NA	NA	21.3±12.6	8.9±1.5	12.3±4.1	NA	NA	13.6±8.3	3/6**
Minnesota	0	12.6±22.4	NA	NA	22.0±25.6	0	6.4±16.8	NA	NA	10.0±24.5	NA

400p-HA: 400-point Hand Assessment test; NA: non-available; Purdue: Purdue Pegboard test.
 *Most affected side/less affected side.
 **One hand/both hands; no study available in stroke patients.

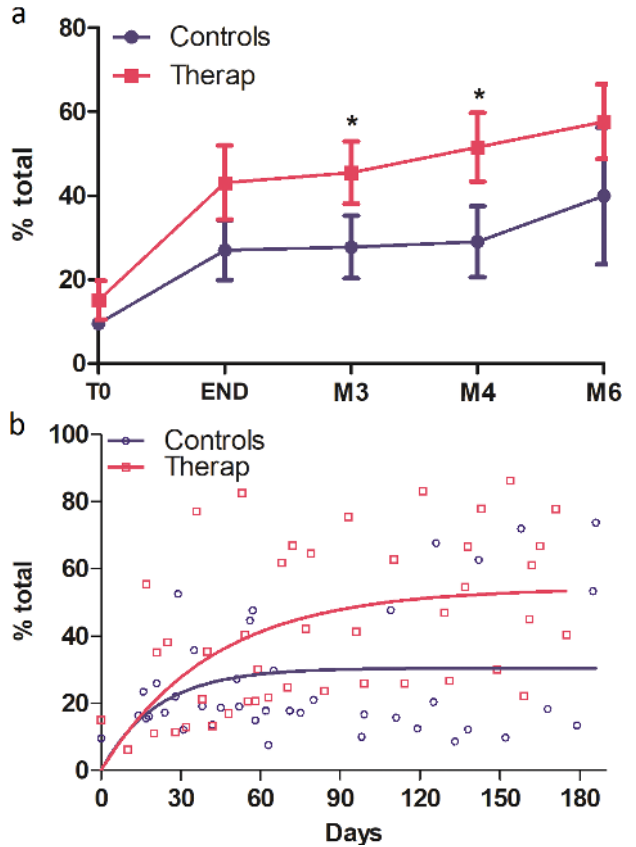


Fig. 2. Temporal evolution of the total 400p-HA test, expressed as percentage of recovery of the maximum score, for the therapeutic group (red dots) and the control group (blue dots); (a) mean difference with SD at fixed times: T0, END of intervention, M3, M4 and M6 poststroke. * $p<0.05$ Mann–Whitney comparison; (b) one-phase exponential modelling for the therapeutic group (red dots and curve) and the control group (blue dots and curve).

DISCUSSION

This proof-of-concept study demonstrated the feasibility of innovative motor training based on immersive visual feedback to improve upper limb function in a small population of subacute stroke patients. By using prerecorded videos of movements normally executed with a healthy limb, this technique provides, similar to mirror therapy, a realistic view of the attended movement from a first-person point of view (22). The main advantages of this technique, compared with

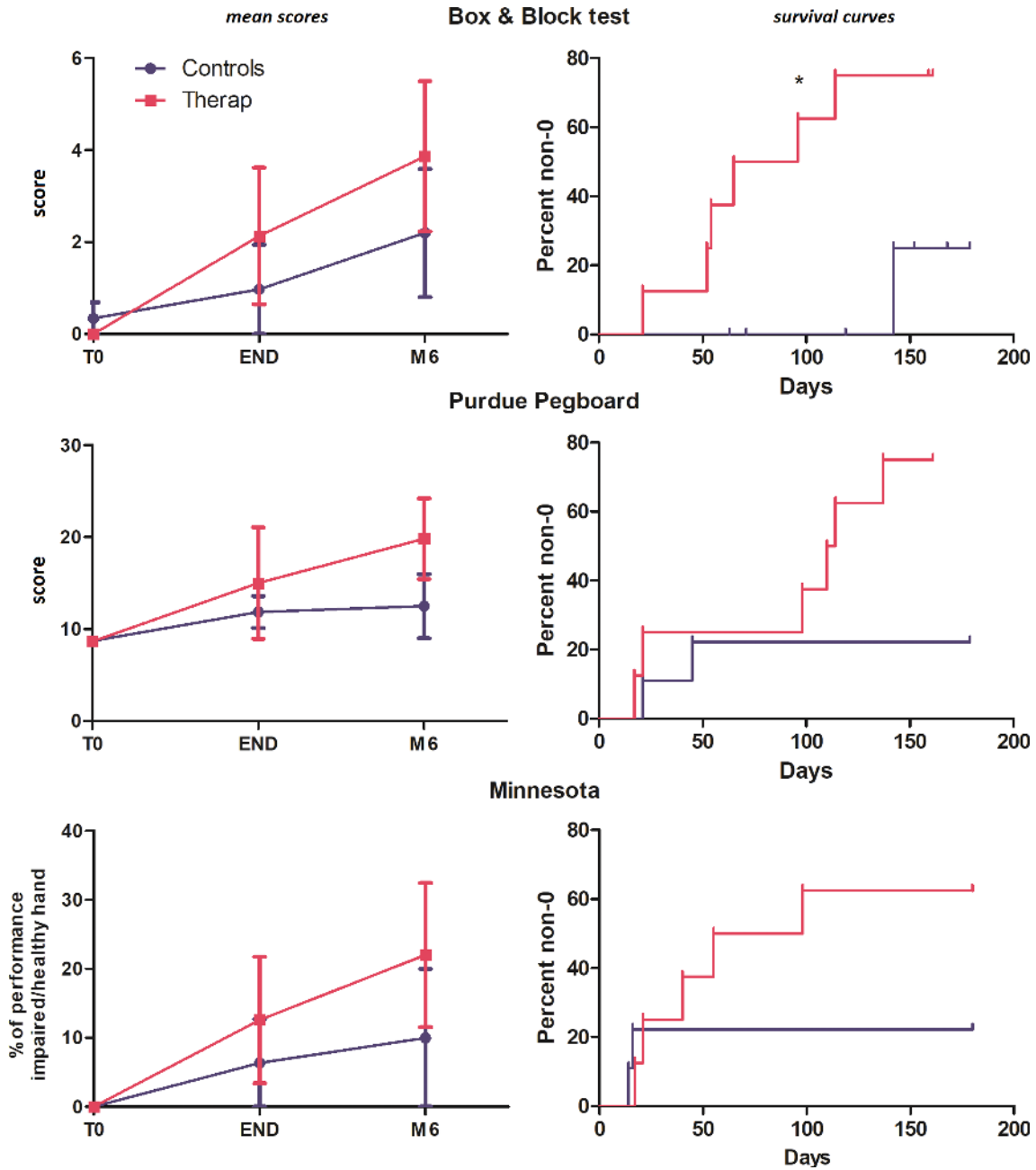


Fig. 3. Left column: temporal evolution for the 3 dexterity tests; right column: survival curves showing the % of participants recovering a non-0 score in the 3 dexterity tests.

mirror therapy, are that (i) the patient is fully focused on the impaired limb and does not have to produce concomitant movements with the healthy limb and (ii) the range of movements can be performed in a large prehensile space and is not limited by the mirror to the hemispace. The simplicity of the task to be performed and the ease of installation on the device probably explain the complete participation of the patients in this intensive training (200 movements per session) at an early subacute stage, less than a month after stroke, as they suffered from a complete motor deficit.

Although conducted on a small population (17 patients), this comparative study provides several positive results supporting the effectiveness of the training with corrected visual feedback, where the device delivers normally executed movements (therapeutic group), versus similar training with uncorrected feedback (control group), on top of a standard rehabilitation programme. The main positive result was obtained with the 400pt Hand Assessment test (400pt-HA), which was defined as the main outcome measure. The mean difference between groups (Mann–Whitney test) was

not significant at the end of the training programme and reached a significant level at 3 and 4 months, respectively around 15 and 20, which is superior to the estimated minimal clinically important difference of 6 (17). This delayed significant difference may, of course, result from the small power of this study but also from the course of motor recovery of the upper limb, which is considered maximal at 3 months, with a plateau after 3 months for most of the patients (3, 23, 24). For this reason, a change in the motor recovery curve due to an early intervention can be statistically detected later in the follow-up period, at the maximum recovery time of approximately 3 months, without questioning the causality of the intervention (5, 24). We may also consider that all the patients received in parallel a standard rehabilitation programme during the intervention period and also during the follow-up period (5 days a week during the inpatient stay, then 2–3 days a week as an outpatient). This standard rehabilitation programme, on top of the spontaneous recovery, also explains part of this continuous improvement after the end of the intervention, and its effect is balanced between groups. At the end of the follow-up period, both groups showed improvement, with a non-significant difference between groups, yet the therapeutic group showed significant improvement earlier. This IVS intervention, thus, may produce an acceleration of recovery, confirming the value of neurofeedback rehabilitation tools for upper limb recovery post-stroke, as supported by literature reviews (5). Because of the sufficient number of repeated measurements available for each patient, approximately 8 measurements were available for a complete follow-up until 6 months, and we were able to construct a recovery curve with the 400pt-HA assessments. This one-phase exponential modelling demonstrated that the therapeutic group reached a significantly greater plateau than the control group. This fitting with a one-phase exponential model is well established for the Fugl–Meyer upper limb test (FM-UL) (3). The 400pt-HA test is a complete and mixed assessment that tests, like the FM-UL test, a panel of elementary movements, and tests graduated functional reaching and grasping movements, like functional tests such as the ARAT. Here, we also showed that the metrological properties of 400pt-HA also respond to one-phase exponential modelling.

The mean scores of the secondary outcome measures, the Box & Block test (B&B) and dexterity test (Purdue, Minnesota), all supported better performance in the therapeutic group, but between-group comparisons at fixed times did not reach the significance threshold. This lack of significance not only results from the small number of patients but also results from a floor effect of the measure, with a mix of delayed ability to perform a non-0 score for some patients and

some patients who never gain this ability during the following period. Another statistical approach was then applied to take advantage of the repeated temporal measures available to test the time difference needed to recover the specific ability tested by each test: grasping and displacing a cube for the B&B test, placing a disc in a hole with the paralyzed hand for the placing test of the Minnesota, and placing a small pin in a hole for the Purdue Pegboard Test. We believe that this temporal approach, testing the time to recovery of a specific ability based on robust time-to-event statistics (survival curves), is a simple and sensitive approach that complements the classical performance comparison at fixed times and is very suitable for small-N studies such as this one. Using this temporal approach, we demonstrated that patients in the B&B therapy group had significantly shorter time-to-non-0 scores than patients in the control group. The Minnesota and Purdue tests did not reach the significance threshold. The B&B test, which is recommended in guidelines for post-stroke protocols (24), seems to be the most sensitive test for this temporal approach, probably because it is easier to perform than the Minnesota and Purdue tests, leading to a higher and suitable probability of success.

This study assessed the effectiveness of a video-based visual feedback therapy synchronized with a coherent motor imagery task (Intensive Visual Simulation) in enhancing motor recovery in the upper limb in subacute stroke patients. To our knowledge, 3 other computerized devices have been described more recently: computerized mirror therapy with augmented video feedback (ART system) provided by an avatar of the hand (25, 26); a camera-based mirror visual feedback device (CBMVF), which has also been tested for its ability to enhance upper-limb motor recovery in stroke patients (27); and a video-augmented wearable reflection device (28). Although mirror therapy (MT) has proven to be effective at improving upper-limb motor recovery in stroke patients (9), these 3 devices have also been proposed to overcome some limitations of MT practice with a sagittal mirror, such as posture pressure, lack of engagement, and sustained attention towards the mirror (29), which hinder treatment effects. The efficacy of these 3 devices has also been supported by proof-of-concept studies in stroke patients (26, 27). Compared with these devices, the IVS device combines all the advantages of these 3 devices, such as naturalistic first-person visual feedback in the frontal position, a large working space, a complete focus on the impaired limb, and a large possibility of training analytic and functional exercises.

Complementary to clinical arguments, Ding et al. (27) also conducted neurophysiological EEG recordings to investigate the change in EEG connectivity induced by CBMVF training, suggesting

improved local efficiency of communication in the visual, somatosensory, and motor areas induced by the therapy. Additional electrophysiological studies with IVS should also be conducted to highlight some of the innovative properties of the IVS training. An initial one is the comparison between unilateral work with IVS and bilateral work with MT. Unilateral versus bimanual training comprises 2 completely different motor tasks, activating different brain networks, which may be complementary approaches. A second characteristic of the IVS training is the possibility for the patient to control and modulate their motor task practised during the video display of movements: passive observation, motor imagery, or execution attempt. The control of this graded motor task is difficult to achieve with a simple mirror. It modulates the sensorimotor network activity (12) and may be useful to monitor at a patient level, for example with EEG recording, to personalize the training.

This clinical study, like most of the recovery studies on hemiplegic stroke, focused on motor recovery with repetitive and intensive motor training and the improvement of performance on analytic or functional motor tests (30). These research objectives underestimate the role of body representations, which are often altered in hemiplegic patients and need to be evaluated and rehabilitated (31). By providing a repeated visualization of our own body practising movements from the first-person point of view, IVS training may also contribute to restoring altered body representations, and this may be one dimension that underpins the efficacy of this technique. Studies with dedicated designs should be conducted to assess this specific dimension.

In conclusion, this controlled study demonstrated the feasibility and efficacy of a new video observational training method (IVS) for motor recovery in the upper limb in subacute stroke patients. The present data showed that, compared with an intervention with uncorrected visual feedback, intensive training with IVS for 6 weeks improved the global functioning of the impaired limb, as assessed by the 400p-HA test. A faster recovery of a non-0 score for the Box & Block test was also demonstrated. If these results are conclusive for the sample of this proof-of-concept study, the generalization of these results requires a confirmatory study conducted on a larger stroke population.

ACKNOWLEDGEMENTS

The authors would like to thank Ms Françoise Pineau, occupational therapist at University Hospital of Saint-Étienne, for her contribution to the planning and delivery of the intervention. The authors thank all the study patients for their contribution.

Conflict of interest declaration: Pascal Giroux is cofounder of the Dessintey Company. He was involved in designing the study and writing the manuscript. He was not involved in carrying out

the patient intervention, patient assessment, or data analysis.

Funding/financial support: Etienne Ojardias and Ahmed Adham received a 1-year research grant from the French Ministry of Health.

Ethical clearance: All methods were performed in accordance with the relevant guidelines and regulations. The protocol was approved by the ethics committee of the Saint-Étienne University Hospital (No. 200102-JV200125). All the included subjects gave written informed consent.

REFERENCES

1. Kyu HH, Abate D, Abate KH, Abay SM, Abbafati C, Abbasi N, et al. Global, regional, and national disability-adjusted life-years (DALYs) for 359 diseases and injuries and healthy life expectancy (HALE) for 195 countries and territories, 1990–2017: a systematic analysis for the Global Burden of Disease Study 2017. *Lancet* 2018; 392: 1859–1922. DOI: 10.1016/S0140-6736(18)32335-3
2. Clery A, Bhalla A, Rudd AG, Wolfe CDA, Wang Y. Trends in prevalence of acute stroke impairments: a population-based cohort study using the South London Stroke Register. Willey JZ, editor. *PLOS Med* 2020; 17: e1003366. DOI: 10.1371/journal.pmed.1003366
3. Vliet R, Selles RW, Andrinopoulou E, Nijland R, Ribbers GM, Frens MA, et al. Predicting upper limb motor impairment recovery after stroke: a mixture model. *Ann Neurol* 2020; 87: 383–393. DOI: 10.1002/ana.25679
4. Hayward KS, Kramer SF, Dalton EJ, Hughes GR, Brodtmann A, Churilov L, et al. Timing and dose of upper limb motor intervention after stroke: a systematic review. *Stroke* 2021; 52: 3706–3717. DOI: 10.1161/STROKEAHA.121.034348
5. Hatem SM, Saussez G, Della Faille M, Prist V, Zhang X, Dispa D, et al. Rehabilitation of motor function after stroke: a multiple systematic review focused on techniques to stimulate upper extremity recovery. *Front Hum Neurosci* 2016; 10: 442. DOI: 10.3389/fnhum.2016.00442
6. Thieme H, Morkisch N, Rietz C, Dohle K, Borgetto B. The efficacy of movement representation techniques for treatment of limb pain: a systematic review and meta-analysis. *J Pain* 2016; 17: 167–180. DOI: 10.1016/j.jpain.2015.10.015
7. Ramachandran V. The perception of phantom limbs. The D. O. Hebb lecture. *Brain* 1998; 121: 1603–1630. DOI: 10.1093/brain/121.9.1603
8. Ramachandran VS, Altschuler EL. The use of visual feedback, in particular mirror visual feedback, in restoring brain function. *Brain* 2009; 132: 1693–1710. DOI: 10.1093/brain/awp135
9. Thieme H, Morkisch N, Mehrholz J, Pohl M, Behrens J, Borgetto B, et al. Mirror therapy for improving motor function after stroke. *Cochrane Database Syst Rev* 2018; 7: CD008449. DOI: 10.1002/14651858.CD008449.pub3
10. Pollock A, Farmer SE, Brady MC, Langhorne P, Mead GE, Mehrholz J, et al. Interventions for improving upper limb function after stroke. *Cochrane Database Syst Rev* 2014; 2014: CD010820. DOI: 10.1002/14651858.CD010820.pub2
11. Barclay RE, Stevenson TJ, Poluha W, Semenko B, Schubert J. Mental practice for treating upper extremity deficits in individuals with hemiparesis after stroke. *Cochrane Database Syst Rev* 2020; 2020; 5: CD005950. DOI: 10.1002/14651858.CD005950.pub5
12. Sun Y, Wei W, Luo Z, Gan H, Hu X. Improving motor imagery practice with synchronous action observation in stroke patients. *Top Stroke Rehabil* 2016; 23: 245–253. DOI: 10.1080/10749357.2016.1141472
13. Giroux P, Sirigu A. Illusory movements of the paralyzed limb restore motor cortex activity. *NeuroImage*

- 2003; 20: S107–S111. DOI: 10.1016/j.neuroimage.2003.09.024
14. Mercier C, Sirigu A. Training with virtual visual feedback to alleviate phantom limb pain. *Neurorehabil Neural Repair* 2009; 23: 587–594. DOI: 10.1177/1545968308328717
 15. Gable C, Xenard J, Makiela E, Chau N. Evaluation fonctionnelle de la main. Bilan 400 points et tests chiffrés. *Ann Réadapt Médecine Phys* 1997; 40: 95–101. DOI: 10.1016/S0168-6054(97)83377-6
 16. Gable C, Kandel M, Moureau F, Beer L, Chau N, Paysant J. Étude de reproductibilité de la cotation du « Bilan 400 points », une mesure de capacité fonctionnelle de la main. *Chir Main* 2012; 31: 76–82. DOI: 10.1016/j.main.2012.01.008
 17. Konzelmann M, Burrus C, Gable C, Luthi F, Paysant J. Prospective multicentre validation study of a new standardised version of the 400-point hand assessment. *BMC Musculoskelet Disord* 2020; 21: 313. DOI: 10.1186/s12891-020-03303-4
 18. Mathiowetz V, Volland G, Kashman N, Weber K. Adult norms for the box and block test of manual dexterity. *Am J Occup Ther* 1985; 39: 386–391. DOI: 10.5014/ajot.39.6.386
 19. Ashford S, Slade M, Malaprade F, Turner-Stokes L. Evaluation of functional outcome measures for the hemiparetic upper limb: a systematic review. *J Rehabil Med* 2008; 40: 787–795. DOI: 10.2340/16501977-0276
 20. Chen H-M, Chen CC, Hsueh I-P, Huang S-L, Hsieh C-L. Test-retest reproducibility and smallest real difference of 5 hand function tests in patients with stroke. *Neurorehabil Neural Repair* 2009; 23: 435–440. DOI: 10.1177/1545968308331146
 21. Gloss DS, Wardle MG. Use of the Minnesota rate of manipulation test for disability evaluation. *Percept Mot Skills* 1982; 55: 527–532. DOI: 10.2466/pms.1982.55.2.527
 22. Morkisch N, Thieme H, Dohle C. How to perform mirror therapy after stroke? Evidence from a meta-analysis. *Restor Neurol Neurosci* 2019; 37: 421–435. DOI: 10.3233/RNN-190935
 23. Lundquist CB, Nguyen BT, Hvidt TB, Stabel HH, Christensen JR, Brunner I. Changes in upper limb capacity and performance in the early and late subacute phase after stroke. *J Stroke Cerebrovasc Dis* 2022; 31: 106590. DOI: 10.1016/j.jstrokecerebrovasdis.2022.106590
 24. Kwakkel G, Lannin NA, Borschmann K, English C, Ali M, Churilov L, et al. Standardized measurement of sensorimotor recovery in stroke trials: consensus-based core recommendations from the Stroke Recovery and Rehabilitation Roundtable. *Int J Stroke* 2017; 12: 451–461. DOI: 10.1177/1747493017711813
 25. Hoermann S, Hale L, Winser SJ, Regenbrecht H. Augmented Reflection Technology for Stroke Rehabilitation – A clinical feasibility study. *Proc. 9th Intl Conf. Disability, Virtual Reality & Associated Technologies (ICDVRAT)*, Laval, France, 10–12 Sept. 2012; ISBN 978-0-7049-1545-9
 26. Hoermann S, Ferreira dos Santos L, Morkisch N, Jettkowski K, Sillis M, Devan H, et al. Computerised mirror therapy with Augmented Reflection Technology for early stroke rehabilitation: clinical feasibility and integration as an adjunct therapy. *Disabil Rehabil* 2017; 39: 1503–1514. DOI: 10.1080/09638288.2017.1291765
 27. Ding L, Wang X, Chen S, Wang H, Tian J, Rong J, et al. Camera-based mirror visual input for priming promotes motor recovery, daily function, and brain network segregation in subacute stroke patients. *Neurorehabil Neural Repair* 2019; 33: 307–318. DOI: 10.1177/1545968319836207
 28. Kim H, Kim J, Jo S, Lee K, Kim J, Song C. Video augmented mirror therapy for upper extremity rehabilitation after stroke: a randomized controlled trial. *J Neurol* 2023; 270: 831–842. DOI: 10.1007/s00415-022-11410-6
 29. Jo S, Kim H, Song C. A Novel approach to increase attention during mirror therapy among stroke patients: a video-based behavioral analysis. *Brain Sci* 2022; 12: 297. DOI: 10.3390/brainsci12030297
 30. Santisteban L, Térémétz M, Bleton J-P, Baron J-C, Maier MA, Lindberg PG. Upper limb outcome measures used in stroke rehabilitation studies: a systematic literature review. *Plos One* 2016; 11: e0154792. DOI: 10.1371/journal.pone.0154792
 31. Risso G, Bassolino M. Assess and rehabilitate body representations via (neuro)robotics: an emergent perspective. *Front Neurobot* 2022; 16: 964720. DOI: 10.3389/fnbot.2022.964720

@ | D

RESEARCH

Open Access



Neural basis of lower-limb visual feedback therapy: an EEG study in healthy subjects

Ahmed Adham^{1,2,6*}, Ba Thien Le³, Julien Bonnal³, Hugo Bessagnet^{1,4}, Etienne Ojardias^{1,4}, Pascal Giraux^{1,2} and Pascal Auzou^{3,5}

Abstract

Background Video-feedback observational therapy (VOT) is an intensive rehabilitation technique based on movement repetition and visualization that has shown benefits for motor rehabilitation of the upper and lower limbs. Despite an increase in recent literature on the neurophysiological effects of VOT in the upper limb, there is little knowledge about the cortical effects of visual feedback therapies when applied to the lower limbs. The aim of our study was to better understand the neurophysiological effects of VOT. Thus, we identified and compared the EEG biomarkers of healthy subjects undergoing lower limb VOT during three tasks: passive observation, observation and motor imagery, observation and motor execution.

Methods We recruited 38 healthy volunteers and monitored their EEG activity while they performed a right ankle dorsiflexion task in the VOT. Three graded motor tasks associated with action observation were tested: action observation alone (O), motor imagery with action observation (OI), and motor execution synchronized with action observation (OM). The alpha and beta event-related desynchronization (ERD) and event-related synchronization (or beta rebound, ERS) rhythms were used as biomarkers of cortical activation and compared between conditions with a permutation test. Changes in connectivity during the task were computed with phase locking value (PLV).

Results During the task, in the alpha band, the ERD was comparable between O and OI activities across the precentral, central and parietal electrodes. OM involved the same regions but had greater ERD over the central electrodes. In the beta band, there was a gradation of ERD intensity in O, OI and OM over central electrodes. After the task, the ERS changes were weak during the O task but were strong during the OI and OM (Cz) tasks, with no differences between OI and OM.

Conclusion Alpha band ERD results demonstrated the recruitment of mirror neurons during lower limb VOT due to visual feedback. Beta band ERD reflects strong recruitment of the sensorimotor cortex evoked by motor imagery and action execution. These results also emphasize the need for an active motor task, either motor imagery or motor execution task during VOT, to elicit a post-task ERS, which is absent during passive observation.

Trial Registration NCT05743647

Keywords Video feedback therapy, Lower limb, EEG, Rehabilitation, Mirror neuron system

*Correspondence:

Ahmed Adham

ahmed.adham@chu-st-etienne.fr

Full list of author information is available at the end of the article



© The Author(s) 2024. **Open Access** This article is licensed under a Creative Commons Attribution 4.0 International License, which permits use, sharing, adaptation, distribution and reproduction in any medium or format, as long as you give appropriate credit to the original author(s) and the source, provide a link to the Creative Commons licence, and indicate if changes were made. The images or other third party material in this article are included in the article's Creative Commons licence, unless indicated otherwise in a credit line to the material. If material is not included in the article's Creative Commons licence and your intended use is not permitted by statutory regulation or exceeds the permitted use, you will need to obtain permission directly from the copyright holder. To view a copy of this licence, visit <http://creativecommons.org/licenses/by/4.0/>. The Creative Commons Public Domain Dedication waiver (<http://creativecommons.org/publicdomain/zero/1.0/>) applies to the data made available in this article, unless otherwise stated in a credit line to the data.

Introduction

In recent years, innovative new techniques have emerged in the field of neurological rehabilitation. Among these techniques, visual feedback therapies distinguish themselves by their ease of use, low cost and efficacy. The aim of visual feedback therapies is to provide visual feedback of a movement correctly performed by the affected limb to elicit cortical activation.

Historically, mirror therapy was the first rehabilitation technique used to offer patients subjective visual feedback of correct movement performed by a paretic limb [1, 2]. In lower-limb mirror therapy, a mirror is placed between the subject's legs; the subjects are invited to perform a movement with their healthy leg while observing the mirror's reflection, which gives them the subjective illusion of moving their paretic leg. During the last decade, Video Observational Therapy (VOT) and Virtual Reality have emerged as alternatives to mirror therapy. In these therapies, the subject observes on a screen or in a virtual reality headset a projection of the paretic lower limb performing the action. This projection can be made by using a pre-recorded video of the healthy limb performing the action flipped on the horizontal axis (mirror image) in video observational therapy or by using a robotic avatar in virtual reality. According to multiple meta-analyses, lower limb visual feedback techniques (mirror therapy, VOT, virtual reality) have been shown to improve lower limb function in stroke patients. Mirror therapy has proven to be effective at improving mobility, motor recovery, balance, spasticity, step length and walking speed in stroke patients [3–5], hemineglect [6] and pain [7]. Video feedback therapies (VOT and virtual reality) have shown improvements in dynamic and static balance [8] and in the composite criterion of mobility (10-m walk test, time up and go, functional ambulation category) [9].

Neurophysiological studies carried out on the upper limb provide us with a better understanding of the effects of these therapies. Observing the action during mirror therapy reduces beta rhythms in sensorimotor regions, indicating a rebalancing of the interhemispheric balance [10, 11]. These results were also found for video observational therapy on the upper limb [12]. This motor facilitation is associated with an increase in cortico-spinal excitability in the mirror therapy of the upper limb [13]. This stimulation of sensory-motor regions is achieved through recruitment of the mirror neuron system [14]. There are also changes in cortico-cortical connectivity, particularly between motor areas, the posterior cingulate cortex, the precuneus and visual areas, linked to visuospatial attentional recruitment [15]. For the lower limb, however, we have little physiological data. Mirrored visual feedback leads to recruitment of the ipsilesional

sensory-motor cortex during ankle dorsiflexion movement on fMRI [16]. There is also a reorganization of fMRI functional connectivity within the sensorimotor cortex during passive action observation with mirrored visual feedback [17]. However, there is little information on the modulations of EEG rhythms (desynchronizations, beta rebounds, functional connectivity) induced by visual feedback rehabilitation of the lower limb, especially via video feedback techniques. As the healthy limb remains immobile in VOT, this therapy is also a better model than mirror therapy for specifically studying the brain dynamics induced by visual feedback since it allows us to study the effects of pure visual feedback and motor intention of the trained limb, uncontaminated by the cortical activity induced by healthy limb movement in mirror therapy. Furthermore, VOT gives the subjects visual feedback of their own limb movement (appearance, etc.), thus maximizing the embodiment of the therapy, which is less common in virtual reality with a robotic avatar.

Interestingly, a multitude of ways in which the patient can work on these visual feedback therapies exist for rehabilitation. The subject could simply observe the visual feedback passively (simple observation, O). They could also observe it while attempting to produce motor imagery of the movement (motor imagery, OI). Finally, the subject could observe visual feedback while attempting to reproduce the movement (motor execution, OM) [18]. These task differences are significant from a physiological point of view. Indeed, in the upper limb, under conditions similar to first-person VOT, EEG differences have been shown between execution and motor imagery [19]. Similarly, in fMRI, the gradation of engagement in action (OI/OM) is associated with increased activation of sensory-motor areas [20]. Despite these results for the upper limb, we have few points of comparison in the literature on the neurophysiological differences between the O, OI and OM conditions for lower limb tasks in rehabilitation.

The aim of this study was to explore the EEG correlates of video feedback therapy. To this end, we studied a cohort of 38 healthy subjects who passively observed (O) or observed while imagining (OI) or observed while performing (OM) a dorsiflexion movement of their right ankle while performing computerized first-person video observational therapy. EEG Biomarkers in the alpha and beta bands (Event related desynchronisation and Event related synchronisation) were studied and compared between conditions and between groups.

Event related desynchronisation (ERD) is defined as a decrease of power in the alpha and beta band during the movement, while the Event related synchronization (ERS or beta rebound) refers to a post-movement synchronization period. ERD and ERS rhythms are generally

observed above the motor regions contralateral to the limb producing the movement. More specifically, alpha desynchronization is generally known to reflect recruitment of mirror neurons [21] and to support somatosensory rhythms [22, 23], while beta desynchronization is also often associated with the recruitment of motor cortex [23, 24]. Beta rebound, on the other hand, is associated with post-movement motor validation phenomena [25, 26]. Therefore, as the subjects observe in all conditions (O, OI, OM) the visual feedback of their moving limb, we hypothesized a systematic recruitment of the mirror neurons system, leading to an alpha band desynchronization over sensori-motor regions in all conditions. We also hypothesized a stronger recruitment of sensorimotor cortex in OI task as compared to O, and in OM task as compared to O and OI, due to the addition of motor imagery and motor execution to action observation. This would be reflected by a gradation in the ERD strength ($OM_{ERD} > OI_{ERD} > O_{ERD}$). We expected the same dynamics for beta ERS.

Functional connectivity was also studied between conditions, to identify and describe network organization changes over time for lower limb movements. Having few points of comparison in the literature, we had no assumptions about the results.

Materials and methods

Participants

Thirty-eight healthy volunteers aged between 20 and 73 y.o. (age: 45.5 y.o. \pm 20 y.o.) participated in the study. There were 26 males and 12 females, 25 subjects aged younger than 60 y.o. and 13 subjects aged older than 60 y.o. Prior to the recording, the subjects' handedness was assessed with the Edinburgh Handedness Inventory [27]. Patients who presented with neurological disease or psychiatric illness or who were receiving neuro-modulatory treatments were excluded from our study. Participants signed a consent form prior to participating in the study. The study was conducted in accordance with the Declaration of Helsinki and was approved by the ethics committee "Comité de protection des personnes Sud-Est III" (2022-A02375-38) and registered in Clinical Trials (NCT05743647).

Material

Participants were comfortably seated in a standardized (hip knees and ankles flexed at a 90° angle) position on a chair in front of a height-adjustable table on which they trained on VOT. We used the IVS4™ (Dessintey Co., France) device (Fig. 1), which uses a large screen precisely placed between the subject's eye and the trained hand. The device is equipped with a camera placed in front of the legs. The camera recorded the left lower limb



Fig. 1 First-person lower-limb video feedback therapy—IVS4—DESSINTEY

movement of the subject. The recorded videos were mirrored and later projected on a screen, giving the subject a visual illusion that the movement was performed by the right limb. The advantage of this device is that it can easily provide first-person feedback congruent with the visual axis, thus maximizing subjective illusions. It is to be noted that the subjects didn't directly perform a right foot movement, despite being healthy controls, since the VOT device automatically mirrors the image.

EEG data were recorded with a 32-channel ENOBIO™ device (Neuroelectrics Co., Spain) placed in a standard position on the head of the subjects with Ag/AgCl electrodes. The data were sampled at 500 Hz, and the impedance was maintained below 5 kΩ. The protocol displayed on the IVS panel was designed with Open-Sesame software [28]. An Open-Sesame TTL trigger was sent on the EEG recording at the beginning of each experimental condition for precise synchronization of the visual cues in further analysis.

Experimental device

Subjects underwent a single EEG recording session. Prior to the experiment, we recorded a video of the subject's left foot performing a movement of ankle dorsiflexion. The video was then manually extracted from the VOT device, mirrored, cut and resampled in Adobe Premiere Pro for the whole movement to last exactly two seconds, with two seconds of pause before and after the movement. The movement displayed and performed by the subjects via both techniques consisted of smooth dorsiflexion of the right foot (one second) immediately followed by flexion of the foot (one second). At rest, the foot was on the ground and completely relaxed. The timing of the whole video was as follows: two seconds of

presentation of the right foot at rest, two seconds of task, and two seconds of rest (Fig. 2). We added a randomized time of 500 to 1000 ms at the end of each 6-s video.

Each session was divided into three sub-sessions, separated by a one-minute pause. In each sub-session, the subject performed thirty movements: (1) action observation alone, (2) action observation + motor imagination, and (3) action observation + motor execution. The order of the sub-sessions was randomized between subjects.

Data analysis

Time–frequency analysis

After filtering (0.5–70 Hz bandpass filter, 50 Hz notch filter), the data were segmented into 6-s epochs. The epochs containing a peak-to-peak voltage above 100 mV were considered too noisy and rejected. Then, a visual inspection of the data was conducted while rejecting the remaining noisy epochs, and bad channels were interpolated. Approximately 80% of the data in our study were considered valid. The data were referenced to an infinite source with the REST algorithm [29]. Ocular artifacts were removed via independent component analysis (ICA). This whole process was conducted with

the MATLAB EEGLab Toolbox (UC San Diego, USA, 30). After this pre-treatment, for each epoch and each EEG channel, time–frequency maps were generated. We implemented time–frequency analysis by convolving the signal with a set of complex Morlet wavelets, defined as complex sine waves tapered by a Gaussian function. The frequencies of the wavelets ranged from 2 to 40 Hz in 80 linearly spaced steps. The full width at half maximum (FWHM) ranged from 1000 to 200 ms [31, 32].

For each electrode, ERD (event-related desynchronization) and ERS (event-related synchronization) magnitudes were then expressed as a percentage of the power in the defined time and frequency window relative to the power measured during the corresponding baseline [33] and were expressed as a percentage change. The baseline was chosen between 1500 and 500 ms before the onset of the movement. We analyzed (i) alpha band power during the task (2500–3500 ms) to determine the alpha component of the Mu motor rhythm (Alpha ERD), (ii) beta band power during the task (2500–3500 ms) to obtain the beta component of the Mu motor rhythm (Beta ERD), and (iii) beta band power after the task (4000–5000 ms) to obtain the post-movement beta rebound power (ERS). We chose


<i>Duration:</i>	2 seconds	1 second	1 second	2 seconds + 500 to 1000 mS
<i>Video</i>	Right Foot at Rest	Right Foot Dorsiflexion	Right Foot coming back to rest position	Right Foot at Rest
<i>Visual feedback:</i>				
Action Observation alone (O)	Rest	Passive video observation		Rest
Action Observation + Motor Imagery (OI)	Rest	Video observation + Motor Imagery		Rest
Action Observation + Motor Execution (OM)	Rest	Video observation + Motor Execution		Rest

Fig. 2 Experimental paradigm for O (Action Observation alone), OI (Action Observation + Motor Imagery) and OM (Action Observation + Motor Execution M) conditions

to remove the first and last 500ms around the task in the time–frequency analysis since during the motor execution condition (OM) the subjects weren't always perfectly synchronized with the video in the beginning or ending of the movement: some subjects started or ended the movement a little earlier or later, which may have confused statistical analysis.

The alpha and beta central frequency bands were adaptively adapted to each subject: the mean and full-width at half-maximum of the alpha and beta spectral distributions were defined for each subject as described in Stolk et al. [23] using a two- or three-way Gaussian model depending on the presence or absence of slow theta-delta waves. On average, the alpha band central frequency was 9.3 ± 1.3 Hz, and the beta band central frequency was 16.2 ± 1.7 Hz. This adaptive central frequency choice diminished the overlaps between signals in the alpha and beta bands that can occur with a canonical choice of frequency bands.

Connectivity analysis

Connectivity analyses were performed before and during the task for each subject. First, the broadband time-domain source signals were bandpass filtered in the alpha or beta central frequency for each subject. A space Laplacian filter was applied to the data to minimize the effects of volume conduction [34]. A Hilbert transform was then applied to the data before assessing connectivity with the phase locking value (PLV). The PLV is a normalized value that gives for each pair of electrodes a value ranging from 0 (no phase locking) to 1 (complete phase locking) and is defined by Eq. (1), from [35], where n indexes the trial number and N is the total number of trials.

Equation 1: Phase locking value formula, from Aydore et al.

$$\widehat{PLV}_{sample} \triangleq \left| \frac{1}{N} \sum_{n=1}^N e^{j\Delta\varphi_n(t)} \right| \quad (1)$$

For each electrode, we computed the connectivity strength, defined as the sum of weights of links connected to the node. We then subtracted the connectivity strength map during the movement from the connectivity strength map before the movement to visualize how connectivity changed during and after the movement compared to the baseline. We also plotted maps of the individual links that increased by more than 2 standard deviations compared with the average change in the PLV.

Statistical comparison

For the time–frequency and connectivity statistical comparisons, we compared the different conditions with a nonparametric permutation test (10,000 permutations,

$p < 0.025$, 36). Multiple comparison correction was performed with a Holm–Bonferroni correction. To ease the visualization of the data, we plotted cortical maps showing the power modifications expressed as percentages of change only in regions with suprathreshold significant differences.

Results

Time–frequency and connectivity maps are shown in Figs. 3, 4, 5, 6. Tables presenting the quantitative data from the time–frequency analyses are available in the supplementary materials (Tables 4, 5 and 6). In this section, ERD and ERS are expressed in percent change. The sensor names and positions can be found in the Table 1 of the Supplementary Materials.

Changes in power during the task

In the alpha band during the task, we observed desynchronization in O, involving the centro-frontal, central left, and parietal electrodes. In the OI condition, desynchronization involved the fronto-central, bilateral central and parietal electrodes. In the OM condition, desynchronization was much more diffuse and powerful and was mainly centered on C3 (central left, -22.4% —CI95 [-29.13 ; -15.67]) and C4 (central right; -17.45% —CI95 [-25.19 ; -9.7]). Analysis of the Cz band-power time course showed that there was Cz desynchronization in all conditions, with gradations between O, OI and OM (-8.53% —CI95 [-12.7 ; -4.37] in O; -9.1% —CI95 [-15.2 ; -3] in OI, and -16.21% —CI95 [-22.41 ; -10] in OM). However, in the alpha band, this Cz desynchronization remained less powerful than C3 desynchronization in all conditions (stronger C3 desynchronization).

Statistical analysis revealed no differences between the O and OI maps but confirmed that desynchronization was more powerful in the OM condition above the central and precentral electrodes than in the O and OI conditions (Fig. 3). Additional data can be found in tables 2 and 4 of Supplementary Materials.

In the beta band, in the O condition, the desynchronization was very weak, mainly over left central and the left parietal cortex (for C3 -10.81% ; CI95 [-16.6 ; -5.03], for CP5 -10.68% ; CI95 [-17.33 ; -4.02]). In the OI condition, the desynchronization recruited bilateral central, precentral and parietal electrodes and appeared stronger than in the O condition (for Cz -12.73% ; CI95 [-17.76 ; -7.7] in OI, versus -8.99% ; CI95 [-13.68 ; -4.29] in O). In the OM condition, the desynchronization was mainly centered on centro-parietal electrodes and appeared much stronger than in the O and OI conditions (for exemplar, for C3: -24.8% ; CI95 [-31.37 ; -18.24] in OM).

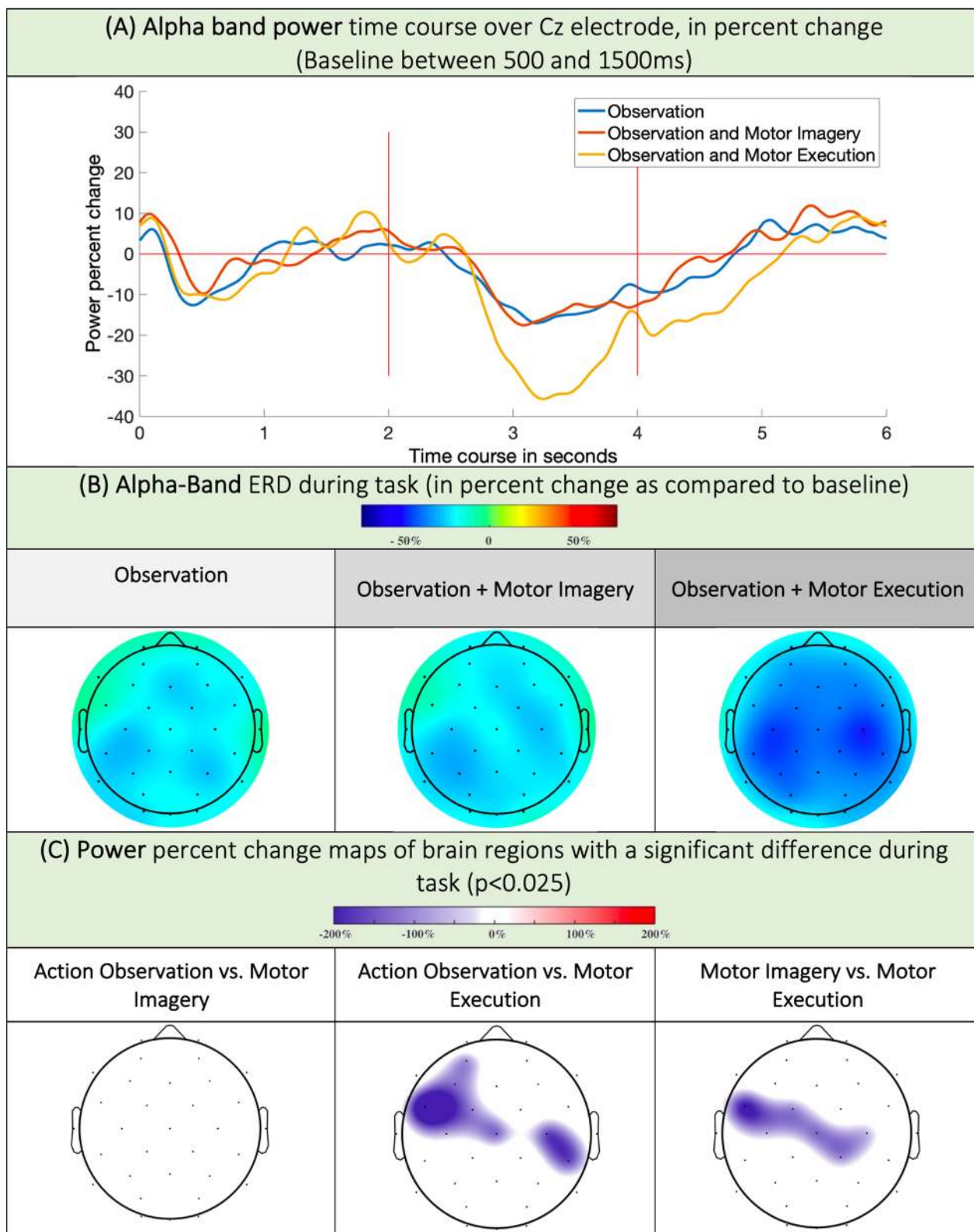


Fig. 3 **A** Alpha band power time course, expressed as the percent change relative to the baseline (500-1500ms) band power in all conditions. **B** ERD maps in the alpha band during movement in the O, OI and OM conditions. **C** ERD relative magnitude in regions with statistically relevant changes in the alpha band. A blue color means the ERD was stronger in condition 2 versus condition 1 (i.e.: stronger ERD in Motor Execution than in Action Observation over Cz)

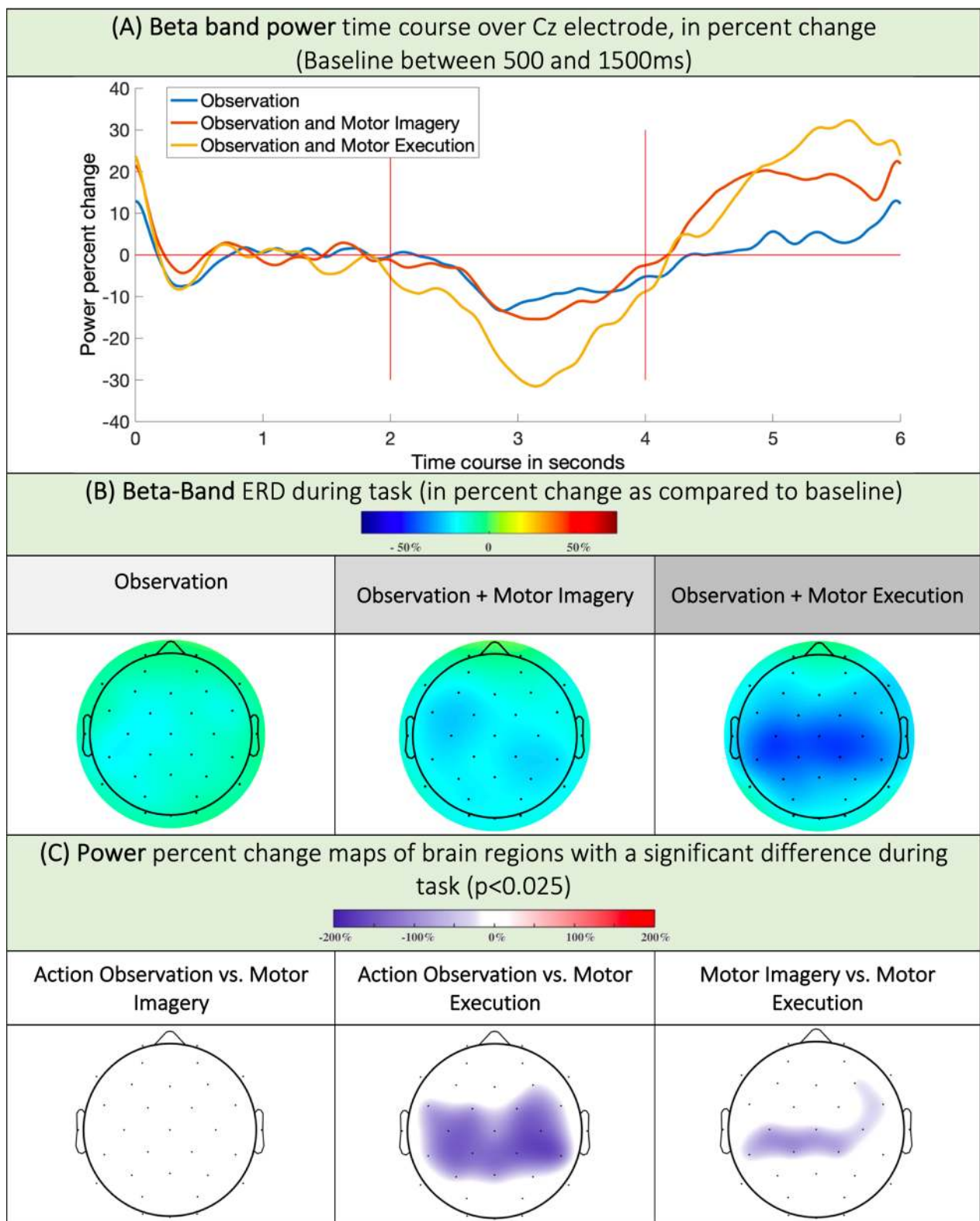


Fig. 4 **A** Beta band power time course, expressed as the percent change relative to the baseline (500-1500ms) band power in all conditions. **B** ERD maps in the beta band during movement in the O, OI and OM conditions. **C** ERD relative magnitude in regions with statistically relevant changes in the beta band. A blue color means the ERD was stronger in condition 2 versus condition 1 (i.e.: stronger ERD in Motor Execution than in Action Observation over Cz)

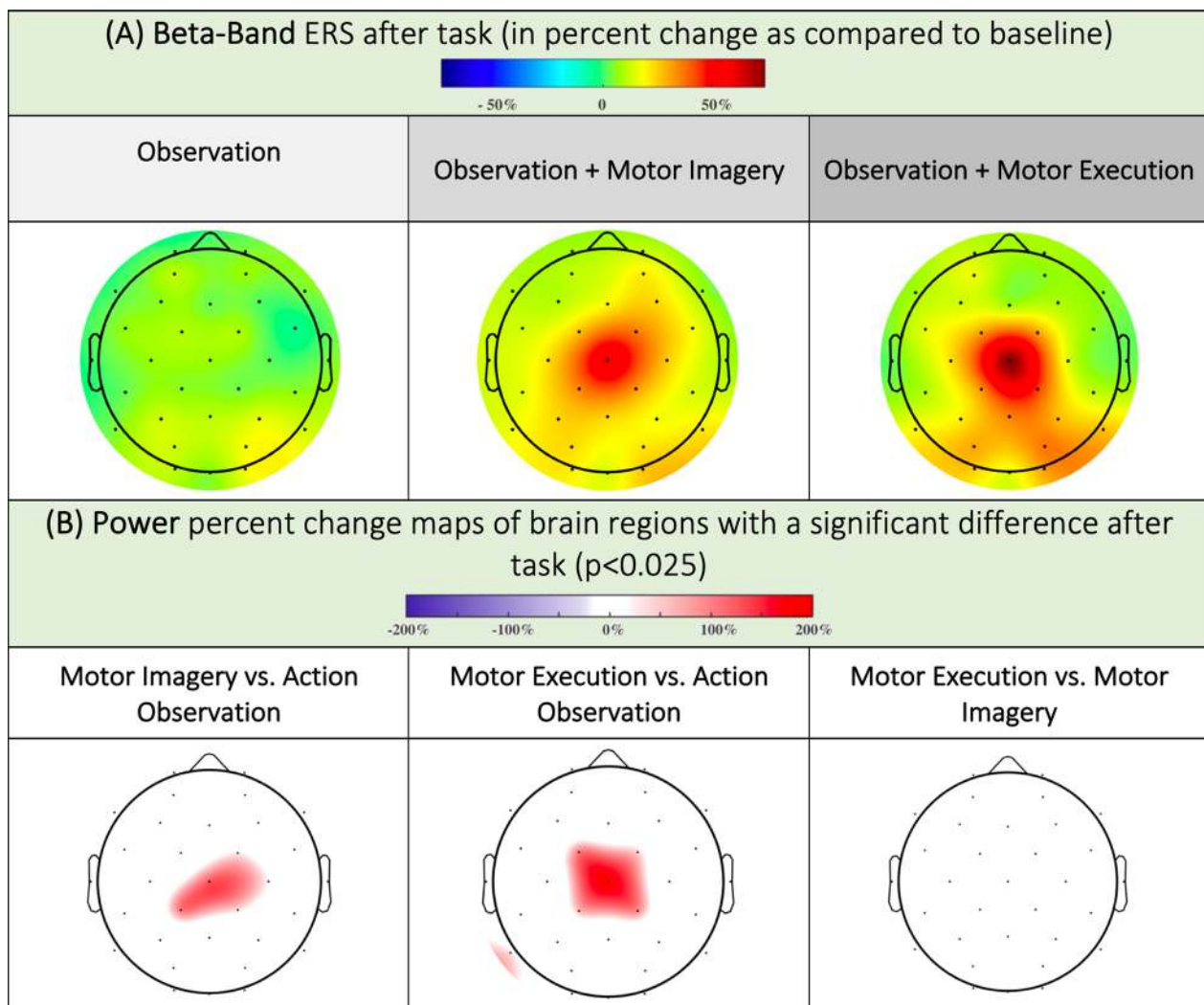


Fig. 5 A ERS maps in the beta band during movement in the O, OI and OM conditions (B) ERS relative magnitude in regions with statistically relevant changes in the beta band. A red color means the ERS was stronger in condition 1 versus condition 2 (Stronger ERS in Motor Execution than in Action Observation over Cz and stronger ERS in Motor Imagery than in Action Observation over Cz)

Statistically, no difference was observed between the O and OI conditions, despite visually visible differences in the time–frequency maps. However, we confirmed a more powerful desynchronization above the bilateral precentral, central, parietal, and parieto-occipital electrodes in the OM condition than in the O condition. Desynchronization was also greater in the OM than in the OI, but only above the central and parietal electrodes but not in the precentral electrodes (Fig. 4). Additional data can be found in tables 3 and 5 of Supplementary Materials.

Changes in power after the task

After the execution of the task, we observed a powerful rebound in the OI and OM conditions. The statistical

analysis confirmed this result, with a significant difference centered on the Cz electrode (vertex) in the OI and OM conditions compared to O (for Cz: 31.87%; CI95 [18.84; 44.9] in OM versus 3.51; CI95 [6.5; 0.53] in O). There was also a visible beta rebound in the OM above the parieto-occipital electrodes (PO3: 17.59%; CI95 [10.1; 25.08], PO4: 15.27%; CI95 [9.1; 21.44]). We found no difference in rebound intensity between OIs and OMs (Fig. 5) according to the Bonferroni correction. However, without Bonferroni correction, the difference was significant, with a stronger ERS in the OM than in the OI over the Cz ($p < 0.025$). The time course of the rebound in the beta band is shown in Fig. 4A. Additional data can be found in tables 3 and 6 of Supplementary Materials.

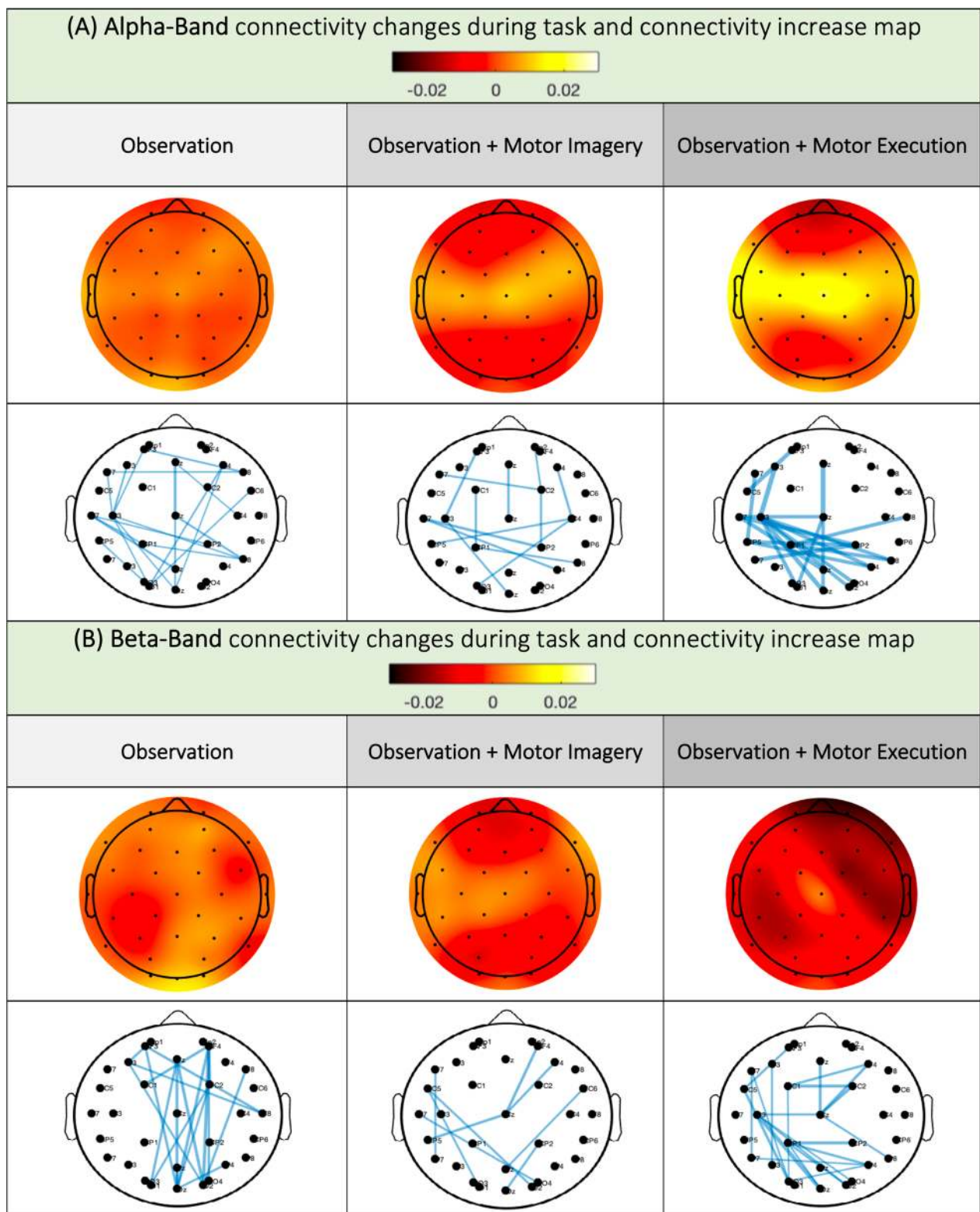


Fig. 6 Changes in the PLV in the alpha (A) and beta (B) bands during movement compared to before movement

Changes in connectivity during the task

In the alpha band, we observed an increase in connectivity strength compared to connectivity before the task in O, OI and OM, above the C3, Cz, and C4 electrodes, with the greatest increase in connectivity occurring during OM conditions. Judging from the links maps, in all 3 conditions, there seemed to be strong left centro-parieto-occipital links.

In the beta band, we observed increased connectivity in the occipital regions in O and no clear change in connectivity above C3, Cz or C4. In the OI, we observed a clear increase in connectivity at Cz and C3. In the OM, there was a clear increase in connectivity above the Cz electrode, with a decrease in connectivity in the right prefrontal and left parietal regions. Interestingly, in the O condition, the links' map showed an increase in fronto-occipital links, while in the OI and

OM conditions, we again found a strong left-central-parietal-occipital link (Fig. 6).

For alpha and beta band connectivity, statistical analysis did not reveal any differences, probably because of high inter-subjects' variability and very tenuous connectivity variations (Supplementary Materials, Table 7A and Table 8A).

Connectivity changes after task

After the task, compared to the pre-task connectivity, we found an increase in the alpha band connectivity in the frontal, parietal and occipital areas with a gradation between O, OI and OM. The connectivity was unchanged in the central and precentral areas. Beta band connectivity after the task showed an increase in connectivity in the prefrontal and occipital areas in O. In OI and OM, the connectivity was unchanged, even above the Cz

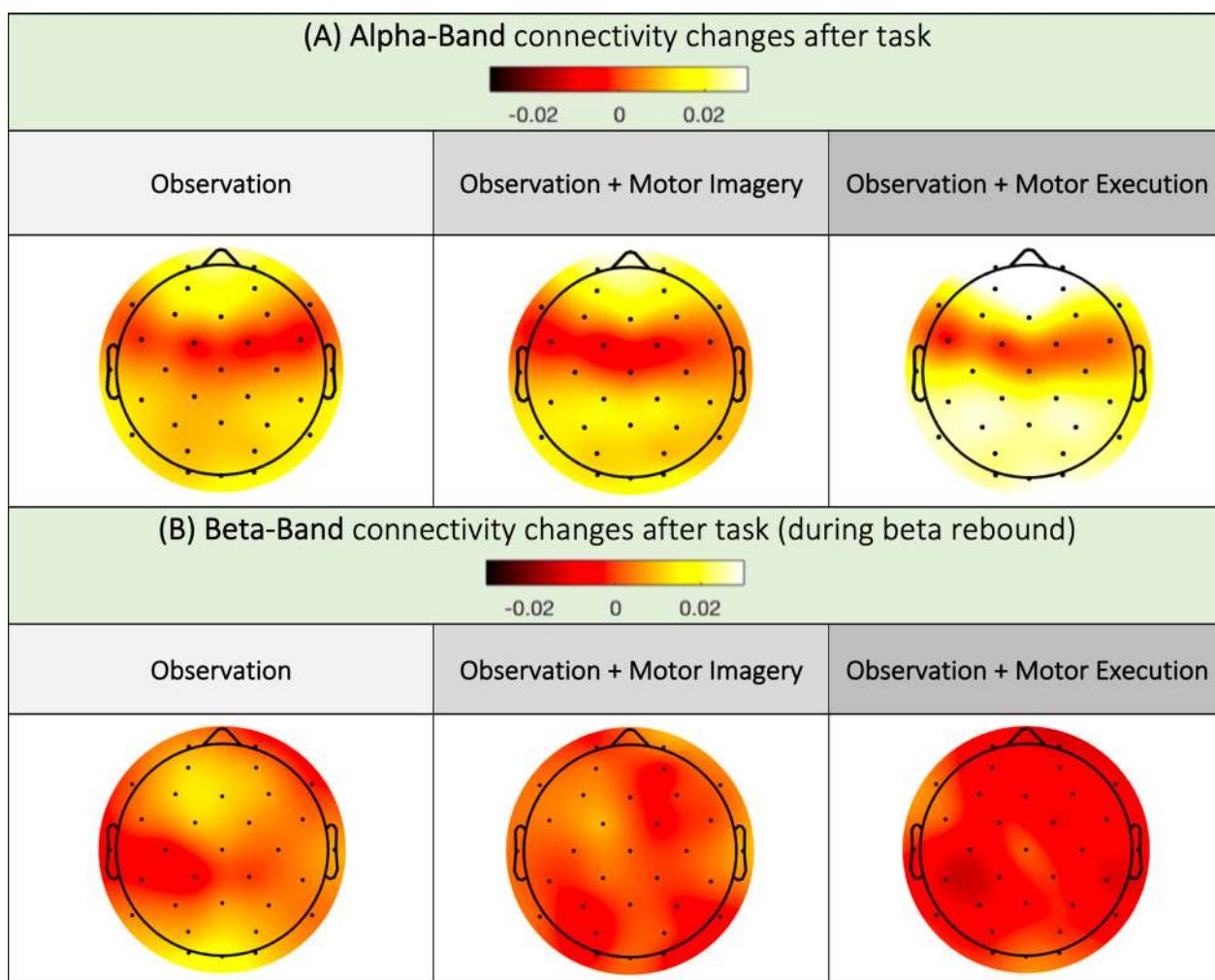


Fig. 7 Changes in the PLV in the alpha (A) and beta (B) bands after movement compared to before movement

electrode (Fig. 7). The statistical analysis showed no difference between conditions. Additional data is provided in Supplementary Materials (Table 7B and Table 8B).

Discussion

In the course of this work, for the first time, to our knowledge, we studied motor rhythms via electroencephalography during video feedback therapy of the lower limb. During the task, in the alpha band, we found a comparable ERD in O and OI over precentral, central and parietal electrodes. In the OM, the ERD involved the same regions but was stronger over central electrodes. In the beta band, there was a gradation of ERD intensity in O, OI and OM over central electrodes. After the task, the ERS (beta rebound) changes were weak during the O task but were strong in the OI and OM (Cz) groups, with no differences between the OI and OM groups.

Recruitment of the mirror neuron system

In our study, in the O condition, we found topographies similar to those in the literature, with bilateral central and parietal desynchronization [37]. However, we observed no difference between the O and OI conditions, particularly in the parietal regions, while other works found greater alpha desynchronization in an observation task than during imagery alone [37]. Moreover, in the OM condition, the topography of desynchronization was bilateral and comparable to that in the O and OI conditions but with stronger desynchronization in the precentral and central regions; however, in a high-density EEG study, alpha desynchronization during a motor task without visual feedback led to centro-parietal recruitment only contralateral to movement [38]. These differences are probably due to the addition of an action observation task to the motor imagery and execution task. This phenomenon has already been shown in fMRI data of upper limb movements, where the addition of action observation to a motor task results in bilateral centro-parieto-occipital recruitment, whereas the motor task alone was much more lateralized [39]. We assumed that this phenomenon was linked to the recruitment of mirror neurons. Indeed, above the sensory-motor regions, alpha band desynchronization is linked to Mu desynchronization [40]. The Mu rhythm is a well-known EEG rhythm containing two independent components, one in the alpha band and one in the beta band, encoding different parameters related to motricity [23]. In the alpha band, Mu desynchronization is generally considered to indicate the activity of the mirror neuron system (MNS, 21); this activity is present not only during action observation, motor imagery, and motor execution but also in other more complex tasks recruiting mirror neurons, notably in social cognition [41]. Mu rhythm is used as a biomarker

of MNS recruitment and is generated around the centro-parietal regions [42]. The observation of bilateral, centro-parietal Mu desynchronization in our O, OI and OM conditions suggested that the observation of action in video therapy in the lower limb results in recruitment of the mirror neuron system, with activation of a bilateral centro-parietal network, which we also observe in connectivity. This recruitment of the mirror neuron system has been described in mirror therapy, notably for the upper limb in healthy subjects but also for stroke patients [11, 43, 44]. For the lower limb VOT, MNS recruitment has not been documented to our knowledge.

In the OM condition, we observed significant desynchronization in the precentral and central regions compared with the O and OI conditions. It is difficult to conclude whether this greater desynchronization reflects an increase in the activity of mirror neurons or whether it is linked to other phenomena involved in motor planning or execution. Indeed, during a movement, the Mu rhythm is involved in the integration of the movement's somatosensory parameters [23], which may enhance desynchronization in the OM task. Similarly, although there are many similarities between the observation, imagery and motor execution networks, we know that there are also some differences since, according to fMRI, only action execution systematically recruits the primary motor cortex [46]. Therefore, although it is logically expected that motor execution leads to desynchronizations of greater intensity than motor observation or imagery through greater cortical recruitment, we must remain cautious about the precise interpretation of the neurophysiological mechanism at the source of this greater alpha desynchronization in OM.

One of the pitfalls of interpreting Mu rhythms is contamination by alpha occipital activity during signal analysis, which is present in the same frequency band [41]. In this work, we did not observe desynchronization in the occipital regions, probably because the subjects were constantly focusing their visual attention on the screen. Additionally, desynchronizations seem to emerge strictly from the central and parietal regions, making the hypothesis of contamination of the observed centro-parietal desynchronization by the alpha-occipital less plausible.

Modulation of beta activity according to the motor task

In O, we observed a weak, left parietal beta ERD. In the OI, the beta ERD was bilateral and centroparietal, and in the OM, the beta ERD was intense in the bilateral centro-parietal regions. In O and OI patients, statistical analysis revealed no difference in the intensity of desynchronization. Interestingly, in OM, there was an increase in desynchronization in the motor, premotor and parietal regions

compared to O. A comparison of OM and OI showed only an increase in desynchronization with respect to the central and parietal regions in favour of OM.

Beta ERD corresponds to disinhibition of somato-motor neuronal populations [23]; for example, there is a correlation between motor response intensity and desynchronization strength in stroke patient populations [24]. For lower limb movements, the beta ERD is classically localized on the vertex opposite to the moving limb [38]. Thus, since the subjects are passive and do not perform any motor planning or motor execution tasks, we did not find any clear desynchronization in O. Additionally, in the OM condition, as the subjects performed a motor task, they recruited the premotor (motor planning) and parietal (integration of proprioceptive feedback) regions, where beta desynchronization was significantly increased compared to that in the O condition. Conversely, the OI and OM comparisons revealed differences only in centro-parietal regions and not in prefrontal regions. This is probably because OIs and OMs need to develop a motor pattern (premotor cortex), but they differ in the recruitment of the primary motor cortex and parietal regions, which are much stronger in OMs (execution of task and integration of proprioceptive feedback).

Analysis of connectivity during action also reflected this gradation between the O, OI and OM conditions, with a gradation in the strength of connectivity in relation to the Cz between conditions. When analyzing connectivity links, we observed in O a fronto-occipital network, probably linked to the activation of an action observation network, whereas in OI and OM, the recruitment is mainly centro-parietal contralateral to movement and may be linked to an action planning or execution network. However, one must remain cautious about these descriptive connectivity results since no statistical difference was found between conditions.

The need for a motor plan for post-movement validation

In our study, we observed a beta rebound emerging from the vertex, with a topography different from that of beta and alpha desynchronization; this rebound was absent in O but present in OI and OM. Beta rebounding corresponds to hypersynchrony in the beta band following movement [33, 48]. It originates in the precentral gyrus, more precisely, in the motor cortex [49, 50]. Initially, described as participating in the maintenance of an idling state in sensorimotor regions, its interpretation has been broadened [51]. It appears that beta rebound is modulated by motor validation phenomena and temporal integration of somatosensory and motor parameters [26]. For example, the observation of an erroneous movement can modulate beta rebound [25], as can the introduction of errors in a motor task [52]. It is possible that

this modulation of beta rebound emerges following the detection of a mismatch between the forward model and the sensory afferents, allowing an update of the motor pattern [53]. Our results seem to confirm this hypothesis, as we observed one desynchronization in OI and OM but no desynchronization in O. This finding confirms that the vision of a movement, even from a 1st-person point of view, will trigger a significant beta rebound only if it is perceived as feedback for a motor pattern, which is either executed (OM) or simulated (OI).

No significant difference in rebound intensity was observed between the OI and OM groups, although there was a proprioceptive/visual mismatch in the OI group (the leg was motionless during the video in the OI group). Negative proprioceptive feedback is known to negatively modulate beta rebound [51]. Providing correct visual feedback in video therapy could therefore minimize the effects of incorrect proprioceptive feedback on rebound formation. This result is of particular interest in neurological rehabilitation, where beta rebound is known to be a marker for monitoring neurological recovery [24]. However, to test this hypothesis, it would be interesting to study beta rebound in patients with cerebellar stroke (alteration of the forward model [54, 55]) and patients with proprioceptive disorders.

Interestingly, in terms of connectivity after the task, we did not observe an increase in connectivity in the beta band over the Cz, suggesting a topographically localized phenomenon. However, we observed an increase in connectivity in the frontal, parietal and occipital regions in the alpha band, with a gradation between the O, OI and OM tasks. This increase in connectivity was associated with a decrease in prefrontal connectivity. To our knowledge, this change in connectivity has never been described previously. We know that there are differences in low-beta and high-beta band function during beta rebound [53], with involvement of the frontal and parietal cortices in addition to the motor regions [56]. However, our observations were in the alpha band and may be indicative of another mechanism involved. Additionally, PLV connectivity is sensitive to volume conduction, making topographical analysis of such broad phenomena less robust. We must therefore remain cautious when interpreting these observations.

From healthy subjects to neurological patients

As this study was carried out on healthy subjects, we must remain cautious regarding the transposition of these results to a pathological population, with extremely different functional cortical dynamics and brain rhythms [57]. However, some general conclusions can be formulated.

Firstly, this work demonstrates a gradation of engagement between the tasks (O, OI, OM), that

enables personalization of the therapy offered to patients according to their level of recovery. Indeed, we demonstrate that passive observation in lower limb video feedback therapy leads to sensori-motor cortical recruitment. Although weak, this activation could be of interest in the very early phases of neurological rehabilitation, for example to tackle maladaptive plasticity as demonstrated for upper limb video feedback therapy [58]. However, it seems necessary to work with motor imagery or motor execution tasks as soon as possible, to maximize cortical recruitment and to trigger motor validation phenomena such as beta rebound, which are absent in passive observation task.

Also, this work provides a physiological basis for understanding the specific effects of visual feedback. Indeed, many rehabilitation studies focus on mirror therapy, which combines two distinct tasks: (1) a systematic movement of the patient's healthy hand or foot, and (2) an observation of the visual feedback on the mirror. Yet these two tasks have distinct neurological effects, whose interpretation often gets mixed up. Indeed, for the upper limb a bimanual movement may lead to bimanual facilitation [59], with an increase of motor cortex excitability [60] and a modulation of EEG rhythms and connectivity [61], which can bias the understanding of the specific effects of the visual feedback. Yet, the understanding of these specific effects is crucial to the personalization of the therapies. For example, we don't know how the visual feedback is integrated in patients with neuro-visual disorders, or if proprioceptive disorders may conflict with correct the visual feedback, and thus decrease the sensori-motor cortex recruitment.

We also have few points of comparison between lower and upper limb video feedback therapy since most of the studies on visual feedback focus on upper limb rehabilitation. The main EEG rhythms dynamics (ERD, ERS) seem to be generally the same, with a different topography above for motor areas, with a gradation between O, OI, and OM cortical recruitment between tasks, and enhanced recruitment in action observation as compared to motor imagery alone [37]. Yet, many questions hypothesis demonstrated for upper limb rehabilitation remain to be tested for lower limb rehabilitation. For example, for upper limb rehabilitation, in an action observation and motor imagery condition (similar to our OI), it appears that the alpha band ERD is enhanced by the vision of own hand movement, as compared to a non-subjective movement [19], especially in a first person perspective [45]. Considering that action observation facilitates motor cortical activity after stroke [12], we believe that lower limb rehabilitation with action observation should always try to implement a first person subjective visual

feedback, in order to maximize the cortical recruitment. This hypothesis remains however to be tested.

Our next step will be to study the specific effects of the visual feedback for stroke patients, regarding their lesion topography.

Limitations

There are several limitations to this work. First, we chose to add a two second interval between the end of the video and the beginning of the next epoch, in order to monitor the beta rebound. However, this interval appeared to be short since the beta rebound had not entirely returned to baseline at the start of the next epoch. For future work we will consider putting at least three seconds between the end of a video and the beginning of the next epoch.

A longer time at the beginning of the epochs should also be considered. Indeed, we observed in all the time-frequency maps an artifact at the beginning of the signal, that may have been caused by an event related potential due to a slight saccade in the video loop, maximal over occipital brain regions. Our baseline may also have been contaminated by some motor-preparation rhythms. Statistical comparison was performed between time-frequency maps with different baselines (500–1500 ms baseline versus 700–1200 ms baseline) and found no difference. Even if this did not change the overall significance of our results, further studies should include at least three seconds of pause at the beginning of each epoch.

Finally, for connectivity we chose to perform a PLV analysis, which can be sensitive to volume conduction effects. We tried to mitigate these volume conduction effects by using a surface Laplacian filter [34]. However, PLI (Phase Lag Index) and wPLI (Weighted Phase Lag Index) connectivity analysis, which are insensitive to volume conduction artifacts, showed no interpretable results. Though this work presents original connectivity data during lower limb visual-feedback therapy tasks, interpretation of these connectivity changes between conditions must be cautious, especially considering the absence of statistically significant results. A specific study of connectivity changes using a high-density EEG headset and a source level analysis could prove interesting.

Conclusion

In this work, we investigated for the first time the EEG correlates of video feedback therapy to the lower limb under three conditions: action observation alone, action observation with motor imaging, and action observation with motor execution.

We observed bilateral centro-parietal alpha desynchronization in all conditions, corresponding to the activation of the mirror neuron system, with strong

sensory-motor recruitment in motor execution. The study of beta desynchronization showed a gradation according to motor task O, OI and OM, with recruitment of the premotor cortex in the OI and OM and of the motor cortex and parietal regions in the OM. Finally, the study of beta rebounds highlights the need to add motor intention to action observation to trigger motor validation mechanisms.

This study provides a better understanding of the neurophysiological effects of video observational therapy and supports the benefits of adding visual feedback in support of motor imagery or motor execution during rehabilitation of the lower limb.

Abbreviations

EEG	Electroencephalography
ERD	Event related desynchronization
ERS	Event related synchronization
fMRI	Functional MRI
FWHM	Full width at half maximum
O	Passive action observation
OI	Action observation with motor imagery
OM	Action observation with motor execution
PLV	Phase locking value
VOT	Video observational therapy

Supplementary Information

The online version contains supplementary material available at <https://doi.org/10.1186/s12984-024-01408-8>.

Additional file 1: Table 1: EEG sensors map. C3 electrode is placed over left sensori-motor cortex, while C4 electrode is placed over right sensori-motor cortex.

Additional file 2: Table 2: Power time course in the alpha band expressed in percent change as compared to baseline (500—1500ms) over C3, Cz and C4 electrodes, in all conditions. The shaded area represents the 95% confidence interval.

Additional file 3: Table 3: Power time course in the beta band expressed in percent change as compared to baseline (500—1500ms) over C3, Cz and C4 electrodes, in all conditions. The shaded area represents the 95% confidence interval.

Additional file 4: Table 4: Mean power value in the alpha band during task for all electrodes, in the three conditions, expressed in percent change as compared to baseline (500—1500 ms), with 95% confidence interval. Sensors placed above sensori-motor cortex are highlighted in grey (C3, Cz, C4).

Additional file 5: Table 5: Mean power value in the alpha band during task for all electrodes, in the three conditions, expressed in percent change as compared to baseline (500—1500 ms), with 95% confidence interval. Sensors placed above sensori-motor cortex are highlighted in grey (C3, Cz, C4).

Additional file 6: Table 6: Mean power value in the beta band after task for all electrodes, in the three conditions, expressed in percent change as compared to baseline (500—1500 ms), with 95% confidence interval. Sensors placed above sensori-motor cortex are highlighted in grey (C3, Cz, C4).

Additional file 7: Table 7: Alpha-band PLV changes distribution and mean between subjects during task (A) and after task (B). Mean value is represented by a grey square.

Additional file 8: Table 8: Beta-band PLV changes distribution and mean between subjects during task (A) and after task (B). Mean value is represented by a grey square.

Additional file 9: Table 9: Time frequency percent changes distribution and mean between subjects during task in the alpha band (A), during task in the beta band (B) and after task in the beta band (C). Mean value is represented by a grey square.

Acknowledgements

This article was edited for proper English language at AJE (0FB0-0D7B-88CB-FB55-E0C9).

Author contributions

AA and LBT performed the experiments. AA analyzed the data. AA wrote the paper with BH and OE. AA, LBT, AP, GP and BJ conceived the study. GP and AP supervised the study. All the authors contributed to the editing of this paper.

Funding

The EEG device and disposable were funded by the Association AIRE (St-Etienne, France) and by the Foundation Neurodis (St-Etienne, France). Merz Pharma provided funding for the acquisition of the Brite MKII fNIRS device. The funders had no role in the study design, data collection and analysis, decision to publish or preparation of the manuscript.

Availability of data and materials

The datasets supporting the conclusions of this article are available upon reasonable request.

Declarations

Ethics approval and consent to participate

The study was registered and approved by the ethics committee "Comité de protection des personnes Sud-Est III" (2022-A02375-38) and registered in Clinical Trials (NCT05743647). Written consent was obtained from the subjects for participation and publication. The study was conducted in accordance with the Declaration of Helsinki.

Competing interests

The authors declare that the research was conducted in the absence of any commercial or financial relationships that could be construed as potential conflicts of interest.

Author details

¹Department of Physical Rehabilitation, CHU of St Etienne, Saint-Étienne, France. ²Laboratory Trajectoires, INSERM 1028, CNRS 5229, University of Lyon-St-Etienne, Saint-Étienne, France. ³Department of Neurology, CHU of Orleans, Orleans, France. ⁴Jean Monnet University, Lyon 1, Université Savoie Mont-Blanc, "Laboratoire Inter-Universitaire de Biologie de La Motricité", 42023 Saint-Étienne, France. ⁵"Laboratoire Interdisciplinaire d'innovation et de Recherche en Santé d'Orléans", LI2RSO, University of Orleans, Orleans, France. ⁶Univ. Grenoble Alpes, CEA, LETI, Clinatec, Grenoble, France.

Received: 15 February 2024 Accepted: 20 June 2024

Published online: 08 July 2024

References

- Kim H, Lee E, Jung J, Lee S. Utilization of mirror visual feedback for upper limb function in poststroke patients: a systematic review and meta-analysis. *Vision*. 2023;7(4):75.
- Altschuler EL, Wisdom SB, Stone L, Foster C, Galasko D, Llewellyn DME, et al. Rehabilitation of hemiparesis after stroke with a mirror. *The Lancet*. 1999;353(9169):2035–6.
- Louie DR, Lim SB, Eng JJ. The efficacy of lower extremity mirror therapy for improving balance, gait, and motor function poststroke: a systematic review and meta-analysis. *J Stroke Cerebrovasc Dis*. 2019;28(1):107–20.
- Li Y, Wei Q, Gou W, He C. Effects of mirror therapy on walking ability, balance and lower limb motor recovery after stroke: a systematic review and meta-analysis of randomized controlled trials. *Clin Rehabil*. 2018;32(8):1007–21.

5. Broderick P, Horgan F, Blake C, Ehrensberger M, Simpson D, Monaghan K. Mirror therapy for improving lower limb motor function and mobility after stroke: a systematic review and meta-analysis. *Gait Posture*. 2018;63:208–20.
6. Thieme H, Bayn M, Wurg M, Zange C, Pohl M, Behrens J. Mirror therapy for patients with severe arm paresis after stroke—a randomized controlled trial. *Clin Rehabil*. 2013;27(4):314–24.
7. Wittkopf PG, Johnson MI. Mirror therapy: a potential intervention for pain management. *Revista da Associacao Medica Brasileira* (1992). 2017;63(11):1000–5.
8. In T, Lee K, Song C. Virtual reality reflection therapy improves balance and gait in patients with chronic stroke: randomized controlled trials. *Med Sci Monit*. 2016;28(22):4046–53.
9. Buchignani B, Beani E, Pomeroy V, Iacono O, Sicola E, Perazza S, et al. Action observation training for rehabilitation in brain injuries: a systematic review and meta-analysis. *BMC Neurol*. 2019;19(1):344.
10. Bartur G, Pratt H, Dickstein R, Frenkel-Toledo S, Geva A, Soroker N. Electrophysiological manifestations of mirror visual feedback during manual movement. *Brain Res*. 2015;1606:113–24.
11. Bartur G, Pratt H, Frenkel-Toledo S, Soroker N. Neurophysiological effects of mirror visual feedback in stroke patients with unilateral hemispheric damage. *Brain Res*. 2018;1700:170–80.
12. Tani M, Ono Y, Matsubara M, Ohmatsu S, Yukawa Y, Kohno M, et al. Action observation facilitates motor cortical activity in patients with stroke and hemiplegia. *Neurosci Res*. 2018;133:7–14.
13. Zult T, Goodall S, Thomas K, Hortobágyi T, Howatson G. Mirror illusion reduces motor cortical inhibition in the ipsilateral primary motor cortex during forceful unilateral muscle contractions. *J Neurophysiol*. 2015;113(7):2262–70.
14. Hamzei F, Lämpchen CH, Glauche V, Mader I, Rijntjes M, Weiller C. Functional plasticity induced by mirror training: the mirror as the element connecting both hands to one hemisphere. *Neurorehabil Neural Repair*. 2012;26(5):484–96.
15. Tai RY, Zhu JD, Chen CC, Hsieh YW, Cheng CH. Modulation of functional connectivity in response to mirror visual feedback in stroke survivors: an MEG study. *Brain Sci*. 2021;11(10):1284.
16. Michielsen ME, Smits M, Ribbers GM, Stam HJ, van der Geest JN, Bussmann JBJ, et al. The neuronal correlates of mirror therapy: an fMRI study on mirror induced visual illusions in patients with stroke. *J Neurol Neurosurg Psychiatry*. 2011;82(4):393–8.
17. Cui W, Huang L, Tian Y, Luo H, Chen S, Yang Y, et al. Effect and mechanism of mirror therapy on lower limb rehabilitation after ischemic stroke: a fMRI study. *NeuroRehabilitation*. 2022;51(1):65–77.
18. Ding L, Wang X, Chen S, Wang H, Tian J, Rong J, et al. Camera-based mirror visual input for priming promotes motor recovery, daily function, and brain network segregation in subacute stroke patients. *Neurorehabil Neural Repair*. 2019;33(4):307–18.
19. Nagai H, Tanaka T. Action observation of own hand movement enhances event-related desynchronization. *IEEE Trans Neural Syst Rehabil Eng*. 2019;27(7):1407–15.
20. Mizuguchi N, Kanosue K. Changes in brain activity during action observation and motor imagery: their relationship with motor learning. *Prog Brain Res*. 2017;234:189–204.
21. Fox NA, Bakermans-Kranenburg MJ, Yoo KH, Bowman LC, Cannon EN, Vanderwert RE, et al. Assessing human mirror activity with EEG mu rhythm: a meta-analysis. *Psychol Bull*. 2016;142(3):291–313.
22. Park W, Kim SP, Eid M. Neural coding of vibration intensity. *Front Neurosci*. 2021;15(15): 682113.
23. Stolk A, Brinkman L, Vansteensel MJ, Aarnoutse E, Leijten FS, Dijkerman CH, et al. Electroencephalographic dissociation of alpha and beta rhythmic activity in the human sensorimotor system. *Elife*. 2019;8:e48065.
24. Shiner CT, Tang H, Johnson BW, McNulty PA. Cortical beta oscillations and motor thresholds differ across the spectrum of post-stroke motor impairment, a preliminary MEG and TMS study. *Brain Res*. 2015;1629:26–37.
25. Koelwijn T, Van Schie HT, Bekkering H, Oostenveld R, Jensen O. Motor-cortical beta oscillations are modulated by correctness of observed action. *Neuroimage*. 2008;40(2):767–75.
26. Cardellicchio P, Hilt PM, Dolfini E, Fadiga L, D'Ausilio A. Beta rebound as an index of temporal integration of somatosensory and motor signals. *Front Syst Neurosci*. 2020;2(14):63.
27. Oldfield RC. The assessment and analysis of handedness: the Edinburgh inventory. *Neuropsychologia*. 1971;9(1):97–113.
28. Mathôt S, Schreij D, Theeuwes J. OpenSesame: an open-source, graphical experiment builder for the social sciences. *Behav Res Methods*. 2012;44(2):314–24.
29. Dong L, Li F, Liu Q, Wen X, Lai Y, Xu P, et al. MATLAB toolboxes for reference electrode standardization technique (REST) of scalp EEG. *Front Neurosci*. 2017;30(11):601.
30. Delorme A, Makeig S. EEGLAB: an open source toolbox for analysis of single-trial EEG dynamics including independent component analysis. *J Neurosci Methods*. 2004;134(1):9–21.
31. Cohen MX. A better way to define and describe Morlet wavelets for time-frequency analysis. *Neuroimage*. 2019;199:81–6.
32. Allen DP, MacKinnon CD. Time-frequency analysis of movement-related spectral power in EEG during repetitive movements: a comparison of methods. *J Neurosci Methods*. 2010;186(1):107–15.
33. Pfurtscheller G, Lopes da Silva FH. Event-related EEG/MEG synchronization and desynchronization: basic principles. *Clin Neurophysiol*. 1999;110(11):1842–57.
34. Cohen MX. Comparison of different spatial transformations applied to EEG data: a case study of error processing. *Int J Psychophysiol*. 2015;97(3):245–57.
35. Aydore S, Pantazis D, Leahy RM. A note on the phase locking value and its properties. *Neuroimage*. 2013;74:231–44.
36. Maris E, Oostenveld R. Nonparametric statistical testing of EEG- and MEG-data. *J Neurosci Methods*. 2007;164(1):177–90.
37. Gonzalez-Rosa JJ, Natali F, Tettamanti A, Cursi M, Velikova S, Comi G, et al. Action observation and motor imagery in performance of complex movements: evidence from EEG and kinematics analysis. *Behav Brain Res*. 2015;281:290–300.
38. Zhao M, Marino M, Samogin J, Swinnen SP, Mantini D. Hand, foot and lip representations in primary sensorimotor cortex: a high-density electroencephalography study. *Sci Rep*. 2019;9(1):19464.
39. Gatti R, Rocca MA, Fumagalli S, Cattrysse E, Kerckhofs E, Falini A, et al. The effect of action observation/execution on mirror neuron system recruitment: an fMRI study in healthy individuals. *Brain Imaging Behav*. 2017;11(2):565–76.
40. Debnath R, Salo VC, Buzzell GA, Yoo KH, Fox NA. Mu rhythm desynchronization is specific to action execution and observation: evidence from time-frequency and connectivity analysis. *Neuroimage*. 2019;184:496–507.
41. Hobson HM, Bishop DVM. The interpretation of mu suppression as an index of mirror neuron activity: past, present and future. *Royal Soc Open Sci*. 2017;4(3):160662.
42. Thorpe SG, Cannon EN, Fox NA. Spectral and source structural development of mu and alpha rhythms from infancy through adulthood. *Clin Neurophysiol*. 2016;127(1):254–69.
43. Zhang JJQ, Fong KNK, Welage N, Liu KPY. The activation of the mirror neuron system during action observation and action execution with mirror visual feedback in stroke: a systematic review. *Neural Plast*. 2018;2018:1–14.
44. Sun Y, Wei W, Luo Z, Gan H, Hu X. Improving motor imagery practice with synchronous action observation in stroke patients. *Top Stroke Rehabil*. 2016;23(4):245–53.
45. Angelini M, Fabbri-Destro M, Lopomo NF, Gobbo M, Rizzolatti G, Avanzini P. Perspective-dependent reactivity of sensorimotor mu rhythm in alpha and beta ranges during action observation: an EEG study. *Sci Rep*. 2018;8(1):12429.
46. Hardwick RM, Caspers S, Eickhoff SB, Swinnen SP. Neural correlates of action: comparing meta-analyses of imagery, observation, and execution. *Neurosci Biobehav Rev*. 2018;94:31–44.
47. Fong KNK, Ting KH, Zhang JJQ, Yau CSF, Li LSW. Event-related desynchronization during mirror visual feedback: a comparison of older adults and people after stroke. *Front Hum Neurosci*. 2021;15:629592.
48. Pfurtscheller G, Neuper C, Brunner C, Da Silva FL. Beta rebound after different types of motor imagery in man. *Neurosci Lett*. 2005;378(3):156–9.
49. Jurkiewicz MT, Gaetz WC, Bostan AC, Cheyne D. Post-movement beta rebound is generated in motor cortex: evidence from neuromagnetic recordings. *Neuroimage*. 2006;32(3):1281–9.

50. Mary A, Bourguignon M, Wens V, Op De Beeck M, Leproult R, De Tiège X, et al. Aging reduces experience-induced sensorimotor plasticity. A magnetoencephalographic study. *Neuroimage*. 2015;104:59–68.
51. Cassim F, Monaca C, Szurhaj W, Bourriez JL, Defebvre L, Derambure P, Guieu JD. Does post-movement beta synchronization reflect an idling motor cortex? *NeuroReport*. 2001;12(17):3859–63.
52. Torrecillos F, Alayrangues J, Kilavik BE, Malfait N. Distinct modulations in sensorimotor postmovement and foreperiod β -band activities related to error salience processing and sensorimotor adaptation. *J Neurosci*. 2015;35(37):12753–65.
53. Cao L, Hu YM. Beta rebound in visuomotor adaptation: still the status quo? *J Neurosci*. 2016;36(24):6365–7.
54. Bhanpuri NH, Okamura AM, Bastian AJ. Predictive modeling by the cerebellum improves proprioception. *J Neurosci*. 2013;33(36):14301–6.
55. Casartelli L, Federici A, Cesareo A, Biffi E, Valtorta G, Molteni M, et al. Role of the cerebellum in high stages of motor planning hierarchy. *J Neurophysiol*. 2017;117(4):1474–82.
56. Heinrichs-Graham E, Kurz MJ, Gehringer JE, Wilson TW. The functional role of post-movement beta oscillations in motor termination. *Brain Struct Funct*. 2017;222(7):3075–86.
57. Kancheva I, Van Der Salm SMA, Ramsey NF, Vansteensel MJ. Association between lesion location and sensorimotor rhythms in stroke—a systematic review with narrative synthesis. *Neurol Sci*. 2023;44(12):4263–89.
58. Giroux P, Sirigu A. Illusory movements of the paralyzed limb restore motor cortex activity. *Neuroimage*. 2003;20:S107–11.
59. McCombe Waller S, Forrester L, Villagra F, Whittall J. Intracortical inhibition and facilitation with unilateral dominant, unilateral nondominant and bilateral movement tasks in left- and right-handed adults. *J Neurol Sci*. 2008;269(1–2):96–104.
60. Byblow WD, Stinear CM, Smith MC, Bjerre L, Flaskager BK, McCambridge AB. Mirror symmetric bimanual movement priming can increase corticomotor excitability and enhance motor learning. *PLoS ONE*. 2012;7(3):e33882.
61. Muthuraman M, Arning K, Govindan RB, Heute U, Deuschl G, Raethjen J. Cortical representation of different motor rhythms during bimanual movements. *Exp Brain Res*. 2012;223(4):489–504.

Publisher's Note

Springer Nature remains neutral with regard to jurisdictional claims in published maps and institutional affiliations.



Head office FR

Parc Techno. Metrotech, Bât. 6
FR - 42650 St-Jean-Bonnefonds

Dessintey GmbH DE

Worringer Straße 30
DE - 50668 Köln

contact@dessintey.com

dessintey.com